Title: Hybrid lead-free polymer-based scaffolds with improved piezoelectric response for biomedical energy-harvesting applications: A review

Article Type: Review article

Corresponding Author: Dr. Roman Anatolievich Surmenev, Ph.D.

Corresponding Author's Institution: National Research Tomsk Polytechnic University

First Author: Roman Anatolievich Surmenev, Ph.D.

Order of Authors: Roman Anatolievich Surmenev, Ph.D.; Tetiana Orlova, Dr; Roman Chernozem; Anna Ivanova, Dr; Ausrine Bartasyte, Dr; Sanjay Mathur, Dr; Maria Surmeneva, Dr

Abstract: Lead-free alternatives to convert mechanical energy into electrical energy through piezoelectric transduction are of significant value in biomedical applications. This review describes novel approaches in the fabrication of hybrid piezoelectric polymer-based materials for biomedical energy-harvesting applications. The most promising routes to improve the piezoelectric response and energy-harvesting performance of such materials are discussed. The effects of the presence of various lead-free components in the structure of the piezoelectric polymers on their piezoresponse or energy-harvesting performance are reviewed. The piezocomposites described are mostly based on poly-(vinylidene fluoride) (PVDF), or its copolymer, poly-(vinylidene fluoride)-trifluoroethylene PVDF-TrFE, loaded with various nanofillers such as reduced graphene oxide (rGO), inorganic compounds (nanoparticles such as barium titanate BaTiO3, and potassium sodium niobate (KNaNbO3)), salts (LaCl3, ErCl3, GdCl3, etc), metal oxides (ZnO, MgO, TiO2), metallic nanoparticles (Ag, Pt), and carbon nanotubes (CNTs). Non-biodegradable hybrid piezocomposites developed with potential or actually demonstrated applications in biomedical devices and sensors, including implantable nanogenerators and stimulatory materials for wound healing and tissue regeneration form the focus of the current research. It is concluded that novel piezoelectric material systems and device architectures can promote the development of flexible self-powered multifunctional e-skin for the detection of the motion rate of humans, the degradation of many kinds of organic pollutants, and the sterilization of bacteria on its surface. Various implantable devices that require no external energy input for biomedical energy-harvesting or bone defect repair applications in vivo, as well as sensors or detectors for human motion, health monitoring, independent temperature monitoring, and pressure control that can be prepared based on piezoelectric polymer materials are also discussed.

Suggested Reviewers: Matthias Epple Dr

Professor, University of Duisburg-Essen
matthias.epple@uni-due.de
Professor Epple is a leading scientist in the field of biomedical
implants inclduing permanent and biodegradable ones as well as hybrid
scaffolds

Andre Skirtach Dr
Professor, Ghent University
andre.skirtach@ugent.be
Professor Skirtach is an expert in the field of biomedical materials
science, implants surface modification and functionalization.

Timothy Douglas Dr
Group leader, Lancaster University
t.douglas@lancaster.ac.uk
Dr Douglas is an expert in the field of polymer-based scaffolds for
regenerative medicine and piezoelectric materials for energy-harvesting
applications.

Opposed Reviewers:

МИНИСТЕРСТВО ОБРАЗОВАНИЯ И НАУКИ РОССИЙСКОЙ ФЕДЕРАЦИИ

634050, г. Томск,
пр. Ленина, 30,
ТПУ
Россия

Tomsk Polytechnic University
30, Lenin Avenue,
Tomsk, 634050, Russia

«НАЦИОНАЛЬНЫЙ ИССЛЕДОВАТЕЛЬСКИЙ

ТОМСКИЙ ПОЛИТЕХНИЧЕСКИЙ УНИВЕРСИТЕТ»

Тел. (382-2) 70-17-79   Факс: (382-2) 56-38-65. УФК по Томской области
р/с 40501810500002000002 в ГРКЦ ГУ Банка России по Томской области г.Томск
БИК 046902001 ИНН 7018007264 ТПУ л/с 20656У20990 ОКПО 02069303; E-mail:
tpu@tpu.ru

18/01/2019 № 1.1568

Dear Professor Wang,

Thank you for editing Nano Energy. We would like to submit our review manuscript titled "**Hybrid lead-free polymer-based scaffolds with improved piezoelectric response for biomedical energy-harvesting applications: A review**".

To the best of our knowledge, no reviews are available on piezoelectric hybrid polymer-based composites with improved piezoelectric response and, thus, energy-harvesting performance.

This review describes novel approaches in the fabrication of hybrid piezoelectric polymer-based materials for biomedical energy-harvesting applications. The most promising routes to improve the piezoelectric response and energy-harvesting performance of such materials are discussed. The effects of the presence of various lead-free components in the structure of the piezoelectric polymers on their piezoresponse or energy-harvesting performance are reviewed. The piezocomposites described are mostly based on poly-(vinylidene fluoride) (PVDF), or its copolymer, poly-(vinylidene fluoride)-trifluoroethylene PVDF-TrFE, loaded with various nanofillers such as reduced graphene oxide (rGO), inorganic compounds (nanoparticles such as barium titanate $BaTiO_3$, and potassium sodium niobate ($KNaNbO_3$)), salts ($LaCl_3$, $ErCl_3$, $GdCl_3$ etc), metal oxides (ZnO, MgO, TiO_2), metallic nanoparticles (Ag, Pt), and carbon nanotubes (CNTs).

Piezoresponsive polymer-based nanocomposite materials offer the potential of developing a new generation of high-performance and flexible energy harvesters for biomedical applications. By developing new polymer-based nanocomposites for piezoelectric energy harvesting, materials scientists now possess a number of potential lead-free alternatives that can be used to convert mechanical energy into electrical energy through piezoelectric transduction, which is of significant value in biomedical applications.

Non-biodegradable hybrid piezocomposites developed with potential or actually demonstrated applications in biomedical devices and sensors, including implantable nanogenerators and stimulatory materials for wound healing and tissue regeneration form the focus of the current research. It is concluded that novel piezoelectric material systems and device architectures can promote the development of flexible self-powered multifunctional e-skin for the detection of the motion rate of humans, the degradation of many kinds of organic pollutants, and the sterilization of bacteria on its surface. Various implantable devices that require no external energy input for biomedical energy-harvesting or bone defect repair applications *in vivo*, as well as sensors or detectors for human motion, health monitoring, independent temperature monitoring, and pressure control that can be prepared based on piezoelectric polymer materials are also discussed.

Sincerely yours,
Roman A. Surmenev, Dr,
Associate Professor, Director of Physical Materials Science and Composite Materials Centre,
National Research Tomsk Polytechnic University,
E-mail: rsurmenev@gmail.com

- Novel approaches to the fabrication of hybrid piezoelectric materials are discussed

- Routes to improve energy-harvesting performance are described

- Novel piezoelectric material systems and device architectures are proposed

- Implantable devices for biomedical energy-harvesting or bone repair are reported

Hybrid lead-free polymer-based scaffolds with improved piezoelectric response for biomedical energy-harvesting applications: A review

Roman A. Surmenev[1,2, *], Tetiana N. Orlova[1], Roman V. Chernozem[1], Anna A. Ivanova[1],

Ausrine Bartasyte[3], Sanjay Mathur[2], Maria A. Surmeneva[1]

[1] Physical Materials Science and Composite Materials Centre, National Research Tomsk

Polytechnic University, 634050 Tomsk, Russia

[2] Institute of Inorganic Chemistry, University of Cologne, Greinstr. 6, 50939 Cologne, Germany

[3] Institut FEMTO-ST, Université Franche-Comté, 26 rue de l'Epitaphe, F-25030 BESANCON

Cedex, France

[*]correspondence author: Roman A. Surmenev, rsurmenev@mail.ru

Contents

List of abbreviations

BT – barium titanate ($BaTiO_3$)

PVDF – poly-(vinylidene fluoride)

PVDF-TrFE – poly-(vinylidene fluoride)-trifluoroethylene

PVDF-HFP – poly-(vinylidene fluoride-co-hexafluoropropylene)

Gr – graphene

GO –graphene oxide

rGO – reduced graphene oxide

PLLA – poly(L-lactice acid)

PLA – polylactide

PHB – polyhydroxybutyrate

PANi – polyaniline

CNT – carbon nanotubes

MWCNT – multiwalled carbon nanotubes

PZT – lead zirconate titanate

KNN – potassium sodium niobate ($(Na,K)-NbO_3$)

NG – nanogenerator

PENG – piezoelectric nanogenerator

PEMG – piezoelectric microgenerator

PET – polyethylenterephthalat

PMN-PT – $(1-x)Pb(Mg_{1/3}Nb_{2/3})O_3 - xPbTiO_3$ (x<1, lead magnesium niobate-lead titanate)

NPs – nanoparticles

NF – nanofiber

PDMS – polydimethylsiloxane

NR – nanorod

AAO – anodized aluminum oxide

ZTO – perovskite zinc titanate (ZnTiO$_3$)

TFB – 4-azidotetrafluorobenzoic acid

ROS – reactive oxygen species

Abstract

Lead-free alternatives to convert mechanical energy into electrical energy through piezoelectric transduction are of significant value in biomedical applications. This review describes novel approaches in the fabrication of hybrid piezoelectric polymer-based materials for biomedical energy-harvesting applications. The most promising routes to improve the piezoelectric response and energy-harvesting performance of such materials are discussed. The effects of the presence of various lead-free components in the structure of the piezoelectric polymers on their piezoresponse or energy-harvesting performance are reviewed. The piezocomposites described are mostly based on poly-(vinylidene fluoride) (PVDF), or its copolymer, poly-(vinylidene fluoride)-trifluoroethylene PVDF-TrFE, loaded with various nanofillers such as reduced graphene oxide (rGO), inorganic compounds (nanoparticles such as barium titanate BaTiO$_3$, and potassium sodium niobate (KNaNbO$_3$)), salts (LaCl$_3$, ErCl$_3$, GdCl$_3$, etc), metal oxides (ZnO, MgO, TiO$_2$), metallic nanoparticles (Ag, Pt), and carbon nanotubes (CNTs). Non-biodegradable hybrid piezocomposites developed with potential or actually demonstrated applications in biomedical devices and sensors, including implantable nanogenerators and stimulatory materials for wound healing and tissue regeneration form the focus of the current research. It is concluded that novel piezoelectric material systems and device architectures can promote the development of flexible self-powered multifunctional e-skin for the detection of the motion rate of humans, the degradation of many kinds of organic pollutants, and the sterilization of bacteria on its

surface. Various implantable devices that require no external energy input for biomedical energy-harvesting or bone defect repair applications *in vivo*, as well as sensors or detectors for human motion, health monitoring, independent temperature monitoring, and pressure control that can be prepared based on piezoelectric polymer materials are also discussed.

Keywords: piezoelectric polymer; nanogenerator; energy harvesting; sensor; piezo-catalysis

Highlights:

- Novel approaches to the fabrication of hybrid piezoelectric materials are discussed

- Routes to improve energy-harvesting performance are described

- Novel piezoelectric material systems and device architectures are proposed

- Implantable devices for biomedical energy-harvesting or bone repair are reported

Introduction

The word piezoelectricity is derived from the Greek word "piezein", which means "to press", and "ēlektron", which means "amber", and thus refers to stress-induced electricity [1]. The piezoelectric effect describes the capability of certain materials to generate spatially separated opposite electrical charges in response to mechanical deformation produced by an external force [1]. For a single piece of deformed material, electrical charges of different polarity are generated at opposite sides, i.e. an electric dipole or piezopotential is thus formed.

Piezoelectric ceramics are commonly used as piezoelectric elements in energy harvesting devices due to their excellent piezoelectric characteristics, low production cost, and ability to be incorporated into energy harvesting devices. The lead-based piezoelectric PZT $((PbZr)TiO_3)$ is especially important because it has a high Curie temperature [2], higher piezoelectric charge constants higher than many other ceramic materials, e.g. ZnO [3], and a relatively low production cost [4]. PZT materials have been broadly commercialised; for example, a flexible

4

multi-layered composite for low frequency energy harvesting applications was prepared based on PET/Al/PZT/Al/PET [5]. Well-aligned PZT NRs prepared *via* hydrothermal treatment with (001)-orientated tetragonal single crystalline structures exhibited a high piezoelectric response with a d_{33} value of up to 1600 pm·V^{-1}. A piezoelectric energy harvester was fabricated based on the PZT NR arrays and exhibited an outstanding energy harvesting performance with open-circuit output voltages of 3.3 V and 8 V when subjected to a compressive 10 N force and a finger tapping motion, respectively. Moreover, the average power densities generated under these two mechanical stimuli were up to 3.16 and 5.92 µW cm^{-2} with an external load of 1 MΩ [6]. Pb-based materials are still being prepared and investigated for energy-harvesting applications [7], including hybrids such as 30 vol% PMN-PT/CNT/PVDF [8]. Multimaterial piezoelectric fibres fabricated from perovskite ceramic NPs (BT/PZT)-PVDF and CNT-PVDF composites *via* fibre drawing have also been reported [9]. However, due to the high toxicity of PZT, PZT-PVDF fibres are probably not suitable for wearable applications [10]. Despite their advantages, hazardous lead-based substances have been removed from a wide range of applications [11].

Various alternative concepts for piezoelectric materials and composites based on inorganic piezoelectric ceramics have been developed [4], including lead-free inorganic materials such as $(Na,K)NbO_3$ [12] and organic polymer hybrids, e.g. PHB/PANi [13]. Polymer-based piezoelectric materials, such as PVDF or its copolymer poly-(vinylidene fluoride)-trifluoroethylene (PVDF-TrFE), have several unique advantages over inorganic materials, such as good mechanical flexibility, ease of moulding, chemical stability, and biocompatibility [14]. These polymers are multifunctional and exhibit ferroelectric, piezoelectric, pyroelectric, and superior dielectric properties [15]. They have been reported to occur in α-phase, β-phase, γ-phase, and δ-phase forms; however, only the β-phase manifests spontaneous polarization and thus exhibits piezoelectricity [16, 17].

Studies of the formation, characterization, and *in vitro* cytocompatibility of electrospun PVDF-TrFE fibres have revealed that this non-biodegradable piezoelectric polymer scaffold is a

promising base material for manipulating cell behaviour and proliferation in a three-dimensional matrix [18]. PVDF or PVDF-TrFE fibre webs, as well as other polymer nanofibres, e.g. PVDF-HFP [19] and PLLA [20, 21], are typically produced by the conventional electrospinning process [17, 22-24]. Their higher mechanical strength results in a more robust interconnected fibre web that can maintain its structural integrity during compression and decompression. Although PVDF fibre mats are usually prepared for energy harvesting applications, other polymers such as poly(γ-benzyl-α,L-glutamate), which has a maximum d_{33} of 27 pC·N^{-1} [25], and PLLA [20] have been also reported. Electrospun PVDF nanofibres showed a high β-phase fraction due to the application of a high voltage during electrospinning [23]. The electrospinning process can be effectively utilised for loaded polymers, for example, polymers with incorporated ZnO particles, to form β-phase crystalline structures and improve the piezoelectric properties of the resulting nanofibre mats. The application of high voltages during the electrospinning process essentially leads to the alignment of the electric dipoles present in the PVDF solution, with the degree of alignment being proportional to the magnitude of the applied electric field [26]. Various electrospun hybrid composites for energy-harvesting applications based on PVDF or PVDF-TrFE nanofibre mats, including graphene nanosheets and BT NPs [27], (Na0.5,K0.5)NbO$_3$ (NKN) NPs embedded in PVDF-TrFE [12], BT NPs embedded in PVDF-TrFE [28, 29], PVDF-ZnO nanofibre mats [26], PVDF/KNN NRs [30], K0.5Na0.5NbO$_3$-BT/PVDF [31], Ag/PVDF-TrFE [32], and PVDF-TrFE-BT with rGO contents of 0.1%, 0.3%, 0.5%, and 0.7% [33] have been reported. Structurally robust, reproducibly scalable, substrate-independent, and large-area NGs have been successfully fabricated utilizing the near-field electrospinning direct-write technique to massively align the piezoelectric PVDF nanofibres (NFs) on flexible substrates [34]. The maximum output voltage reached 20 V using a three-layered NG with serial connections, and the maximum output current exceeded 390 nA with a parallel integration setup. An NF-based device with a length of ∼5 cm was easily attached on a human finger, and its

output voltage and current in response to a ~45° folding-releasing movement reached 0.8 V and 30 nA, respectively [34].

PVDF scaffolds were also prepared by melt spinning [35], and from PVDF/clay components (modified or unmodified clay with an organic modifier) containing up to 5 wt% of an additive [36]. Stretchable PVDF piezoelectric generators that exhibited excellent responses under extremely large applied strains (more than 100%), were prepared by electrohydrodynamic direct-writing using a mechano-electrospinning process [37]. Spin-coating, in addition to being an alternative to evaporative deposition, is also interesting because it readily results in the formation of the β-phase of PVDF [38]. Benz et al. prepared 2 μm thick PVDF thin films with a high β-phase content on highly-polished single-crystal silicon wafers by spin coating PVDF solutions with acetone/DMF as the solvent [39]. The spin speed and humidity were reported to be the main factors that determined the β-phase content and surface roughness of the resulting thin films [17, 39].

Piezoelectric polymer fibres can also be fabricated using the fibre drawing technique. In this method, a preformed geometrically complex multimaterial fibre with a length of tens of centimetres is first assembled by stacking tubes, rods, multilayered films, or other functional components [9]. A transformative additive manufacturing-based novel process was presented to fabricate freeform-shaped volumetric piezoelectric devices by combining additive manufacturing and electric poling processes in a single processing and fabrication step. The poling-assisted additive manufacturing process can align the dipoles of the polymer molecular chain and transform the polymer from the α phase to the β phase by applying a strong electric field during printing [40, 41].

The degree of crystallinity plays an important role in the d_{33} piezoelectric response, which increases with the degree of crystallinity for a piezoelectric polymer [42], allowing greater piezoelectric potential values to be obtained. For example, a PVDF harvester provided an average output power of 1 mW during a walk at a frequency of roughly 1 Hz [43]. The amount

7

and direction of the strain induced in a PVDF film can be changed by varying the direction of the applied force; thus, the output power generated can be tuned. The maximum output peak voltages measured for the harvester were 1.75, 1.29, and 0.98 V when an input force of 4 N (2 Hz) was applied at an angle of 0°, 45°, and 90°, respectively; the corresponding maximum output power values were 0.064, 0.026, and 0.02 µW, respectively. Moreover, the harvester generated a stable output voltage over 1.4×10^4 cycles, and successfully identified and converted the strain energy produced by multi-directional input forces from various human motions into electrical energy [22].

In spite of the many reviews on the topic of piezoelectric polymers, none have focused on surveying the effect of different additives on their piezoelectric responses and energy-harvesting performances. Thus, this review summarises the most recent achievements in the development of novel piezoelectric materials and their biomedical applications. Future perspectives and challenges, as well as existing sensors and devices based on hybrid piezoelectric materials for biomedical energy harvesting, are also discussed.

1. Methods for the improvement of the piezoelectric response of polymeric materials and scaffolds

1.1 Inorganic non-conductive additives

The content and orientation of the γ and β phases and the degree of crystallinity are the essential features that determine the piezoelectric performance of polymer NGs based on PVDF and its copolymers [44]. Recently, researchers have attempted to improve the dielectric and piezoelectric characteristics of this polymer without compromising its mechanical strength or flexibility through the incorporation of various nucleating agents (nanofillers) into the polymer matrix [45-47]. This approach has emerged as a new paradigm for the development of high-energy-density capacitors. Numerous studies have shown that the crystallization behaviour of the

polymer depends on specific interfacial interactions between the nucleating agents and polymer chains [45, 47-51]. Therefore, the nucleation effect of the nanofillers depends on the particle surface charge and surface area, concentration, dispersion, lattice matching, and processing conditions [47, 52, 53]. The presence of nanofillers was shown to reduce the nucleation energy barrier, enhancing the crystallization rate and the degree of crystallinity of the polymer [47]. Lead-free piezoceramic particles (BT, KNN) [48-51, 54, 55], metal oxide NPs (ZnO, MgO, TiO_2) [19, 56-59], CNTs [60-65], graphene and graphene derivatives such as rGO [27, 66, 67], hydrated ionic salts [68], nanoclays [69, 70], and metal NPs (Ag, Pt) [71, 72] have all proven to be highly efficient as nucleating fillers that can induce a polar electroactive phase without applying electrical polarization. By optimizing the concentration and uniformity of the distribution of the fillers in the polymer matrix, superior piezoelectricity and dielectric values are obtained. The addition of these types of nanofillers leads to significant changes in the breakdown field, charge transport, and charge distribution of the dielectric materials. The increased content of the polar electroactive phase and the enhancement of the dielectric features of polymer-based nanocomposites open the possibility for these materials to be used in energy harvesting and energy storage for biomedical applications.

Barium titanate ($BaTiO_3$, BT)

BT is a well-known dielectric ceramic with moderate piezoelectric coefficients (d_{33}) of 90 and 190 pC/N along the [001] and [111] directions of the perovskite cubic crystal [51]. BT is a promising nucleating filler for PVDF-based composites due to its easy preparation via a procedure that allows for the precise control of its chemical composition. Other advantages include its high piezoelectric coefficient, scalable and low-cost processing, and biocompatibility as a lead-free material [49]. The improved dielectric and piezoelectric features of PVDF/BT nanocomposites have recently been demonstrated by a number of authors [49, 51, 55, 73, 74]. The majority of studies have shown that solution-cast films and electrospun PVDF/BT fibre mats

exhibit enhanced dielectric constants, and consequently, increased electric energy density [49, 51, 55, 62, 75]. Flexible energy harvesting devices fabricated using PVDF loaded with BT nanowires with a length of 4 μm and a width of 150 nm exhibited high performance with a high current output [49]. BT NPs have also been used as guiderails for the delivery of anticancer drugs, making BT NPs of 40–100 nm a versatile tool in biomedicine [62]. A recent study of an electrospun PVDF scaffold filled with BT NPs of up to 100 nm in diameter reported that the piezoelectric coefficient increased with the nanofiller weight percentage, reaching a value of up to 130 pm/V at a 20 wt% loading of BT NPs [51]. *In vitro* assays performed by the authors demonstrated the enhanced viability of epithelial cells and neural-like cells in physiological-like conditions. Membranes and films composed of ferroelectric PVDF-TrFE and BT nanostructures have been effectively utilised in a number of studies to enhance osteoblast-like cell differentiation [76-78], human neuroblastoma cell stimulation [79], and *in vivo* bone regeneration [76]. *In vitro* and *in vivo* experiments demonstrated that the observed effects were directly connected to the electrical microenvironment generated by the piezoelectric composites. The transverse piezoelectric coefficient d_{31} was enhanced 1.8-fold by embedding multi-walled BT tubes with an average diameter of 10 nm and lengths of up to a micrometre in the PVDF-TrFE matrix [77], and the addition of 300 nm tetragonal BT NPs resulted in a 4.5-fold increase of the coefficient d_{31} [79]. The incorporation of highly crystalline $BaTi_{(1-x)}Zr_xO_3$ (BTZO) nanocubes with dimensions of around 200 nm into PVDF was shown to provide a high electrical output of up to ~11.9 V and ~1.35 μA in response to a 21 Hz cyclic stress with a constant load (11 N) [55]. For comparison, a BT/PVDF film exhibited outputs of 7.99 V and 1.01 μA under the same loading conditions. The piezoelectric performance of a BTZO/PVDF NG increased as the molar substitution ratio (Zr^{4+}/Ti^{4+}) was increased up to 0.2.

Bodkhe et al. studied the nucleation behaviour of 3D -printed PVDF in the presence of BT NPs with a diameter of 100 nm [48]. The authors confirmed that the content of the electroactive phase increased from ~45 to ~56 % with the addition of 15 wt% of BT NPs. The 3D-printed

PVDF/BT NP sensor was demonstrated to provide a maximum voltage output of up to 4 V in response to finger tapping.

Hollow BT nanospheres (diameter: 20 nm) treated with different silane coupling agents were incorporated into PVDF, and the crystallization behaviour of the resulting nanocomposite was explored in ref. [75]. A significantly higher β-phase content was detected when the surface-modified BT nanospheres were added than for the neat PVDF and untreated BT/PVDF. The changes in crystallinity were shown to increase the dielectric constant (ε' ~109.6) and energy density (U_e ~21.7 J/cm^3) with a breakdown strength (E_b) of 3.81×10^3 kV/cm compared to pristine PVDF (ε' ~11.6 and U_e ~2.16 J/cm^3 at 3.98×10^3 kV/cm).

Although a great deal of work has been carried out using these materials, some limitations related to the agglomeration and phase separation of the BT fillers in the polymer matrix, which cause poor interfacial interactions and high defect density, still exist. Moreover, the dielectric constant of the BT particles is unstable at elevated temperatures, which may influence the performance of the composites. Therefore, several key issues should be considered in order to achieve practically applicable composites. For instance, Nunes-Pereira and coworkers performed comparative studies of the piezoelectric performance of spin-coated and electrospun PVDF-TrFE containing BT particles of various dimensions, in particular, 10 nm (cubic), 100 nm (cubic), and 500 nm (tetragonal) particles [80, 81]. The electrospun composite fibres were compared to neat PVDF fibres [81]. The obtained results demonstrated that the size and content of the filler and its crystalline structure determined the piezoelectric and energy harvesting properties of the nanocomposites. The authors reported that the enhanced mechanical stiffness of composites with greater nanofiller dimensions and contents reduced the energy harvesting performance of the samples. Among the studied spin-coated PVDF-TrFE-based composites, the highest output power (0.28 μW) was measured for the samples with 20 wt% of the 10 nm particles and 5 wt% of the larger particles [80]. More interestingly, the PVDF fibres showed the highest power output under mechanical deformation; values of 0.02 W

and 25 W were measured under low and high deformation. The authors considered three possible mechanisms that could contribute to the decrease in the output power of the composites. Firstly, defects induced by the nanofiller in the polymer matrix could act as dampers and therefore reduce the mechanical-to-electrical energy transformation [80]. Additionally, the random orientation of the domains in the inorganic electroactive filler could lead to an overall decrease in the piezoelectric polarization of the composite compared to that of the neat polymer. Finally, the opposite signs of the piezoelectric coefficients of the polymer and the nanofillers could contribute to the final piezoelectric response of the composite.

Theoretical simulations conducted by several authors have indicated that the filler morphology affects the energy harvesting performance of composite materials. A polymer-based composite containing low-dimensional piezoceramic fillers was found to exhibit poor stress transfer from the polymer matrix to the active ceramic particles [82]. Several researchers demonstrated that the use of fillers with a high aspect ratio is an effective way to improve the intrinsic polarization of the fillers, the interface polarization, and the electric field distribution between the fillers and the matrix [83, 84]. For instance, a comparative study of the dielectric properties of PVDF composites filled with spherical and rod-like BTs revealed that the composites loaded with rod-like fillers had a higher permittivity and superior energy storage performance due to the stronger internal electric field density distribution. The results of this simulation are depicted in Figure 1 [84].

Modelling of the electric field intensity distribution across the PVDF composites embedded with rod-like BT and spherical fillers revealed that the inorganic particles, which had a higher dielectric permittivity, induced electric field deformation, as evidenced by the darker colour of the filler area (Figure 1a). The magnitude of the alteration of the electric field intensity across the BT NRs, BT NPs, and PVDF matrix are depicted in Figure 1b and c. The high-aspect-ratio fillers obviously exhibited a stronger electric field strength (10.240 kV/mm) than the fillers with a low aspect ratio (2.260 kV/mm) (Figure 1b). Figure 1c depicts the electric field strength distribution

along the fillers. Interestingly, nanorods with different lengths had different electric field distributions, and the electric field strength was stronger in the centre of the fillers. Nevertheless, even at the ends of the NRs, the electric field strength was higher than that of the NPs. Thus, the BT NRs were more efficiently polarised than the BT NPs, and the former led to higher dielectric permittivity in the PVDF composites. The relationship between the electric field strength of the nanorods and their spatial position along the horizontal direction is depicted in Figure 1d. As shown, the electric field strength increases gradually as the angle between the NRs and horizontal axis reaches 90°. The mean electric field intensity of the randomly distributed BT NRs was greater than that of the BT NPs; thus, the composites filled with high aspect ratio particles had a superior piezoelectric performance.

Shin et al. developed a composite thin film composed of tetragonal BT NPs with a an average size of 200 nm embedded in hemispherical PVDF-HFP clusters, which exhibited a surprisingly high piezoelectric power output owing to the alignment of the dipoles combined with effective stress transfer [74]. More recently, Jeong et al. reported a high-performance PVDF-TrFE-based hybrid NG using 1D BT nanowires [49] that achieved high output parameters (14 V and 4 μA).

The finite element analysis method provided a more in-depth understanding of the origin of the high piezoelectric performance of the PVDF-TrFE/ BT nanowires composite (Figure 2). The simulation showed that both the PVDF-TrFE matrix and the embedded fillers produced a high piezoelectric response (Figure 2a (i, ii)), which caused a synergetic effect. The BT nanowires included in the low-Young's-modulus PDMS matrix possessed very weak piezopotential due to external stress dissipation within the matrix, as shown in Figure 2b (i, ii). Thus, the effective stress transfer of PVDF-TrFE was responsible for the high performance of the PVDF-TrFE-based NG. Figure 2c depicts the relationship between the output voltage, the instantaneous power of the PVDF-TrFE/ BT nanowire NG, and the external resistance of the circuit. Increasing the load resistance enhanced the output voltage up to the open-circuit value. The developed composite exhibited a power output as high as 1.5 μW, which exceeds the power performance of

recently reported PVDF-based NGs at the lower resistance. Therefore, the available findings indicate that the development of novel piezoelectric composites should be based on controlling the morphology of the ferroelectric filler.
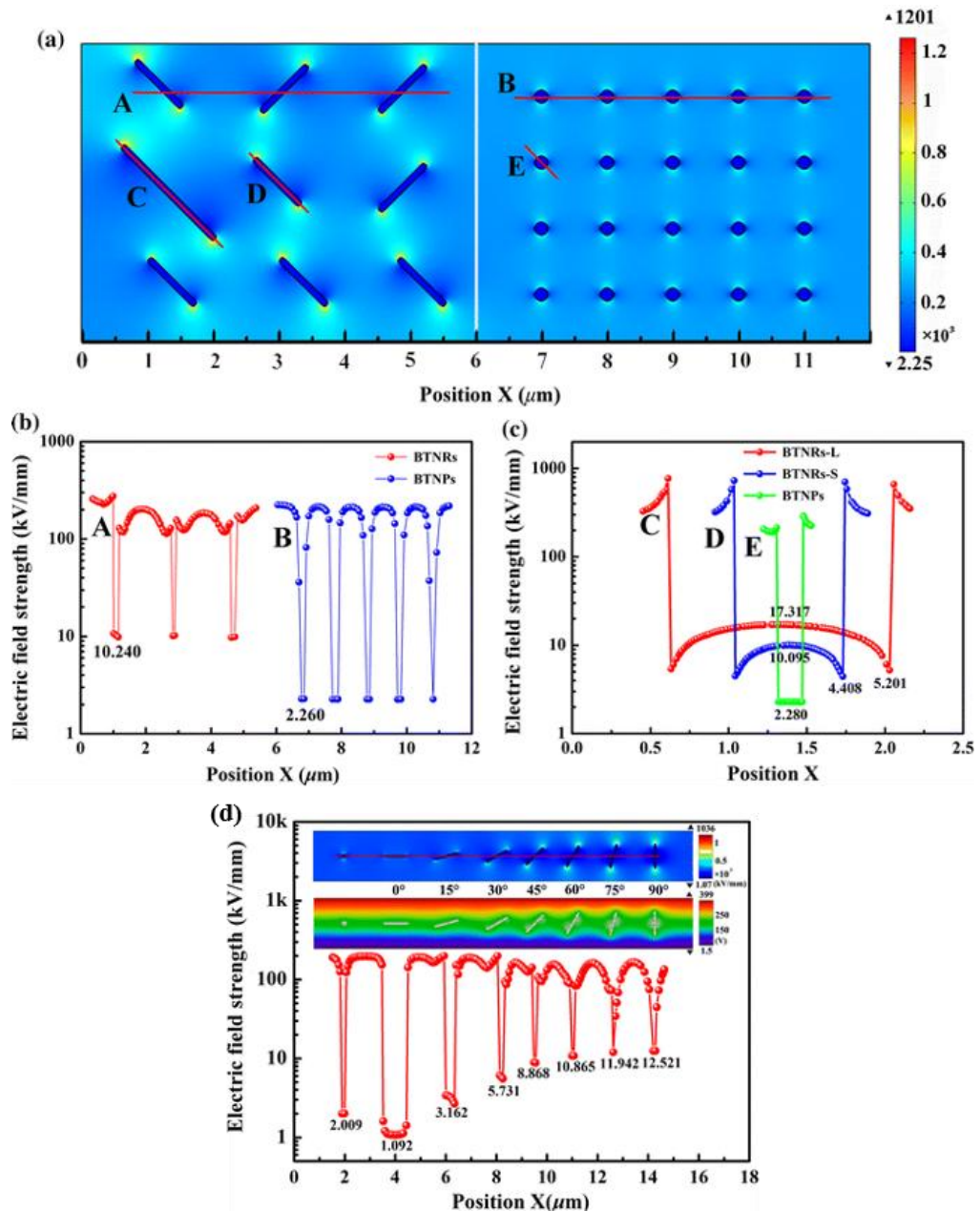
Figure 1. a) Simulated distribution of the electric field for BT/PVDF composites filled with BT NRs and BT NPs. Distribution of electric field along b) line A and line B, and c) lines C, D, and E. d) Simulated distributions of the electric field and potential for the BT/PVDF composites filled with BT NPs and BT NRs in different arrangements, and the distribution of electric field along the red line. Reprinted from [84] with the permission from Springer.
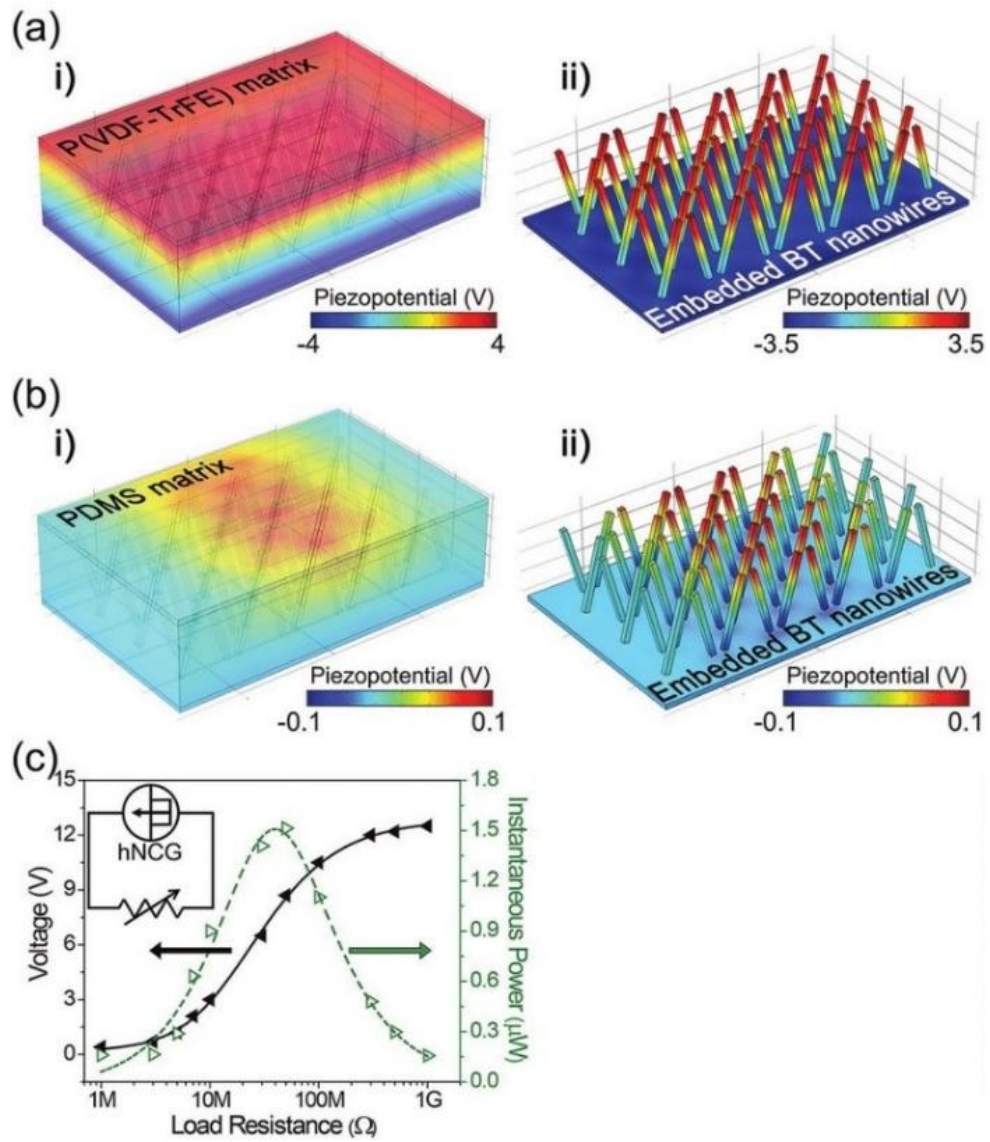
Figure 2. a,b) Results of a simulation performed using COMSOL Multiphysics programming software, which depicts the piezopotential levels of components in a) a BT nanowire-embedded PVDF-TrFE nano-composite and b) a BT nanowire-embedded PDMS nanocomposite to compare the potential generation of the piezoelectric nanocomposites. c) Output voltage and relevant instantaneous power levels as a function of the variable load resistance. Reprinted from [49] with the permission from Wiley.

Potassium sodium niobate ((Na,K)-NbO₃, KNN)

KNN is another lead-free piezoelectric filler with a complex orthorhombic structure that exhibits spontaneous polarization along the [110] direction, and has been widely studied due to its favourable electromechanical properties ($k_p = 0.36$, $d_{33} = 80$ pC/N) [46].

15

A KNN/PVDF-based NG exposed to a vibrational load with a compressive force of 50 N and a frequency of 1 Hz was shown to generate an output voltage of up to 18 V and a current of up to 2.6 μA [54]. Kang et al. studied the energy harvesting performance of a nanocomposite based on a PVDF-TrFE matrix filled with perovskite KNN NPs ranging from 30 to 105 nm in size [12]. Surface modification and the KNN NP volume fraction were considered to be the critical parameters responsible for the high performance of the NG. An output voltage of 0.98 V and an output current of 78 nA were obtained using NFs containing 10 vol% KNN. According to ref. [46], PVDF containing 70 vol% of micron-sized orthorhombic crystallites of KNN demonstrated a piezoelectric coefficient d_{33} of up to 35 pC/N, while the nanocrystals included in the polymer matrix did not exhibit any piezoelectric response. A synergetic enhancement in the piezoelectric performance of the PVDF/KNN nanocomposite was induced by the incorporation of KNN nanocrystals with a higher aspect ratio into electrospun PVDF fibres in the study in ref. [30]. The presence of 5 wt% KNN in PVDF was shown to provide a high degree of improvement in the output properties of the NG without any additional poling procedure. An output voltage of 1.9 V was detected from the PVDF/KNN fibre web, which was 40-fold higher than that of the neat PVDF web [30]. One drawback of KNN is its high leakage current density, which significantly reduces the piezoelectric performance of the composite [85]. Simply varying the composition of this material can significantly improve its piezoelectric properties [12]. In particular, it was shown that by replacing the Nb^{5+} ions in the perovskite structure of KNN with Cu^{2+}, Zr^{4+}, Li^{+}, Ta^{5+}, or Sb^{5+}, complex defects are created in the form of oxygen vacancies, and prevent the movement of the domain walls, reduce the dielectric losses, and stabilize the piezoelectric performance [86]. However, to the best of our knowledge, there is a lack of studies on the piezoelectric performance of PVDF doped with substituted KNN.

Metal oxides

Zinc oxide (ZnO) with a hexagonal wurtzite structure is considered to be one of the most promising materials for piezoelectric devices [87, 88] due to its excellent piezoelectric performance. ZnO nanofillers have been widely used for the development of piezoelectric NGs because of their biocompatibility and facile and versatile growth method [89]. The introduction of ZnO NPs (average diameter: ~50–150 nm) into a PVDF matrix enhanced the β-phase content up to 84% at a ZnO loading of 0.85 vol%. The piezoelectric coefficient was increased to 50 pC/N at 50 Hz, and the dielectric constant to 109 at 1.7 vol%, as reported by Thakur et al. [90].

Ferroelectric PVDF-HFP was coupled with Co-doped ZnO fillers [19]. An increase in the amount of the crystalline β-phase of PVDF-HFP was observed with increasing nanofiller concentration in the polymer matrix. The output voltage increased proportionally with the concentration of the polar electroactive phase present in the nanocomposites [19].

A numerical study performed by Choi et al. demonstrated that the addition of ZnO nanowires (size: ~50 nm) into the polymer matrix allowed better electric field redistribution within the polymer and a greater improvement in the piezoelectric performance than that observed for piezoceramic fillers [57]. The latter have been shown to mainly affect the dielectric permittivity of ZnO, which is close to that of PVDF and its copolymers. The second reason is related to the transfer of strain from ZnO to the polymer matrix. The electrical outputs of the PVDF/ZnO nanocomposite were superior to those of the neat PVDF device, with a 2.7-fold and 6.5-fold enhancement in output voltage and current, respectively [57]. It was also demonstrated that as-synthesised ZnO-containing paper ash can be used as an alternative to conventional semiconducting fillers used to improve the electroactive β-phase content in electrospun PVDF NFs [91].

Singh et al. used MgO NPs with a size of <50 nm and a rock salt structure as fillers in PVDF-TrFE [58]. The dielectric constant of MgO is ~10, which is close to that of PVDF-TrFE; hence, the incorporation of MgO NPs is unlikely to result in any inhomogeneity in the electric field distribution in the composite, and it can be considered a filler material. Moreover, the beneficial

role of MgO in increasing the breakdown strength and imparting a low leakage current was recently reported [92, 93]. Thus, in addition to improving the ferroelectric and piezoelectric properties of PVDF-TrFE, MgO fillers may improve the long-standing issue of its large leakage current. The addition of MgO into the polymer matrix reportedly induced an improvement in the crystallinity of the latter, which was attributed to the formation of hydrogen bonds between the inherently present −OH groups on the MgO surface and the F atoms of PVDF-TrFE [58]. The values of the piezoelectric coefficient d_{33} followed a similar trend to that of the remnant polarization, with the highest value (-65 pm/V) being obtained for the 2 wt% MgO/PVDF-TrFE nanocomposite film. In contrast, devices with pure PVDF-TrFE exhibit a d_{33} value of approximately -40 pm/V. Thus, the addition of 2 wt% MgO NPs to PVDF-TrFE films leads to an almost 50% improvement in the piezoelectric coefficient, confirming the efficacy of the addition of MgO to the PVDF-TrFE matrix to achieve superior ferroelectric and piezoelectric responses [58].

Recently, Dutta et al. reported the development of a NiO@SiO$_2$/PVDF nanocomposite [59]. In order to overcome the agglomeration of the metal oxide particles and the formation of a conductive nanofiller path in the polymer matrix, rhombohedral NiO NPs with a size of <100 nm were coated with non-conductive SiO$_2$ prior to being added to the polymer. The piezoelectric NG fabricated using the resulting NiO@SiO$_2$ (15 wt%)/PVDF nanocomposite had very promising output parameters in response to the application of biomechanical force, with an output voltage of up to 53 V, a current density of ~0.3 μA/cm^2, a high power density of 685 W/m^3, and a superior conversion efficiency of up to 13.86%. The use of the NiO@SiO$_2$/PVDF NG in tactile e-skin mechanosensors was proposed [59].

Owing to its exceptional mechanical and thermal stability, TiO$_2$ is another semiconductor that can be used to develop high-performance PVDF-based NGs for energy harvesting and storage applications [91]. Alam et al. prepared a flexible and wearable NG for harvesting mechanical energy from normal human activities and acoustic vibrations from an electrospun PVDF/TiO$_2$

fibre mat from an electrospun PVDF/TiO_2 fibre mat. Within 50 seconds, a 1 µF capacitor could be charged to 20 V, and power a LED tape and LCD screen individually.

Salts

A number of researchers have reported the effect of rare earth salts (R^{3+} cations) on the structure, dielectric properties, and piezoelectric performance of PVDF and its co-polymers [94, 95]. Thakur et al. reported electroactive β-phase crystallization and an increase in the dielectric constant with the incorporation of cerium (III)/yttrium (III) nitrate hexahydrate in PVDF [96]. Hassen et al. and El-Sayed et al. also studied the dielectric properties of lanthanum (III) chloride ($LaCl_3$)/PVDF [94] and $ErCl_3$ or $GdCl_3$/PVDF [95] thin films, respectively. Erbium (III) chloride hexahydrate/PVDF (5 wt%) and iron nitrate (III) nonahydrate/PVDF (10 wt%) thin films exhibited d_{33} values of -124 pC/N and -72.4 pC/N, respectively [68]. The complex cerium(III)-N,N-dimethylformamide-bisulphate [$Ce(DMF)(HSO_4)_3$] was loaded into PVDF to induce a higher yield (99%) of the electroactive phases (β- and γ-phases) [97]. A remarkable enhancement in the output voltage (∼32 V) of a NG based on a PVDF composite film containing the non-electrically poled cerium (III) complex was achieved by simple repeated human finger tapping, whereas neat PVDF did not show this kind of behaviour. This high electrical output was assumed to be the result of the generation of a self-poled electroactive β-phase in PVDF due to electrostatic interactions between the fluoride of PVDF and the surface-active positively charged cloud of the cerium complex *via* H-bonding and/or bipolar interaction between the opposite charges of the cerium complex and PVDF, respectively [97]. Under finger tapping, erbium (III) chloride hexahydrate/PVDF was produced an open circuit voltage of up to 115 V and a short circuit current of up to 32 µA with a power density of 160 mW/cm^3. The output signal of an iron nitrate (III) nonahydrate/PVDF generator reached a voltage of up to 75 V and a current of up to 17 µA with a power density of 55.34 mW/cm^3. The incorporation of ytterbium (III) chloride hexahydrate (Yb^{3+}) into a PVDF film resulted in a high β-phase content (80%) and an increased

piezoelectric output signal [98]. In response to finger movement with a pressure of approximately 0.17 MPa, an open circuit voltage and short circuit current of 10 V and 63 µA, respectively, were detected. Adhikary and co-authors performed an extensive investigation into the performance of piezopolymer composites doped with Eu^{3+}, Zn^{2+}, Ce^{3+}, Mn^{2+}, and Al^{3+} salt fillers [97, 99-101]. An enhancement of the piezoelectric response was detected without the application of mechanical stretching or electrical poling. Moreover, the composites exhibited intense light emission, which opens new prospects for the development of flexible light emitters. The obtained electromechanical output values are summarised in Table 2.

An organic modifier (quaternary ammonium salt) influenced the crystalline form of melt-electrospun PVDF and led to a high β phase content [36]. Filling dioctadecyl dimethyl ammonium chloride (which is found in C15A - Cloisite®) into PVDF provided a 150% increase in the β-phase content. The formation of strong hydrogen bonds and the interfacial polarization between the salt molecules and the polymer chains were considered to be the key factors affecting the enrichment of the self-poled β-phase and improvement of dielectric properties and consequently, the piezoelectric output of the salt-filler composites [68, 97, 101]. The maximum value of the piezoelectric coefficient d_{33} was determined for different material compositions and concentrations of the doping component [102]; electrospun PVDF fibres containing 10 wt.% Al $(NO_3)_3 \cdot 9H_2O$ were found to give a d_{33} coefficient of **-**116 pm·V^{-1} [102]. When the salt concentration was increased further, the effective piezoelectric coefficient began to decrease, which was consistent with the degradation of the crystalline structure and dielectric properties at an excessive level of the hydrated salt.

Metal NPs

Metal NPs can also be used as nucleating agents in piezoelectric polymer matrices to enhance the electroactive phase content. As discussed above, the interfacial interactions between the inorganic particles and polymer chains play a crucial role in β-phase crystallization. The effect of

metal NPs on the piezoelectric performance of PVDF is comparable to that of other types of additives; however, metal nanofillers impart additional functional properties. For instance, silver NPs (Ag NPs) with a diameter of ~100 nm were added to a PVDF matrix to increase the electroactive phase content and as an antibacterial agent [103]. The resulting PVDF/Ag NP electrospun fibres demonstrated piezoelectric behaviour as well as a bactericidal effect. The output voltage of the nanocomposite with 0.4 wt% of Ag was 2 V. Superior piezoelectric properties were achieved for a self-poled porous polymer consisting of platinum NPs embedded in a PVDF-HFP matrix [71]. This nanocomposite synergistically combined the functionality of the self-polarised β-phase and micropores as charge trapping sites and was developed by applying a conventional solvent evaporation method. The porous Ag-filled PVDF-HFP film exhibited a remnant polarization of 61.7 $\mu C/cm^2$, an outstanding piezoelectric charge coefficient d_{33} of −686 pC/N, and high dielectric properties (ε'=2678 and tan δ=0.79 at 1 kHz). Moreover, a high output signal was achieved. The NG exhibited an open-circuit voltage of approximately 18 V and a short-circuit current of 17.7 μA under a 4 MPa compressive stress [71].

Carbon nanotubes

CNTs have attracted great interest among scientists as reinforcing nanofillers for polymers due to their outstanding properties, low mass density, and high aspect ratio, which make them an ideal candidate for chemical functionalization and for the insertion of electromechanical and electrochemical sensing transduction mechanisms within a composite structure [64, 65]. When conventional solution-mixing methods such as melt-cooling and melt-spinning are utilized for the production of polymer/CNT composite films, sonication is required to induce β-phase crystallization, as reported by Mendez et al.[17] and Alluri et al. [60]. In the latter work, the CNT fillers in PVDF were demonstrated to act as electrically conductive paths between the − CH_2− and −CF_2− electric dipoles of PVDF, inducing an improved piezoelectric response. The

PVDF/CNT composites showed a ~30% increase in voltage and a ~96% increase in current compared to the pristine PVDF film [60].

A spin-coated PVDF film containing 0.7 wt% CNTs (8.5 nm in diameter and 1.5 μm in length) was shown to consist of the polar electroactive γ-phase mixed with the non-polar α-phase. The γ-phase domains yielded a d_{33} value of 13 pm/V [104]. Composite CNT-filled PVDF films prepared by the spray coating method exhibited an approximately 50-fold increase in the output power as the CNT concentration was increased from 0.015 to 0.075 wt% [105]. A synergetic improvement in the crystal structure and piezoelectric performance of electrospun PVDF/CNT nanofibres was observed by several authors [65, 106, 107]. Wu et al. showed that electrospinning itself promotes β-phase crystallization and dipole alignment, and that the addition of CNTs into the PVDF matrix allows further improvement in the piezoelectricity of the electrospun PVDF [65]. The d_{33} value of the obtained scaffold was 1.8-fold higher than that of the neat PVDF fibres.

The dispersion and alignment of the CNTs in the polymer matrix are the principal conditions that have been proven to affect PVDF/CNT matrix performance [64, 107]. CNTs can be modified by mechanical methods and chemical functionalization. The approaches used for the dispersion of CNTs are described in detail elsewhere [61, 108].

Recent reports have shown that it is possible to obtain a β phase content of up to 100% of in PVDF/CNT composites with the proper modification of the surface of the nanofiller [63]. Functionalization of the CNT surface by carboxyl (-COOH) [109], hydroxyl (-OH) [110], 3,4,5-trifluorobromobenzene (TFBB) [111], and amino (-NH$_2$) [112] groups was demonstrated to improve the filler dispersion and enhance the nucleation efficiency of the β-phase in the polymer matrix. Composites with well-dispersed CNTs were shown to exhibit remarkably improved ferro-, pyro-, and piezoelectric properties [65, 113].

The most challenging issue presented by PVDF/CNTs composites is the drastic decrease in breakdown strength due to the high conductivity of the fillers [114]. The latter limits the

improvement of the piezoelectric performance of PVDF/CNTs, because the composites cannot be poled under sufficiently high electric fields. One convenient approach to overcome the this limitation is to align the fillers perpendicular to the applied electric field [114].

Several authors have reported the effect of CNT templating on the crystallization and orientation of the β-phase crystals in PVDF or co-polymer matrices. Wang et al. demonstrated that the molecular chain axis (c axis) of the β-phase crystals in PVDF-TrFE is oriented parallel to the long axis of the CNTs [115]. Thus, the dipole orientation in the polymer matrix can be controlled by changing the orientation of the CNT long axis. If the CNT long axes are oriented parallel to the substrate, the β-phase has a much higher tendency to align with the polar axis oriented perpendicularly to the substrate.

Another way to improve the breakdown strength is to form insulating or semiconductive shells outside the CNTs. Yang et al. reported a PVDF composite comprising core-shell structured TiO_2-CNT fillers with diameters of 40–60 nm and lengths of 5–15 mm [114]. Using solution casting and mechanical rolling, a high degree of orientation was achieved for both the PVDF domains and the TiO_2-coated CNTs. A maximum piezoelectric coefficient of 41 pC/N was measured for a composite with 0.3 wt% of filler, which was twice as great as that of the neat PVDF. The β phase content in electrospun PVDF determines the output voltage of the NG. CNTs and PANi provided the maximum and minimum β phase content and output voltage [116]. The maximum output voltage of the CNT composites was 0.9 V, which was well-correlated with the maximum β phase content, while the minimum value measured for the PANi-containing composites was 0.46 V. The output voltages of the composites based on different additives followed the order CNT>LiCl>pure PVDF>ZnO>PANi [116]. Comparative data of the piezoelectric performance of polymer-based NGs are presented in Table 1 and Table 2.

Table 1. Comparison of the piezoelectric constants (d_{33} and d_{31}, pC/N=pm/V) for PVDF-based PENGs.

Nanogenerator material	d_{33}	d_{31}	Ref.
Neat PVDF film processed uniaxial elongation at high temperature	-30 pC/N		[117]
Unpoled PVDF nanowires	-6.5 pm/V		[118]
Poled PVDF-TrFE nanofibres		16.17 pC/N	[119]
Unpoled PVDF-TrFE film		6 pm/V	[77]
Self-aligned β-phase PVDF films	-49.6 pm/V		[120]
Core-shell-structured PVDF/1 wt %GO nanofibres	-110 pm/V		[121]
PVDF electrospun fibres filled with Ag–CNTs	54 pm/V		[122]
PVDF/CNT fibres	35 pm/V		
PVDF with highly aligned TiO_2@MWCNTs	41 pC/N		[114]
PVDF fibres filled with BT NPs	50-130 pm/V		[51]
3D printable PVDF with BT NPs		18 pC/N	[123]
Casted PVDF-TrFE/BT NPs film		53.5 pm/V	[79]
Film of casted PVDF-TrFE/BN nanotubes		11 pm/V	[77]
PVDF-TrFE matrix filled with 70 vol.% (Na,K)-NbO$_3$ NPs	35 pC/N		[46]
PVDF matrix loaded with ZnO NPs	50 pC/N		[90]
2 wt% MgO/PVDF-TrFE nanocomposite films	-65 pm/V		[58]
Erbium (III) chloride hexahydrate/PVDF (5 mass%)	-124 pC/N		[68]
Iron nitrate (III) nonahydrate/PVDF (10 mass%) thin films	-72.4 pC/N		[68]
Hybrid porous Pt/ PVDF-HFP film	-686 pC/N		[71]
Electrospun PVDF/CNT fibres	18.8 pC/N		[65]
Spin-coated PVDF-0.7 wt% CNT film	13 pm/V		[104]
Ag/PVDF-TrFE films by tape casting (0.005 vol% Ag)	20.23 pC/N		[32]

Table 2. Comparison of the outputs of nanocomposite-based piezoelectric nanogenerators.

Nanocomposite	Poling	Output voltage, V	Output current, µA	Power density, mW/m^2	Excitation mode	Ref.
PVDF film with embedded $BaTi_{(1-x)}Zr_xO_3$ nanocubes	Poled	11.9	1.35	1.4	Cyclic stress at 21 Hz with a constant load 11 N	[55]
PVDF film with embedded BT NPs	Poled	7.99	1.01		Cyclic stress at 21 Hz with a constant load 11 N	[55]
3D-printed PVDF/15 wt% BT NPs	Unpoled	4			Finger tapping	[48]
(PVDF-TrFE) film containing BT nanowires	Poled	14	4		Bending mode ~0.5 Hz	[49]
Electrospun PVDF with embedded BT NPs	Self-poled	1.4	$0.8 \cdot 10^{-3}$		The moving end of the generator was displaced transversely by 10 mm	[9]
PVDF-TrFE matrix filled with (Na,K)-NbO$_3$ NPs	Poled	18	2.6		Compressive force of 50 N and 1 Hz	[54]
Flexible planar $(1-x)K_{0.5}Na_{0.5}NbO_{3-x}BT/PVDF$ composite films, x = 0.02	Poled	≈160	≈0.4	≈14	Mechanical force of ~0.4 N	[31]
Electrospun PVDF fibre with embedded high-aspect-ratio (Na,K)-NbO$_3$ nanocrystals	Self-poled	1.9			Finger tapping	[30]
PVDF-TrFE nanofibres containing 10 vol% (Na,K)-NbO$_3$ NPs	Self-poled	0.98	0.078		Under bending strain	[12]
ZnO nanowires embedded in a PVDF matrix	Poled	0.4	0.030		Bending strain of 3.2%	[57]

NiO@SiO$_2$ (15 wt%)/PVDF nanocomposite	Unpoled	53		137	Compressing pressure of ~ 0.3 MPa at a frequency of ~4 Hz	[59]
Erbium (III) chloride hexahydrate/PVDF NG	Unpoled	115	32	7680	Finger typing	[68]
Iron nitrate (III) nonahydrate/PVDF generator	Unpoled	75	17	2656	Finger typing	[68]
Eu^{3+}-doped PVDF-HFP hybrid nanocomposite film	Self-poled	5	0.35		Compressing pressure of 10.4 kPa	[101]
Cerium(III)-N,N-dimethylformamide-bisulfate complex (1 wt%) doped into a PVDF film	Self-poled	32			Finger typing	[97]
Sponge-like PVDF-HFP film embedded with MgCl$_2$·6H$_2$O (0.5 wt%)	Unpoled	8			Finger typing	[100]
Zn^{2+}-doped PVDF-HFP hybrid nanocomposite film	Unpoled	6		3.5	Compressing pressure of 14 kPa	[99]
Platinum NPs embedded in a PVDF-HFP matrix	Self-poled	18	17.7	~0.140	Compressing pressure 4 MPa	[71]
Activated carbon nanotubes embedded in a PVDF matrix	Unpoled	37.87	0.831	63.07	Compressing pressure 6.6 kPa	[60]
Carbon nanotubes (0.4 wt%) embedded in electrospun PVDF	Self-poled	3	1.2·10^{-3}		The moving end of the generator was displaced transversely by 10 mm	[9]
30 wt% GaFeO$_3$ NPs/PVDF	Unpoled	~3.5	4·10^{-3}		Mechanical pressing and releasing conditions	[124]

BT NPs stacked with P(VDF-TrFE) electrospun nanofibres	Self-poled	10.1	0.189	17.6	Knee movements during walking [125]
PVDF-BT nanocomposite films on each side of the n-Gr layer	Poled	10	2.5		Applied force of 2 N (pressing–releasing cycles) [126]
PVDF with 2 wt% ZTO	Unpoled	25.7	1.2	82.2	Cyclic loading under a finger imparting a constant pressure (~16.5 KPa) [127]
Sponge-like mesoporous PVDF film (30-500 nm) nanogenerator	Poled	3.8	3.5		Shaker with a frequency of 20 Hz and a force of 6 N [128]
		0.2			Gentle movement of rodent muscle of living mouse

Nanocomposites based on PVDF and its co-polymers and loaded with inorganic fillers are very promising for biomedical applications such as energy-harvesting devices. Despite the progress that has been made in this field, piezoelectric composites still require further optimization to meet the demands of practical applications, as higher sensing performance is required for biomedical devices due to the small physical displacement of the human organs and low working frequency. Thus, an in-depth understanding of the impact of the piezopolymer composite behaviour at the nanoscale on their macroscopic properties is still a key scientific issue. Progress in developing computational methods and suitable piezoelectric models to link domain or even atomic and macroscale behaviours is expected in the near future. Multiple energy harvesting (i.e. thermal and piezoelectric energy) to improve the overall output of the systems may require the introduction of fillers with different functionalities to the polymer matrix, or the development of multilayer structures. Thus, there is still substantial room for improvement and development in the field of polymer-based flexible NGs.

1.2 Graphene and reduced graphene oxide

It is well documented that adding conductive fillers to composite materials can not only further increase their dielectric constant and piezoelectric charge constant values due to the formation of micro-capacitors inside the composite, but also contributes to the stabilization the polar β-phase of the polymer matrix [33]. Uniform dispersion of the piezoelectric particles in composite films is essential for the fabrication of composite-based PENGs with a high output, as it ensures a well-distributed piezopotential within the active energy-harvesting composite layer [129].

rGO is often used to improve the energy-harvesting performance of piezoelectric PVDF or PVDF-TrFE [130]. Modified rGO, e.g. with Fe, has also been reported [45], as have hybrids of rGO with BT NPs and PVDF [27]. rGO plays two major roles in the composite: (1) it facilitates the alignment of the dipoles of the PVDF-TrFE matrix and (2) allows the formation of micro-

capacitors inside the composite. Oxygen-containing functional groups such as carboxyl and carbonyl groups in the rGO basal plane facilitate the alignment of the polymer chains by attracting fluorine atoms to one side [33] and thus improving the crystallinity [130]. Moreover, the dielectric constant shows an increasing trend with increasing rGO concentration [130]. For a pure PVDF-TrFE thin film, the dielectric constant was 35, while after the addition of rGO flakes, it reached a maximum value of approximately 72 at 1 kHz. Two neighbouring rGO fillers can be considered as the electrodes of a local capacitor with a very thin PVDF-TrFE layer as the dielectric medium. These micro-capacitors contribute to the capacitance, which is correlated to the enhancement in the dielectric constant due to the alignment of the dipoles in one direction [130].

Abolhasani et al. investigated the influence of Gr nanoplatelets on the crystallinity, polymorphism, and electrical output of electrospun NF generators. The open circuit voltage of the NFs was 3.8 V, and the addition of 0.1% graphene increased this value to 7.9 V [131]. Few-layer Gr for current generation was prepared by a facile and cost-effective method, and a Gr-Ag-doped PVDF hybrid nanocomposite was synthesised *via* a one-pot method [132]. The nanocomposite induced a voltage of 100 mV and a current of 0.1 nA when the material was subjected to a periodic uniaxial compressive stress of approximately 5.2 kPa.

The mechanism of γ-phase formation in the Fe-doped rGO nanocomposite embedded in the PVDF matrix can be explained *via* the following mechanism. The π-electrons of rGO attract some of the $-CH_2-$ dipoles of PVDF (gauche conformation), which is composed of $-CH_2-CF_2-$ chains. Some of the $-CH_2-$ dipoles (*trans* conformation) are repelled by the Fe/iron oxide particles present within the rGO matrix. In the same way, some $-CF_2-$ dipoles are attracted (gauche conformation) by the Fe/iron oxide particles, and some of the $-CF_2-$ dipoles are repelled (*trans* conformation) by the delocalised π-electrons of rGO, respectively [45]. The oxygen-containing functional groups (like hydroxyl, carbonyl, and carboxyl) present in Fe-rGO may interact with fluorine or hydrogen atoms *via* hydrogen bonding. Additionally, the Fe-rGO

nanosheets develop an electrical potential when exposed to mechanical stress. This potential further aligns the PVDF dipoles in the same direction by stress-induced polarization [133].

Among the fabricated PENGs, the one with 0.1% rGO exhibited the maximum open circuit voltage of 2.4 V and the highest short-circuit current peak of approximately 0.8 mA at an applied force of 2 N. Moreover, it exhibited the highest output power of 3.2 µW at a 1.8 MΩ load resistance; all the outputs were recorded without applying a poling process [130]. The maximum output voltage obtained with 1% filler content and under the maximum applied load in the study (500 g) was ±0.45 V, which was nearly five times greater than that of pure PVDF [134]. The power generation calculated from the electrical output signals was 14 µW/cm^3 for the device made from the 1 wt.% Gr nanohybrid, indicating a linear relationship with the applied stress up to a certain value. Moreover, increased output current and voltage were observed when the content of rGO was increased [134]. The PVDF/GO nanofibres exhibited a melting temperature peak that shifted toward higher temperature and narrower melting point features with the addition of GO [121].

Core-shell-structured electrospun piezoelectric PVDF NFs chemically wrapped with GO lamellae (PVDF/GO nanofibres), in which polar β-phase nanocrystals are formed and uniaxially self-oriented by the synergistic effect of mechanical stretching, high-voltage alignment, and chemical interactions, have been reported. The PVDF/GO NFs showed a desirable out-of-plane piezoelectric constant (d_{33}) of −93.75 pm V^{-1} (at 1.0 wt% GO addition), which was 426% higher than that of the conventional pure PVDF nanofibres [121]. The enhancement of the piezoelectric properties of the PVDF/GO NFs was consistent with the increase in the content of the β-phase nanocrystals and their orientation, which was contributed by interactions with the GO lamellae.

An increase in the content of the β phase and its uniaxial orientation contribute to the excellent piezoelectricity of core-shell-structured PVDF/GO NFs (Figure 3a,b). In a three-dimensional molecular model, the GO lamellae are aligned along the axis of the fibre and distributed near the surface of the NF, producing the following effects: (1) The PVDF chains, which usually exist in

the α phase, are polarised in alternating directions, resulting in nonpolar behaviour. However, here, the PVDF chains twist into a zigzag structure with CF_2 groups in the upward direction and CH_2 groups in the downward direction due to the interaction with the oxygen functionalities of the GO lamellae. (2) The mechanical stretching and electric poling from the electrospinning process result in the extension of the twisted PVDF chains and their reorientation along the fibre axis. (3) Rapid solvent evaporation also contributes to the alignment and distribution of the GO lamellae. Thus, when the PVDF nanocrystals nucleate and grow during the electrospinning process, the GO lamellae move to the surfaces of the NFs because of the internal radial orientation of the electrostatic field and the rapid evaporation of the solvents. Furthermore, Figure 3b shows the interactions that maintain the core-shell structure and β-phase orientation. The details of the π-electron delocalisation in GO and the interactions of $-CH_2/-CF_2$ dipoles of the PVDF can be found elsewhere [121]. The surface area of rGO is very important. rGO has a much higher surface than other conductive fillers, and as a result the percentage of the β phase in the polymer increases with increasing rGO content. The oxygen functionalities detected using XPS confirmed that the GO lamellae are mainly distributed near the surface of the NFs. The GO content near the NF surface was measured to be was 8.3% using a probing depth of ~10 nm; this value was much higher than the original GO content (Figure 3c, left curves). The chemical interactions of the core-shell structure were detected by analysing the vibrational modes using FTIR (Figure 3d). The C−H bending vibration band at $880 \ \mathrm{cm}^{-1}$ was strengthened by the electrostatic attraction between the delocalised π-electrons in GO and the $-CH_2$ dipoles of PVDF.
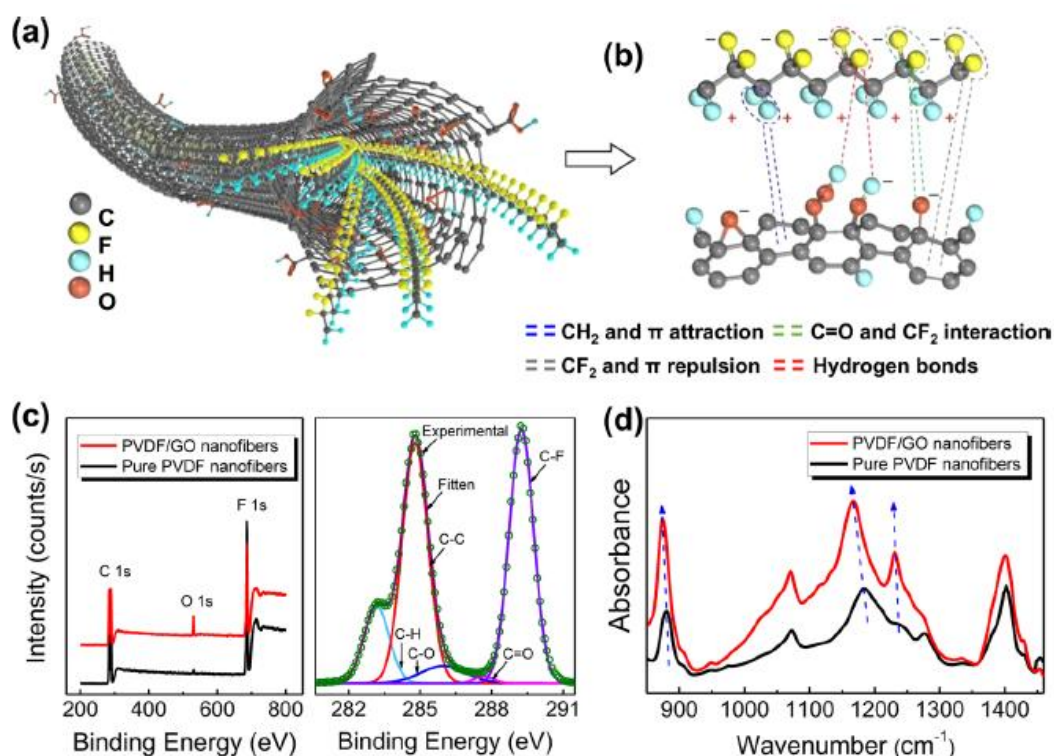
Figure 3. Structure modelling studies demonstrated excellent piezoelectricity of core-shell-structured PVDF/GO NFs. (a) Three-dimensional molecular model for the PVDF/GO NF showing the core-shell structure and the orientation of the β-phase in the PVDF core. (b) The chemical interactions between the GO lamellae and the β-phase nanocrystals of PVDF. (c) Survey spectra (left) of the PVDF/GO and pure PVDF NFs and C 1s spectrum (right) of the PVDF/GO NFs probed by XPS. (d) FTIR spectra of the PVDF/GO and pure PVDF NFs in the range 850−1450 cm^{-1}. Reprinted from [121] with the permission from the American Cemical Society.

PVDF composites with GO and Gr as nanofillers and various concentrations of halloysite (Hal) nanotubes 0.05−3.2 wt/wt%) were fabricated by electrospinning. The PVDF/Hal nanocomposite with a low filler content concentration (<0.1 wt/wt%) and the PVDF/GO with a high filler concentration (>0.4 wt/wt%) exhibited higher polar phase contents. The Hal nanotubes, which had rod-like morphology produced, more oriented and finer NFs than those of the PVDF/GO and PVDF/Gr composites. However, the PVDF/0.8 Hal composite showed a higher output voltage

(0.1 V) than the PVDF/0.8GO composite despite its lower β-phase content. Thus, it was concluded that the piezoelectric response cannot be determined only from the dielectric constant of the nanofiller and the percentage of the β-phase in an electrospun PVDF nanocomposite, but instead, other important factors such as the relative orientation and fineness of the electrospun NFs must be considered [66].

The addition of 0.1 wt% Gr increased the β-phase content in the electrospun PVDF composite NFs from 77% to 83%. However, further addition of Gr decreased the β phase content to 75%. A significant increase in the piezoelectric output of the PVDF NFs was observed when only 0.1 wt% of Gr was used. The open-circuit voltage of the PVDF NF was 3.8 V, while the addition of 0.1% Gr increased this value to 7.9 V [131].

The morphology, structure, dielectric properties, and mechanical strength of rGO nanosheet/PVDF-HFP nanocomposites were investigated [135]. The rGO nanosheets were well dispersed and strongly oriented in the matrix due to the unique spin-assisted preparation process. A dielectric constant of 54 (100 Hz), which was four times higher than that of pure PVDF-HFP, was obtained for a rGO concentration of 0.7 vol%, and the dielectric loss was as low as 0.27. The good dielectric performance of the nanocomposites was attributed to the homogeneous dispersion and good alignment of the rGO nanofillers. The shear force provided by spin-coating, the thickness decreasing process, and the thickness control were assumed to be key factors in the alignment of the rGO nanosheets in the nanocomposite films. At the same time, the aligned rGO sheets increased the percolation threshold of the composite, which indicates a pathway towards the fabrication of low-loss materials [135].

The combination of piezoelectric materials with more than two components in a piezopolymer matrix has also been studied; the synergy of the components provided even better piezoelectric responses and energy-harvesting performances. In a tri-layer PENG, an extra PVDF-BT film between the n-Gr layer and the electrode acted as a blocker to prevent the charges from recombining. Consequently, the charges are sustained at both the upper and the lower surfaces of

the n-Gr. These charges then play a vital role in the alignment of the dipoles on both sides of the n-Gr layer [126]. Additionally, the n-Gr layer also increases also the tensile stress and dielectric constant of the piezoelectric thin film, which can ultimately increase its Young's modulus and piezoelectric charge constant (d_{33}) [126]. AlO-rGO acts as a nucleating agent for the formation of the electroactive β-phase in PVDF [136]. The AlO-rGO nanosheets were well distributed over the PVDF matrix and created a conductive network structure to drain the charges towards the steel fabric electrode, which improved its piezoelectric energy harvesting properties. The PVDF/AlO-rGO-based NG exhibits excellent output without applying traditional electrical poling. The fabricated NG showed an unprecedented shift of the open circuit output voltage to a high value of ~36 V and a short circuit current of ~0.8 μA, which correspond to a power density of ~27.97 μW cm^{-3}, under repeated human finger pressure. These are the highest output values reported up to the present date for PVDF-based PENGs. When the nanocomposite fibre mats were composed of 0.15 wt% Gr nanosheets and 15 wt% BT NPs in an electrospun PVDF NF mat, the open-circuit voltage and electric power of the PENG could reach values as high as 11 V and 4.1 μW under a loading frequency of 2 Hz and a strain of 4 mm, and no apparent decline in the open-circuit voltage was observed after 1800 cycles in the durability test [27]. In addition, the PENG generates a peak voltage as high as 112 V during a finger pressing-releasing process, which coudl light 15 LEDs and drive an electric watch. The improved output of the PENG was attributed to the synergistic contribution of the BT NPs and Gr nanosheets to the piezoelectric performance of the nanocomposite fibres [27]. A scheme explaining this effect is presented in the supplementary information file (Figure S1).

1.3 Additional polarization and other ways to improve electroactive phase content

The piezoelectric constant is well-known to increase with the degree of crystallinity and the orientation of the crystallites in a polymer [137]. There is one other well-known process to increase the piezoelectric constant of a polymer, namely, poling in a high external electrical field

[138-140]. It has also been reported that poling improves the piezoelectric properties of piezo-ceramics [141-143]. To facilitate poling and to collect the piezoelectric output voltage, electrodes must be applied. These electrodes are usually in direct contact with the piezoelectric material. The electrodes should cover as much of the area of the piezoelectric material as possible. Once the electrodes have been applied, the piezoelectric sample can be poled, i.e. subjected to an electric field close to the coercive field, in either contact or non-contact mode [144]. Contact-mode poling with an electric field and heating is illustrated schematically in Figure S2. The applied external electric field strength required to achieve permanent polarization of PVDF has been reported to be 100 MV/m [144], 300 MV/m [145], 220 MV/m [146], 2.7 ± 0.1 MV·m^{-1} [35], and 20 V·µm^{-1} [147]. The poling conditions were as follows: 50 kV cm^{-1} was applied at 100 °C to PVDF-TrFE containing BTO and rGO [33]. The PVDF poled at 110 °C with an electric field of 50 MV·m^{-1} exhibited a ten-fold improvement in its d$_{31}$ compared to that of the same material poled at 25 °C with an electric field of 30 MV·m^{-1} [148]. An electric field of 2 kV was applied to an NG made of PVDF and BT NPs, and the electric field was maintained for 8 h [149].

Recently, E. Nilson et al. reported that a strong piezoelectric effect can be achieved for PVDF fibres with a conductive composite based on carbon black and polyethylene using as high a poling voltage as possible and a poling temperature between 60 °C and 120 °C [144]. This can be explained by the heating of the polymer leading to an increase in the mobility of the molecular chain and, thus, a slight reduction in the coercive field and an increase in the charge-carrier mobility. K. Arlt and M. Wegener showed how the piezoelectric strain coefficient d$_{33}$ of a piezoelectric composite film containing PZT and PVDF could be increased by long-term high-temperature (120 °C) poling at a poling field of 20 MV/m in direct contact mode [150]. Malmonge et al. observed a high piezoelectric strain constant for a film based on a PHB and PZT composite after poling at an external electric field of approximately 12 MV/m and a heating temperature of 100°C [151]. Additionally, it was found that the piezoelectric properties of the

ceramics increased significantly as the poling electric field and poling temperature are increased [141-143].

Non-contact mode poling is based on applying a high-potential corona discharge in the vicinity of the samples [152, 153]. The discharge generates ions which charge the sample surface, causing the molecular dipoles of the polymer matrix to become oriented by the applied electric field between the charged surface and its grounded counterpart [144]. Pärssinen et al. reported that a piezoelectric coefficient d_{33} of 32 pC/N was achieved for a PVDF film by corona discharge poling at 100 °C, 10 kV, and a sample-tip distance of 2 cm [154]. Additionally, it was shown that permanent polarization could be achieved in a time as short as 2 s in corona-poled PVDF fibres with carbon black and polyethylene at poling temperatures between 60-120 °C [144]. The maximum piezoelectric strain constant of the PZT/ PVDF-HFP composite after the corona discharge poling at 110°C was 25 pC/N [150]. PVDF is known to also possess a piezoelectric d_{31} coefficient. The authors of ref. [155] reported a significant increase in d_{31} from 1.0×10^{-3} pC/N to 4.8×10^{-2} pC/N after poling by corona discharge at 12 kV, but increased heating temperature reduced the piezoelectricity of PVDF due to a decrease in the β-phase content.

It was found that a material can be poled by applying a bias in excess of ∼200 V in order to promote the rotation of the polarization and full dipole reversal within a PLA fibre, and the maximum d_{33} achieved in PLA fibres was around 15 pC/N [156]. It should be noted that the crystal structure of the PLA was characterised by a helical structure, i.e. only three shear piezoelectric constants, d_{14}, d_{25}, and d_{36}, were found [157]. Thus, poling can allow the redirection of dipoles, and hence, resulting piezoelectric material can also show a compression piezoelectric constant. The poling electric field, poling temperature, and poling duration had a great influence on the performance of the piezoelectric materials. Thus, polarization plays a crucial role in improving the piezoelectric responses of piezoelectric materials such as polymers, ceramics, and hybrids.

Ferroelectric and lead-free ZTO NPs prepared using a solution casting method mitigate the alignment of the molecular CH_2/CF_2 dipoles of PVDF, promoting the nucleation of the electroactive γ-phase in the PVDF matrix (γ-PVDF), which is responsible for the generation of piezoelectricity in the PENG without any electrical poling treatment [127]. In addition, copolymerization is an effective method to tune the polymorph structure and phase transition behaviour of PVDF. A variety of VDF-copolymers and terpolymers with improved piezoelectric properties have been synthesised by incorporating trifluoroethylene (TrFE), chlorotri-fluoroethylene (CTFE), or hexafluoropropylene (HEP) comonomers [47].

Wetting PVDF into a nanoporous AAO to form a vertically aligned PVDF nanowire array significantly increased the β-phase content in the polymer, as the nanotemplate confinement-induced stress induced α-to-β phase transition in the PVDF [54, 118, 158, 159]. Additionally, the nanotemplate confinement affects the crystallization behaviour of the PVDF and aligns the polarization direction of the molecular chains parallel to the AAO nanochannels. Both of these effects were conducive to the improvement of the piezoelectric effect and energy harvesting performance in PVDF-based PENG. The mechanical stretching during processing provided PVDF fibres with a piezoelectric β-phase content of up to 97%, as determined using FTIR spectroscopy [35].

Completely biodegradable flexible DNA-PVDF films were prepared by a simple solvent-casting method. The nucleation of the electroactive β- and γ- phases was induced and intensified by the presence of single-strand DNA without any electrical poling. This phenomenon can be explained by electrostatic interaction and H-bonding models [160].

In PVDF films produced by the phase inversion technique, the β-phase content increases rapidly as the quenching temperature is reduced, with a nearly pure (~100 %) β-phase being obtained at -20 °C. The β-phase crystals were self-aligned and polarised, and the films showed an abnormally high piezoelectric coefficient of up to -49.6 pm·V^{-1}. Fast quenching at low temperature induced a strong thermal field gradient, which caused the crystals to align along the thermal field direction.

The interaction with polar water is one possible reason for the alignment of the β-crystals [120]. The O–H groups of the water molecule could form hydrogen bonds with the C–F groups of PVDF, leading to the emergence of their orientation [161, 162].

1.4 Size-dependent effects

Piezoelectric polymers and their copolymers are well-known to exhibit much lower power outputs than those of inorganic piezomaterials, which are insufficient to operate self-powered electronics (e.g. sensors, NGs, etc.) continuously. To address this issue, many research groups have been focusing on enhancing the efficiency of the piezoelectric conversion from mechanical to electrical energy. Strategies such as the hybridization of the piezoelectric polymer matrix by adding highly piezoelectric inorganic and conductive fillers to the matrix have been widely adopted to impart flexibility and robustness with good performance. Further processing of the piezopolymer or hybrid composite by thermal or electrical poling can lead to a significant increase in the piezoelectric properties compared to the conventional performance of bulk or thin films. Additionally, it is known that the piezoelectric effect can be enhanced by fabricating a material into nano- or micro-structures. Since the first ZnO nanowire-based NGs were demonstrated in 2006 [163], multiple studies have been conducted using various piezoelectric micro/nanostructures for self-powered systems due to their size effect, higher mechanical flexibility, better strain confinement, and higher sensitivity to small forces.

PVDF has attracted significant interest due to its relatively large remnant polarization values, high piezoelectric voltage constants, low dielectric constants, and high chemical stability. Various kinds of PVDF-based and PVDF-ceramic-based micro/nanostructures, such as porous films [164, 165], electrospun NF mats [23, 26, 166, 167], and trigonal line-shaped and pyramid-shaped films [168], have demonstrated enhanced output compared to conventional bulk films, as have nanowires (pillars) prepared *via* nanoconfinement in AAO [169, 170]. Table 3 summarises the main output parameters of various structured polymer-based composites. It should be

mentioned that all the presented works report an improvement of the piezoelectric response for films that are structured rather than flat; however, the results of these studies cannot be compared directly due to the different approaches, frequencies, and applied mechanical stresses used.

Wang and Cha et al. [164] first introduced porous PVDF NGs fabricated via a template-assisted method. The porous PVDF NG produced a rectified power density of 0.17 mW/cm^3, and the piezoelectric potential and the piezoelectric current were 5.2 times and 6 times higher than those obtained for the bulk PVDF film under the same sonic input. Additionally, the decreased interpore distance led to an increase in the d_{33} value of the porous PVDF film [164]. Recently, Chen et al. demonstrated that the piezoelectric output increased 100% for a modified mesoporous PVDF layer compared to the that of the bulk film, despite the slightly lower crystallinity of the mesoporous sample [165]. The author of the study [165] mentioned that the piezoelectric performance could be doubled with a well-controlled porous film, as shown in Figure S3.

Several studies have reported the fabrication and characterization of vertically aligned nano- and micro-structured piezoelectric polymers; the low stiffness of such nano- and micro-scale pillar arrays makes their fabrication extremely difficult [171]. PVDF-TrFE nanotubes synthesised with the nanoconfinement effect were reported to give a greater piezoelectric d_{33} coefficient value (44 pm·V^{-1}) than poled films (20 pm·V^{-1}) [172]. This can be explained by the fact that the confinement allows the formation of the polar axes of the polymers along the nanotubes (pillars), i.e. confinement initiates a kinetic selection mechanism for the lamellar growth of this desired crystal orientation of the polymer [170]. The mechanisms of the growth of polymer crystals in nanotubes have scarcely been studied.

Piezoelectric polymer fibres fabricated using the electrospinning technique have also shown a significantly enhanced piezoelectric response compared to that of the non-structured films. The authors showed that a PVDF electrospun mat could generate up to 20 V of output voltage depending on the pressure and frequency [173]. Recently, Shi et al. demonstrated that the power

output of the PVDF NF mat could be increased almost three times in comparison with pristine PVDF NF mat by the addition of 0.15 wt% Gr nanosheets and 15 wt% BT NPs [27]. The authors of the study in ref. [174] also observed an output voltage increase of 300% after the addition of ZnO into PVDF electrospun fibres.

In addition to the above-mentioned structurisation methods, micropatterned polymer films, such as films with trigonal line-shaped and pyramid-shaped micropatterns, have also been fabricated [168]. Ju-Hyuck Lee et al. reported that trigonal line-shaped and pyramid-shaped PVDF-TrFE films showed significantly higher output voltage than flat PVDF films; the trigonal line-shaped PVDF-TrFE films showed a voltage of 4.4 V, while the flat PVDF-TrFE had a voltage of 1 V [168]. The influence of micropatterning on the piezoelectric performance can be explained by the increase in the compressive strain [168].

Table 3. A summary of the output parameters of polymer-based composites with different structures.

Structure	Composition	Piezoelectric coefficient, pC/N or pm×V^{-1}	Surface electric potential, V	Reference
Non-structured film	PVDF	-14, -15, -20	0.4, 0.7, 2	[117, 168, 170, 175]
	PVDF-TrFE	-17, -20	0.35, 0.8	[168, 170, 173]
	PLLA	10	-	[176]
Porous film	PVDF	-32.5	2, 2.6	[164, 165]
NFs	PVDF		3, 20	[23, 167]
	PVDF-0.15 wt% BT-0.15 wt% rGO	-	~12	[27]
	PVDF-2 wt% cellulose	-	~60	[177]
	PLLA	15	-	[156]
Nano-pillars (Nanowires)	PVDF-TrFE	-35, -44	4.8	[170, 172]
Trigonal line-shaped film	PVDF-TrFE	-	~4.4	[168]
Pyramid-shaped film	PVDF-TrFE	-	~3.8	[168]

The electric power output from piezoelectric generators based on structured hybrid composites is greater than that of the pristine polymer-based PENGs and PEMGs; however, the preparation of polymer composite-based PENGs/PEMGs still presents problems, such as a complex fabrication process, poor reproducibility, non-uniform power output, low economic effectiveness, and the difficulty of controlling the interface between the inorganic nanostructures and the polymer matrix. The development of simple and low-cost approaches to improve the electric power output of polymer-based PENGs/PEMGs without forming complex composite structures would be promising for the fabrication of various self-powered device applications.

2 Biomedical devices and sensors based on hybrid piezocomposites

Lead-based perovskite ceramics, namely PZT and PMN-PT, are piezoelectric materials that are widely used for energy harvesting devices [3, 178-181], low-power personal electronics [3, 178, 182], and self-powered biomedical nanosensors [178-181, 183]. Piezoelectric NGs with PZT and PMN-PT based mechanosensing elements demonstrate the best device features and capabilities, which originate from the piezoelectric d_{33} constants of PZT and PMN-PT, which are the greatest among all conventional piezoelectric materials [3], combined with effective sensor morphology. For example, a large-area PZT-based NG with an active area of 1.5×1.5 cm^2 was fabricated by synthesizing a PZT film using laser lift-off and transferring it to a flexible substrate, and provided a voltage of ~200 V and a current of ~1.5 µA under bending deformation [7]. Another device consisting of PZT nanoribbons with a total area of ~22 mm^2 and serpentine connections showed the highest sensitivity of ~0.005 Pa and a fast response time of ~0.1 ms [184]. An extremely sensitive mechanosensor with an active area of 1×2.5 cm^2 fabricated by depositing PZT nanoribbons onto a silicon substrate was capable of detecting the deformation of a single living cell at the nanoscale (~1 nm) [185]. While PZT-based devices exhibit high voltage but a low output current of below 10 µA, which is not sufficient for consumer electronics, piezoelectric harvesters based on PMN-PT

ceramics, which have an extremely high piezoelectric charge constant [3], can provide output currents on the microampere level. As the best example, a flexible single-crystal PMN-PT thin film NG with dimensions of 1.7×1.7 cm^2 on a thin plastic substrate yielded a current output of 0.22 mA under light finger tapping [186]. The use of PZT and PMN-PT based mechanosensing elements has been demonstrated for piezoelectric NGs, including energy harvesters for bodily motion [3, 178-180, 182], for monitoring pulse signals, sounds, and touches [179, 180, 183], and for biomedical applications such as direct stimulation of the living heart [180], measurements of the mechanical properties of soft tissues and organ systems [179], and energy collection from organ motions [178, 180].

However, despite their favourable device characteristics for implantable electronic applications, the biocompatibility of PZT and PMN-PT elements is rather low due to the presence of lead oxide, which presents a toxicological risk in the biological context. A shift towards piezoelectric organic materials (PVDF and its co-polymer PVDF-TrFE) and lead-free inorganic ceramics (BT, LiNbO$_3$, ZnO, MgO, hydroxyapatite, KNN, and lithium sodium potassium niobate (LNKN)) has been made with the aim of creating lead-free physical sensors for biomedical applications [1, 178-180, 183, 187]. Significant progress has been reported in the development of energy harvesters [1, 3, 178, 180, 182], pressure, strain, and temperature sensors [178, 179, 183], and the creation of biomedical materials and scaffolds for tissue engineering and stimulating cell growth [1, 179, 188]. Despite these advances, lead-free piezoelectric sensing elements typically provide poorer performance compared to lead-based ones [1, 3, 47, 178-180, 182, 183, 187-193], even in the best case of a powerful curved piezoelectric NG based on PVDF film layers, which exhibited a peak output voltage of ~155 V and a peak output current of ~700 µA (~25 µA/cm^2 of current density) under finger tapping [194]. In comparison, a piezoelectric generator (active area 1 cm^2) based on an Fe-doped BT nanopillar array (diameter ~120 nm, pitch 400 nm, height ~400 nm) demonstrated an output voltage and current density that exceeded ~10 V and ~1.2 µA/cm^{-2} respectively in response to an applied force of 0.3 MPa [195]. Another piezoelectric sensor for motion and temperature

monitoring (area 1×5 cm^2) based on an Li-doped ZnO nanowire array (average length ~20 μm, diameter ~700 nm) generated an output voltage of 6.7 V under an applied pressure of 0.3 MPa and a maximum motion frequency of 5 Hz [196].

In this regard, the incorporation of inorganic piezoelectric fillers in flexible piezopolymer matrices has been considered as a new pathway towards improving the characteristics of NGs to achieve high sensitivity and wide-range responsiveness while preserving the flexibility and light weight of such devices [1, 3, 47, 178, 179, 183, 188, 197, 198]. In this review, we focus on non-biodegradable hybrid piezocomposites developed from 2014 to the present with potential or demonstrated uses in biomedical devices and sensors, including implantable NGs and stimulatory materials for wound healing and tissue regeneration.

2.1 Mechanosensors, gas sensors, and energy harvesters

In the last few years (2014-2018), great progress has been observed in the development of hybrid piezopolymer-based materials with improved electroactive properties, but only a limited number of studies have demonstrated the use of hybrid piezomaterials in biomedical applications, such as monitoring of biomechanical motions and human vital signs, voice detection, and the measurement of levels of biochemical species in the human body. Typically, the polymer PVDF or its copolymer PVDF-TrFE is chosen as the piezopolymer matrix and loaded with metal oxide NPs, ceramics, Gr derivatives, or a mixture of these, in order to create a hybrid piezocomposite for use as the sensing element for high-output NGs and biomedical sensors [199].

A hybrid free-standing ZnO/PVDF film was demonstrated to be a highly sensitive sensor for independent temperature and pressure monitoring [200]. A nanocomposite film with a thickness of 80 μm, which is only 15% of the thickness of the human epidermis, was loaded with vertically grown ZnO NRs ~300 nm in length and ~85 nm in diameter (Figure S4a) to form a 1D array. The density of the ZnO nanostructures was high (1.42×10^{10}) cm^{-2}. In the presence of the ZnO filler, the

β-phase content increased to 85%, while that of commercially available PVDF was only 73%; the increased content of the β-phase enhanced the piezoelectric and pyroelectric responses of the hybrid film. An assembled device with an overlap area of 6×6 cm^2 demonstrated excellent pressure-sensing capabilities, with a smallest detectable pressure of 10 Pa. Moreover, it was able to detect temperature in the range 20–120 °C independently of the pressure measurement. Its simultaneous pressure and temperature sensing abilities were associated with the dipole alignment originating from the vertically grown ZnO NRs and the enriched content of the β phase in the hybrid nanocomposite film. Potentially, such a sensing element could be used as a multifunctional tactile gauge sensor.

In another study [201], PVDF and tetrapod ZnO nanostructures were hybridised on a flexible fabric substrate with an area of 20×7 cm^2 (Figure S6a). The ZnO tetrapods exhibited a very smooth surface, four legs of ~2 μm in length, and a diameter of ~50 nm (Figure S4b), and were uniformly distributed over the whole network and formed a nanoarray structure on the fabric because of their unique 3D geometry (Figure S5a). The developed material demonstrated piezoelectric, photocatalytic, and gas-sensing properties; moreover, the piezoelectric/photocatalytic and piezoelectric/gas-sensing abilities were coupled. The hybrid fabric was tested to measure its bending angle, exposed to different O_2 concentrations and various levels of relative humidity, and was also tested as a self-cleaning material under UV/ultrasonic irradiation. It was demonstrated that the developed flexible e-skin could be used for the detection of the rates of human motions, such as elbow bending (Figure 4a) or finger pressing, and could be extended to other bodily vibrations such as breathing or heartbeat. As an atmosphere sensor, the hybrid material demonstrated a nonlinear response to O_2 in the concentration range 20–50%, while its response to humidity was linear between 55% and 85% (Figure 5). The proposed e-skin can also degrade many kinds of organic pollutants and sterilise bacteria on its surface.
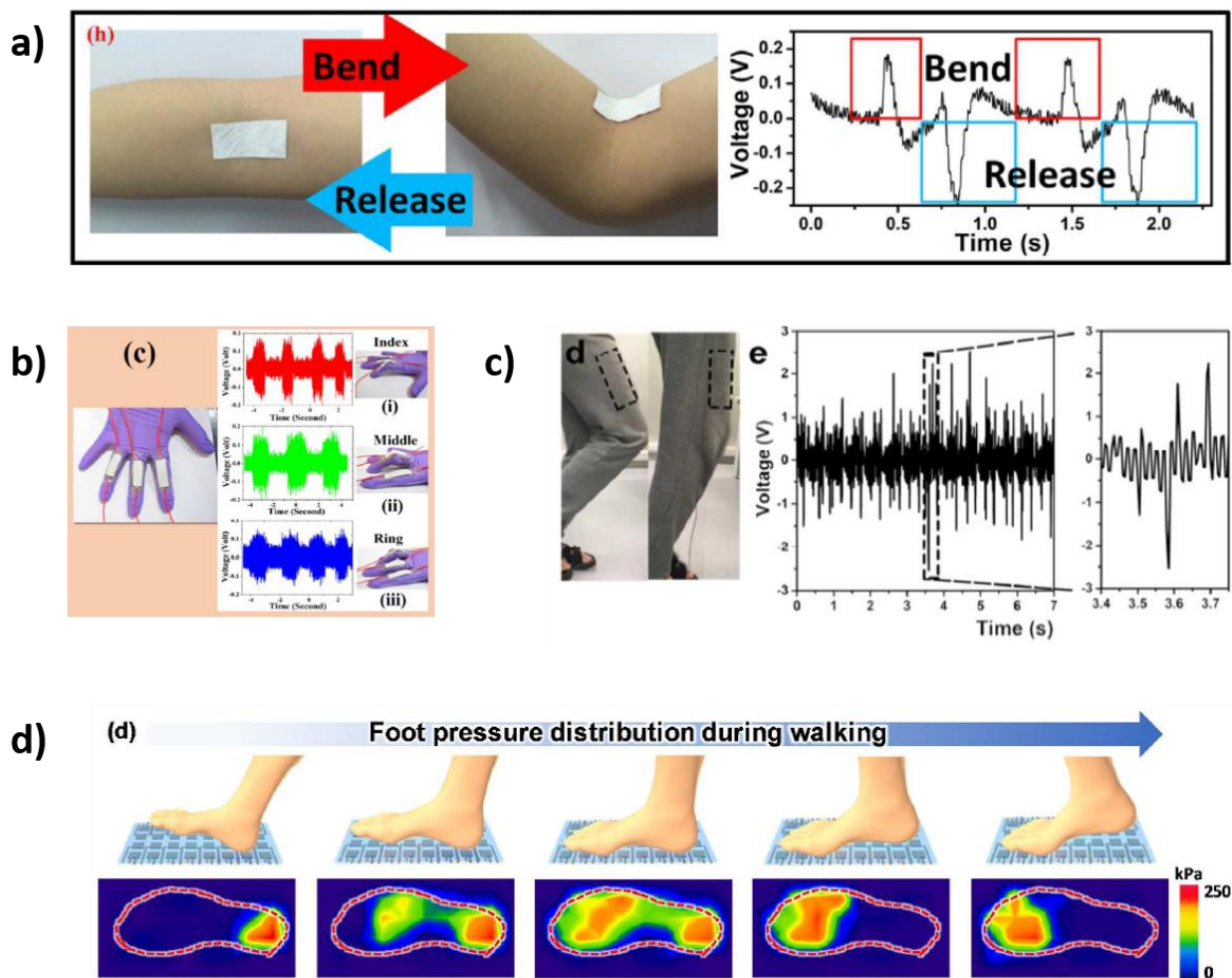
Figure 4. Human motion detectors: (a) elbow bending and releasing [201], (b) bending of the index, middle and ring fingers [59], (c) distinguishing the landing moments of legs [202], (d) plantar pressure measurements [203]. Reprinted with the permission from the American Chemical Society

The incorporation of Co-doped ZnO nanofillers enhanced the nucleation and stabilization of the piezoelectric polar β-phase [19]. A comparative study of flexible nanogenerators manufactured from Co-doped ZnO/PVDF-HFP and ZnO/PVDF-HFP electrospun composite NFs showed that a 2 wt% loading of Co-doped ZnO NRs provided the highest piezoelectric output voltage of 2.8 V under a constant tapping force of 2.5 N and a frequency of 50 Hz due to an increased β-phase content of 54.6% [19]. These hybrid nanofibres could potentially be used in self-powered devices for wearable electronics and in the biomedical field.

Another flexible piezoelectric energy harvester was fabricated from a nanocomposite film containing 2 wt% of <50 nm MgO NPs embedded in PVDF-TrFE. The film had a thickness of 20 ± 2 μm and an area of 7×7 mm^2 [58]. The nanocomposite device exhibited an output voltage of 2 V, which was more than twice the output voltage of 0.9 V generated by the pure PVDF-TrFE film. The improvement in the electrical properties of the MgO-loaded piezopolymer film was associated with the increased crystallinity of the film and β-phase stabilization, which increased the piezoelectric coefficient d_{33} by nearly 50% to a value of −65 pm/V, as compared to −40 pm/V for the pure PVDF-TrFE. In practical demonstration as a touch sensor, the piezocomposite film generated a voltage of ~0.4 V upon repeated finger tapping.

A hybrid nanocomposite film of silica-coated NiO NPs loaded in PVDF 200 μm in thickness and 1.6×2.5 cm^2 in area was fabricated as a piezoelectric NG and demonstrated e-skin properties [59]. The incorporation of the NiO@SiO$_2$ nanofillers led to an 80% increase in the β-phase content at 15 wt% NPs, which improved the piezoelectric and dielectric properties of the hybrid nanocomposite. In the static regime, the sensor was capable of measuring very low pressures in the range from 0.1 kPa to 1.2 kPa with a high sensitivity of 26.58 MPa^{-1}. In dynamic conditions, the developed self-powered e-skin was used to monitor variable pressures at low values from 10 kPa to 35 kPa with a good dynamic pressure sensitivity of ~0.97 V kPa^{-1}. The e-skin sensor precisely detected the stretching and bending motion of the index, middle, and ring fingers (Figure 4b), which would be useful for the monitoring of bed-bound patients in a healthcare setting, as well as for controlling the hands of surgical robots.
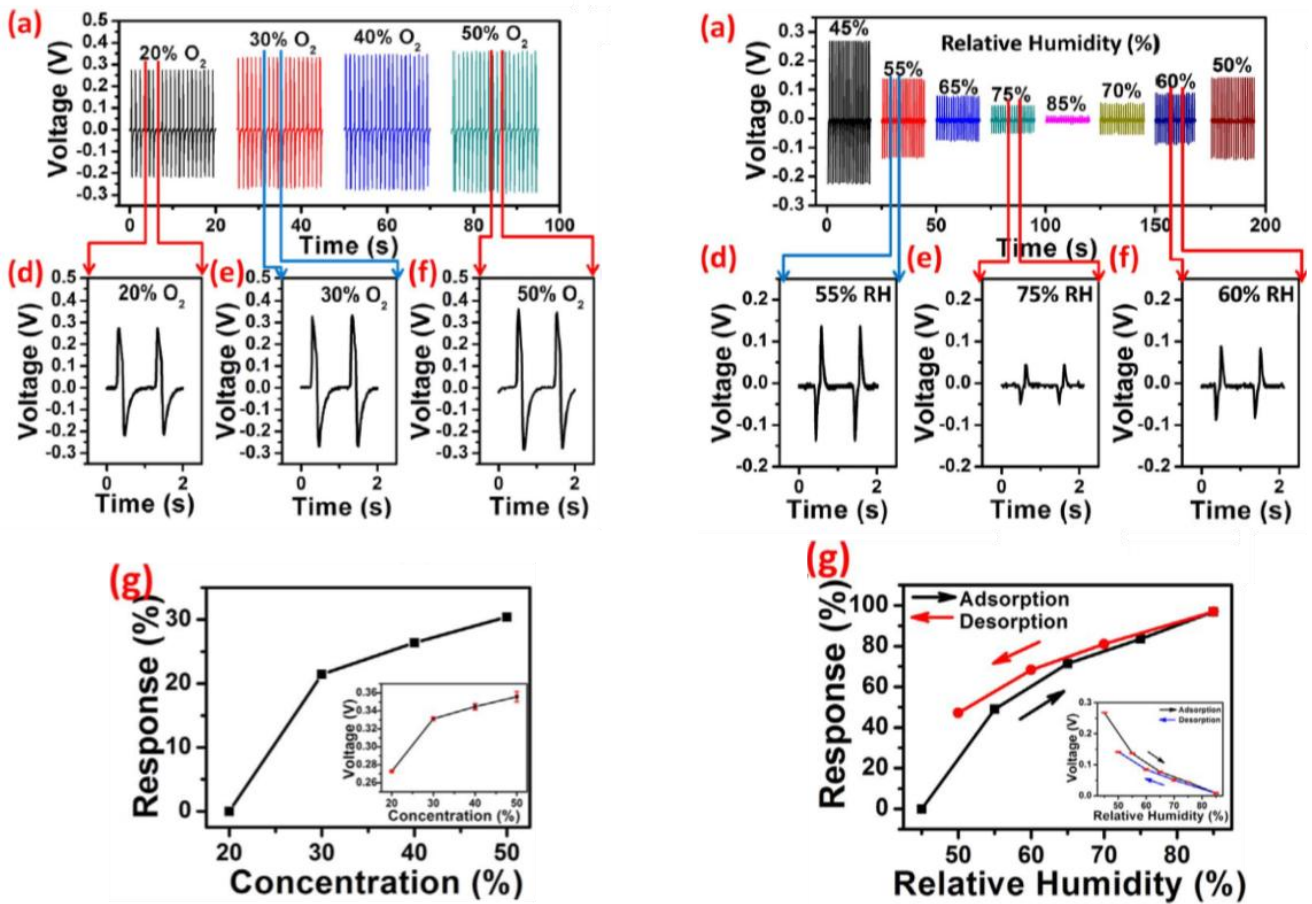
Figure 5. Detection of atmospheric conditions such as O_2 concentration and relative humidity. Reprinted from [201] with the permission from Elsevier.

Another high-performance energy harvester was fabricated using a TiO_2-loaded PVDF NF mat [91]. The electrospun mat was 250 μm in thickness and 9.0×7.5 cm^2 in area. The presence of 0.5 wt% TiO_2 NPs with an average diameter of ~20 nm (Figure S4c) efficiently increased the β-phase content to 93% in the composite NF mat (compared to 77% for the unloaded NF mat) and improved its mechanical properties, with the Young's modulus increasing ~129% to 22 N/mm^2. Because of the improved piezoelectric properties, an open-circuit output (peak-to-peak) voltage of 11.5 V was obtained under compression by a human finger with a force of ~5 N in the vertical direction, while the sensitivity of the acoustic to electrical energy conversion was found to be as high as 26 VPa^{-1}. The energy harvesting ability of the fabricated NG was demonstrated for the swinging motion of the hands (arm) and legs (foot) during walking and running in a normal jogging procedure, from the

motions of the extremities during running, and from a speaker. Altogether, this indicates that the developed piezoelectric NG could be useful for human motion detection and noise pollution monitoring.

Ceramic fillers with piezoelectric properties, such as BT NPs, are also used to amplify the piezoelectric response of composite polymer materials. For example, BT NPs with an average diameter of 200 nm were loaded into a PVDF matrix, and NFs were fabricated to test their performance as piezoelectric generators [10]. First, a 20 wt% BT/PVDF planar NF mat with an active area of several tens of cm^2 and a thickness of 100 μm was shown to generate an open-circuit voltage of ~8 V and a short-circuit current of ~50 nA under a 10 mm bending displacement. Subsequently, a microstructured piezoelectric fibre was fabricated using the fibre drawing technique from a macroscopic preform of ~10 alternating piezoelectric-conductive layers obtained by sandwiching two BT/PVDF NF mats between two carbon-impregnated low-density polyethylene films (thickness: 85 μm) and rolling the layers. The piezoelectric fibre had a length of 10 cm and a diameter of ~1 mm, and provided an open-circuit voltage of ~1 V and a short-circuit current of ~0.7 nA under the same 10 mm bending displacement during cyclic bending with a frequency of 0.1 Hz. A piezoelectric textile made of four piezoelectric fibres with a length of ~15 cm and a diameter of ~1 mm that were woven into cotton fabric and connected generated an open-circuit voltage of up to ~5 V and a short-circuit current of up to ~10 nA in response to repeated irregular tapping and releasing by the human hand. In the second case, the piezoelectric fibre was glued onto the exterior of an airplane model to demonstrate its energy harvesting properties, and generated an open-circuit voltage of 2 V at the maximum rotation speed of the airplane motor.

This research was continued in ref. [9], in which a comparative study of the piezoelectric performance of multimaterial NFs fabricated through drawing a fibre from the BT/PVDF composite (average BT NP diameter: 200 nm), PZT/PVDF (particle size: 10-50 μm) and MWCNTs dispersed in PVDF was performed. The experiments showed that a 10 cm long fibre made of 20 wt% BT loaded in the PVDF matrix provided an open-circuit voltage of 1.4 V and a short-circuit current of

0.8 nA with a 10 mm transverse displacement of the tip. In comparison, the PZT/PVDF NF generator (PZT content: 20 wt%) generated ~6 V and ~4 nA, whereas for the MWCNT/PVDF NF (0.4 wt% MWCNT), the measured voltage and current were ~3 V and ~1.2 nA (Figure S6b), respectively. A fabricated MWCNT/PVDF fibre 10 cm in length was shown to be applicable for surface and underwater sound detection. In open air, the fibre generated an output voltage in the range of 50 to 70 mV in response to a sound pressure level of 0.2 mPa at 1 Hz, while underwater, the registered piezoelectric response reached ~0.37 V at a distance of ~20 cm from an ultrasound source with acoustic power of 8 W at a frequency of ~20 kHz. The piezoelectric BT/PVDF textile generator was utilized as a tactile or motion sensor with an open-circuit voltage of up to ~10 V and a short-circuit current of up to ~15 nA under a 90° bending-release action of the human elbow. For energy harvesting, a textile made of fifteen 20 cm long fibres was used as the seat pad of a vehicle under a 22 kg sandbag load. This generator could charge a capacitor from 0 to ~0.3 V during a 10 min period of urban road driving under regular traffic conditions.

In another study, a piezoelectric nanocomposite film consisting of a PVDF-TrFE polymer matrix with a high 40 wt% loading of BT NPs with an average diameter of 100 nm showed an output voltage of 9.8 V and a current density of 1.4 $\mu A/cm^2$ under cyclic bending [73]. This good performance was achieved due to the combined effect of the high crystallinity of the PVDF-TrFE matrix and the high loading fraction of the nanofillers. An NG based on this material with a tapping area of 12 mm^2 provided an open-circuit voltage of 1.3 V under a constant pressure of 0.5 N/mm^2 with a tapping frequency of 3 Hz. Since a significant peak open-circuit voltage of 7.5 V was registered from a slight movement of the index finger joint, this piezoelectric material could be used as a highly sensitive element for monitoring body movements and as an energy collector for self-powered biomedical sensors and devices.

A piezoelectric-enhanced nanocomposite micropillar array of BT-loaded PVDF-TrFE was demonstrated to be an efficient energy harvester and a highly sensitive pressure sensor (Figure S6c)

[204]. The highest piezoelectric response was obtained using a 20 wt% loading of BT NPs with a rounded shape and an average size of 200 nm. Figure S7 reveals the simulated piezoelectric potential at the top of the two surfaces. The peak voltage of the micropillar array reached 13.1 V, while the output voltage of the bulk film had a lower value of 1.85 V. The simulated results showed that the piezoelectric potential of the micropillars was much higher than that of the flat film, which is in accordance with the experimental data. Thus, the higher strain produced a larger piezoelectric signal, generating a higher voltage for the micropillar-based PENGs [204]. A sensor was fabricated using a nanocomposite film 1×1 cm^2 in area and 60 μm in thickness containing vertically aligned micropillars with an average diameter of 22 μm and a height of 55 μm. This geometry resulted in improved mechanical flexibility in addition to enhanced piezoelectricity of the nanocomposite material, with a measured d_{33} value of 35.3 pC/N in comparison with the value of 14.6 pC/N obtained for the pristine PVDF-TrFE film. Under a mechanical pressure of 0.5 mPa, the piezoelectric NG achieved an average output voltage of 13.2 V, while finger-bending led to a high output voltage of 20-25 V. Due to its enhanced piezoelectric properties, this sensor could be used for pressure monitoring in non-contact mode, such as air flow pressure. Furthermore, it can be fixed on the chest to monitor the respiratory cycle and identify deep-breathing, gasping, laboured breathing, and normal breathing modes (Figure 6a).

To further improve the piezoelectric NG performance, a 1D–3D fully piezoelectric nanocomposite with an active layer thickness of ~50 μm based on BT nanowire-embedded PVDF-TrFE was developed [49]. The BT nanowires had an average length of 4 μm and an average width of 150 nm. The maximum output characteristics of the flexible hybrid NG were found to be ~14 V for voltage and ~4 μA for the current signal under bending stimulation. When attached to the back of the hand, the NG device provided an output voltage and current of up to ~8 V and ~900 nA via clenching and releasing the hand, and three small capacitors connected in parallel were charged to approximately 3.5 V.
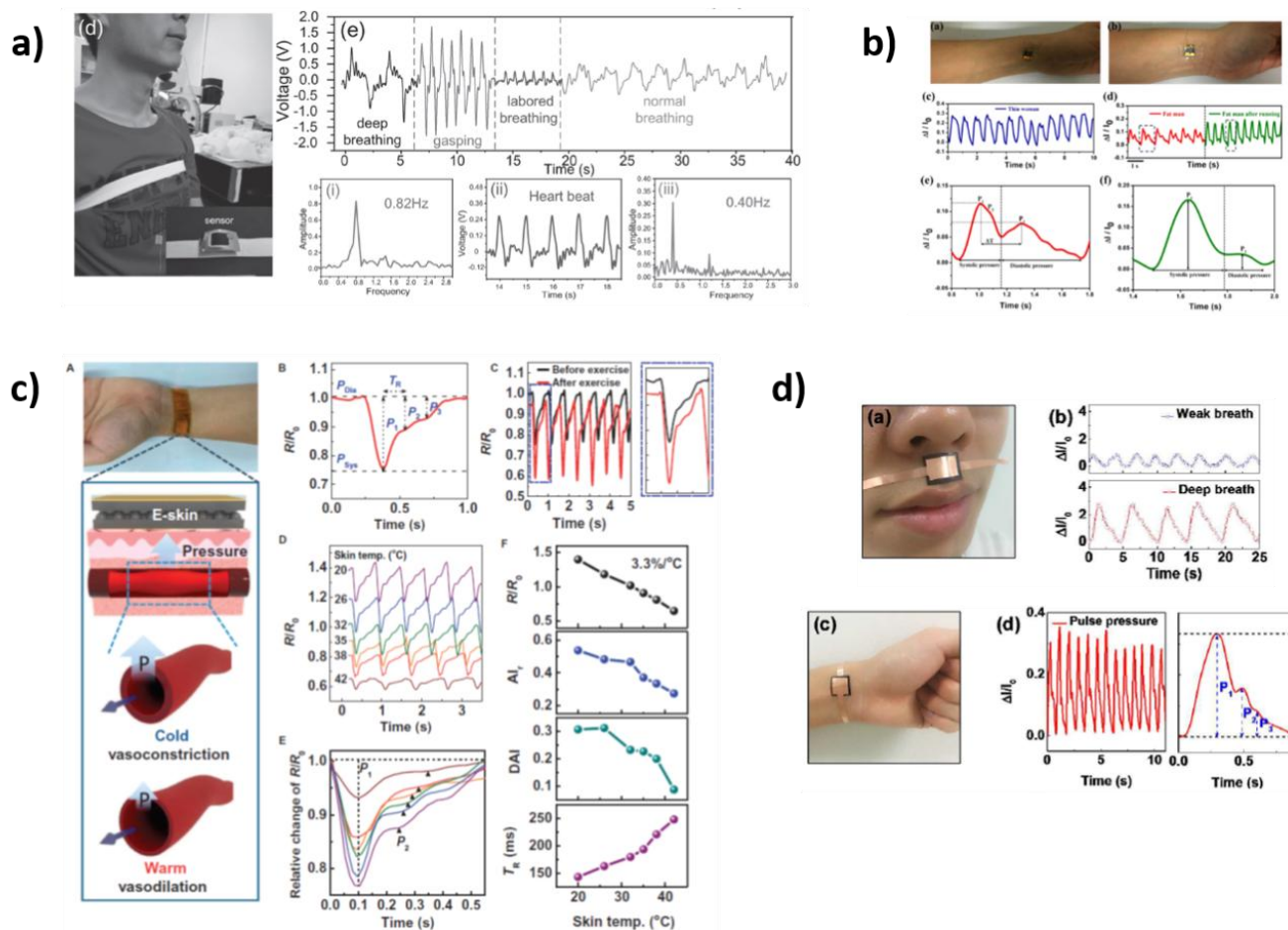
Figure 6. (a) Identification the different breathing modes, labored breathing is additionally enlarged [204] (Reprinted with the permission from Wiley), (b) monitoring of wrist pulse under normal and exercise conditions [205], (c) heart beating and breathing monitoring: simultaneous monitoring of artery pulse and temperature [206], (d) monitored weak and deep breathing and pulse signals [203] (Reprinted with the permission from the American Chemical Society).

A hybrid film of $BaTi_{0.9}Zr_{0.1}O_3$ nanocubes (typical size: 200 nm) dispersed in PVDF at a concentration of 25 wt% were presented as a self-powered sensor for remote monitoring and control applications [55]. Importantly, the average piezoelectric response d_{33} for $BaTi_{0.9}Zr_{0.1}O_3$ at a Zr content of less than <0.1 was measured to be 285-290 pC/cm^2, which was almost twice as high as the BT bulk piezoelectric coefficient of 150 pC/cm^2. Due to the increase in the average piezoelectric

response d_{33}, a developed piezocomposite NG with an area of 2.5×2.5 cm^2 showed an enhanced electrical output of up to ~11.9 V and ~1.35 μA during cyclic push-release cycles with a constant load of 11 N. In comparison, the BT/PVDF NG had an output of 7.99 V and 1.01 μA. The NG sensitivity was tested by repeated gentle tapping with a finger of the right hand, and the generated piezoelectric potential reached up to 4 V. As a water velocity sensor, the hybrid NG could operate at high fluid temperatures of up to 120 °C and over a wide pressure range up to a value corresponding to a water velocity of 125.7 m/s.

A NF nonwoven fabric made from randomly oriented PVDF-based fibres (diameter: 132-714 nm), with a 5 wt% loading of NaNbO$_3$ nanowires with a uniform diameter of ~30 nm, and variable lengths of several microns (Figure S4d) was developed as a novel active piezoelectric component [207]. SEM, TEM, FTIR, and XRD data revealed that the NaNbO$_3$ nanowires were embedded in PVDF in a uniform and fine manner, forming a NaNbO$_3$/PVDF NF core-shell structure (Figure S5b), while the electrospinning process promoted β-phase formation. A composite NG with effective dimensions of $2.5 \times 2.5 \times 0.2$ cm^3 produced a peak open-circuit voltage of 3.4 V and a peak current of 4.4 μA under a series of dynamic impact force pulses with a frequency of 1 Hz and a pulse pressure 0.2 MPa, which is comparable to the normal human walking motion.

A synergistic piezoelectric response was obtained using K$_{0.5}$Na$_{0.5}$NbO$_3$-BT/PVDF composite films fabricated for use as a flexible and planar energy harvesting device [31]. The substitution of lead-free BT NPs into the K$_{0.5}$Na$_{0.5}$NbO$_3$ lattice up to a content of 0.02 improved its piezoelectric properties while preserving the K$_{0.5}$Na$_{0.5}$NbO$_3$ orthorhombic phase. A film fabricated by dispersing the 0.98K$_{0.5}$Na$_{0.5}$NbO$_3$-0.02BT nanocomposite in PVDF provided a high open circuit voltage of ~160 V and a current of ~400 nA under a constant mechanical force of ~0.4 N. A piezoelectric generator based on this nanocomposite material with a thickness of ~121 μm and an area of 3×3 cm^2 exhibited a maximum generated peak-to-peak voltage of 16 V, 12 V, and 9 V in response to the motion of a motorcycle, bicycle, and a human leg moving forward and backward, respectively.

rGO is often used as a nanofiller to improve the electrophysical properties of piezopolymer matrices. A flexible and large-area nanocomposite film (20×15 cm^2) of PVDF loaded with 1 wt% of rGO sheets was obtained as a multifunctional e-skin [206]. The piezoresistive and ferroelectric properties of the fabricated piezomaterial were improved not only by the presence of rGO, but also by the specific geometry of the composite layer, which had the form of an interlocked microdome array (Figure S6d). The prepared e-skin was capable of detecting static pressures as small as ~0.6 Pa, and was sensitive to air flow pressure variations from 0.6 to 2.2 Pa. For dynamic touch, the efficiency of the normal force to current conversion was 35 µm/Pa at pressures below 2.45 kPa and 5 µm/Pa in the pressure range of 2.45-17.15 kPa. A proof-of-concept for the monitoring of wrist pulse pressure depending on skin temperature using this material was demonstrated. Change in the skin temperature leads to vasodilation or vasoconstriction, and thus temperature-dependent pressure monitoring of the artery vessels was achieved based on the measurement of the variation in the relative resistance (R/R_0). The detectable parameters were the difference between the systolic and diastolic pressure (P_1), the radial artery augmentation index ($AI_R = P_2/P_1$), radial diastolic augmentation ($DIA_R = P_3/P_1$), and round-trip time of a reflected wave from the hand periphery (T_R) (Figure 6c). The sound detection capabilities of the material were also tested by monitoring the acoustic waveforms generated by a speaker. Various letters of the alphabet, and then a well-known quotation of R. Feynman, were played to the e-skin, which was able to monitor the full sentence (Figure 7a). Additionally, fingerprint-like patterns were made to test texture perception, and the surface texture recognition of different surfaces was demonstrated.

The flexible e-skin developed in ref. [206] was later improved by increasing its rGO concentration to 2 wt% and fabricating an optimized multilayer structure with three layers of interlocked microdome arrays [203]. Interestingly, for rGO loadings above 0.5 wt%, the α-phase disappeared or was not detectable by X-ray diffraction spectroscopy analysis. The patterned mould used for the preparation of a single layer provided microdomes ~10 µm in diameter and ~4 µm in height with a ~12 µm pitch. The intermediate adhesive layers had approximately the same thickness as a single

nanocomposite film. The multilayer e-skin exhibited linear pressure-sensing capabilities with an ultrahigh sensitivity of 47.7 kPa^{-1} over an exceptionally broad range of pressures from 0.0013 to 353 kPa. This flexible multilayer sensor could be efficiently used as a wearable healthcare device for motions in the medium-pressure regime, such as human breathing and wrist pulse, in applications such as the diagnosis of sudden infant death syndrome (Figure 6d). In the low-pressure regime, it could also be used to detect weak gas flows and acoustic sounds. Finally, in the high-pressure regime, the multilayer e-skin acted as a sensor for plantar pressure (Figure 4d), as it is known that abnormal gait patterns and excessive foot pressure in certain areas may cause diseases such as diabetic foot ulcers, and patients with Parkinson's disease demonstrate representative gait patterns that noticeably differ from normal gait patterns.

Another high-sensitivity pressure sensor for e-skin and health monitoring was fabricated by synthesizing a uniform 3D network composite film of electrospun PVDF-TrFE NFs wrapped with rGO nanosheets [205]. The produced sensing film was 1.3 mm in height, 0.7 cm in width, and 1.4 cm in length. As a static pressure detector, it showed a high sensitivity of 15.6 kPa^{-1} for applied pressures greater than 20 kPa. Moreover, in the low-pressure regime from 0 to 60 Pa, excellent linear response was observed with a sensitivity of 3.1 kPa^{-1}. In the dynamic regime, the sensor showed the ability to measure bending and torsional forces, thus enabling monitoring of the wrist pulse in real time under normal and exercise conditions, with fine recognition of small differences in blood pressure (Figure 6b). In addition, it demonstrated the ability to recognise speech through the capture of subtle muscle movements (Figure 7b). Its ability to map and identify the spatial pressure distribution was also tested for e-skin technological applications.
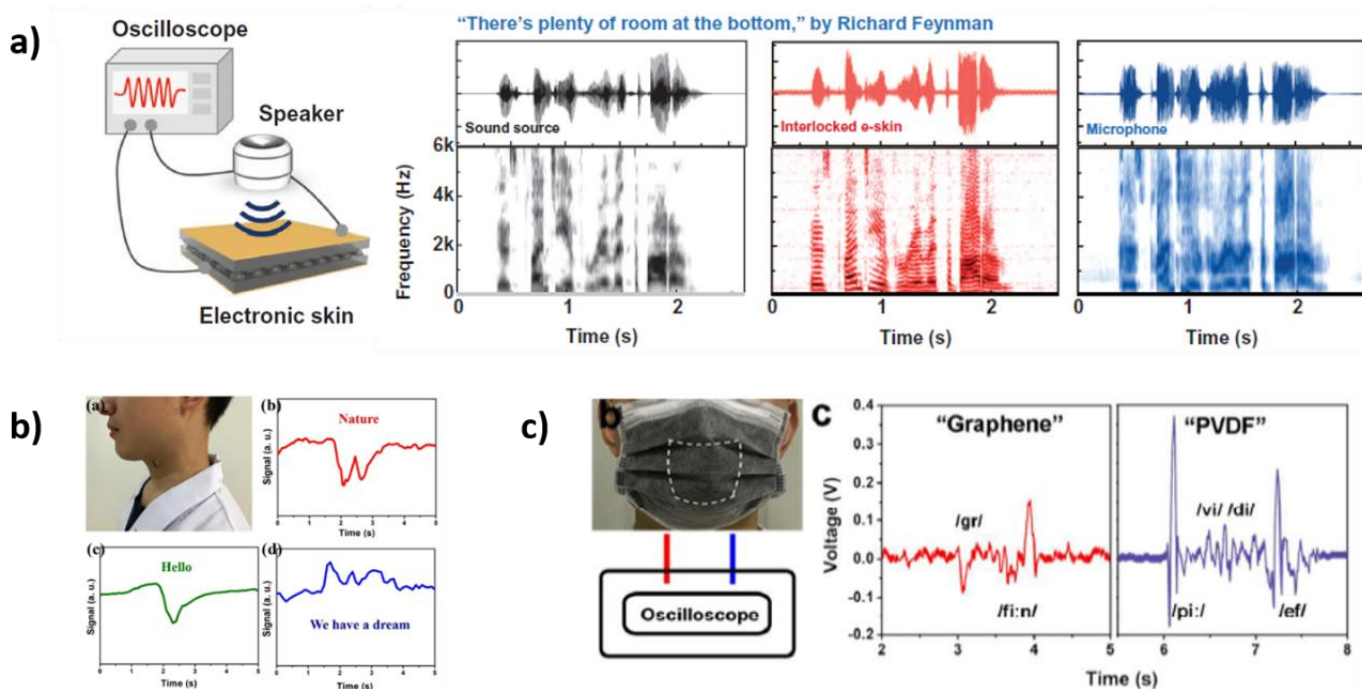
Figure 7. Acoustic sound detectors: (a) readout signals from the interlocked e-skin vs microphone [206], (b) an example of speech recognition by the rGO-encapsulated PVDF-TrFE NF sensor [205], (c) readout signals from the graphene/PVDF composite sensor during speaking [202]. Reprinted with the permission from the American Chemical Society.

A new functional device for energy harvesting from low-frequency random (bio)mechanical movements based on rGO nanofillers chemically modified with TFB and suspended in a PVDF-HFP matrix was developed [208]. Thermogravimetric analysis indicated that the grafting weight density of TFB reached 5.8 wt%, and the covalent modification of rGO by TFB significantly improved its compatibility with PVDF-HFP. Based on a comparative analysis of three composite films (PVDF-HFP, rGO/PVDF-HFP, and rGO-TFB/PVDF-HFP) using FTIR and differential scanning calorimetry, both rGO and rGO-TFB were found to induce structural changes in the composite films; however, the intermolecular interactions of rGO and rGO-TFB with the polymer were different. The rGO-TFB/PVDF-HFP nanocomposite presented the highest β-phase fraction. For the 2.5 wt% rGO-TFB/PVDF-HFP piezopolymer film, the β-phase content calculated from FTIR data reached 42%. The corresponding energy-harvesting device generated an open-circuit

voltage of 2.2 V and a pulse current of 30 nA in response to finger bending motions, while three serially connected devices provided an open-circuit voltage of 4.8 V and a pulse current of 50 nA. It is worth noting that elongating a single film four times led to a remarkable increase in the β-phase content from 42% to 84%; the current generated by finger movement increased accordingly from ~30 to 80 nA, but the dielectric constant of the material dramatically decreased.

A superior piezoelectric energy harvester based on an Fe-doped rGO/PVDF nanocomposite film (2 wt% loading) with an active area of 2×3 cm^2 provided an open circuit output voltage and short circuit current of up to 5.1 V and 0.254 μA, respectively, in response to repeated impulses from a human finger (or, under a 12 kPa pressure amplitude) [45]. Both XRD and FTIR measurements confirmed that the Fe-rGO nanofillers played an important role in the nucleation and stabilization of the polar γ-phase, and at a nanofiller content of 2 wt%, the relative proportion of the γ-phase reached ~99%, remarkably improving the piezo- and ferroelectric properties of the nanocomposite film.

Very recently, a commercially available fabric coated with Gr nanosheets (Figure S4e) dispersed in PVDF was used to monitor speech and body motion [202], similarly to the study carried out in ref. [201]. The average coating thickness achieved during fabrication process, which involved continuous impregnation, phase separation, and drying, was ~1.5 μm. The presence of 0.5 wt% Gr was found to increase the content of the electroactive phases (β/γ) in the nanocomposite to 87%, improving the piezoelectric properties of the material. Further tests revealed that the voltage signal increased linearly from 3 V to 18 V with a sensitivity 34 V/N as the input strength was increased from 0.05 to 0.45 N. The highest detected voltage of over 60 V was measured when the piezoelectric NG was hit with a force of 2 N, while the sensing threshold was found to be 0.6 mN. This means that even tiny changes in air flow during speaking can be measured by the sensor, as the air flow causes it to vibrate (Figure 7c). The sensor was also embedded into trousers and demonstrated the ability to distinguish the landing moments of the legs (Figure 4c).

The synergetic effect of Gr nanosheets and BT NPs in enhancing the piezoelectric performance of a PVDF NF mat was studied in ref. [27]. BT NPs with an average diameter of 200 nm and Gr nanosheets were loaded into a PVDF matrix, and fibre mats with an effective working area of 2.5×2.5 cm^2 and a thickness of 18-20 μm were fabricated from the fibres; the most frequent fibre diameter was 0.4-0.6 μm. The presence of both BT NPs and Gr was demonstrated to be crucial for β-phase formation, with the β-phase content reaching a maximum value of 91.1% for nanocomposite fibres containing 0.15 wt% Gr and 15 wt% BT. The measured open-circuit voltage and electric power of the piezocomposite device were as high as 11 V and 4.1 μW at a loading frequency of 2 Hz and a strain of 4 mm. A high output voltage of 112 V was generated by finger pressing and releasing with fast strain rates. Small strains or slow strain rates, such as those resulting from wrist bending and finger-tapping, produced low output voltages of 7.7 V and 7.5 V, respectively, while output voltages of 7.8 V and 2.8 V were registered under the heel and toe, respectively, for foot-stepping motions.

2.2. Biosensors

Two recent publications demonstrated the use of PVDF-based nanocomposites for sensing biochemical species such as hydrogen peroxide and glucose. In the first study [209], Pt NPs (particle size: <50 nm) and MWCNTs (outer diameter: 10–15 nm, inner diameter: 2–6 nm, length: 0.1–10 μm) were suspended in the piezopolymer PVDF prior to the preparation of a 3D porous membrane from electrospun NFs (width: 150–300 nm). It was revealed that the Pt NPs tend to attach to the side walls of carbon nanotubes, while the nanotubes themselves serve as bridges connecting the dispersed Pt NPs together into hybrid NFs. The assembly of Pt NPs and CNTs (Figure S5c) led to an increase in the nanocomposite conductivity and enhancement of its electrocatalytic properties, while the electrospinning process provided a significantly higher β-phase content in the resulting NFs than the drop-casting method. The hybrid nanofibrous membrane exhibited a regular response to hydrogen peroxide in the range of 0.1 to 75 mM with a low

detection limit of ~0.61 μM, whereas the sensing performance for glucose was moderate with a detectable range of 15 to 100 mM. Additionally, the hybrid membrane was found to have excellent electrochemical activity for the oxygen reduction reaction, most likely due to the high specific surface area of the 3D nanoporous structure in the fabricated membrane and sufficient number of active reaction sites provided by the Pt NPs and MWCNTs.
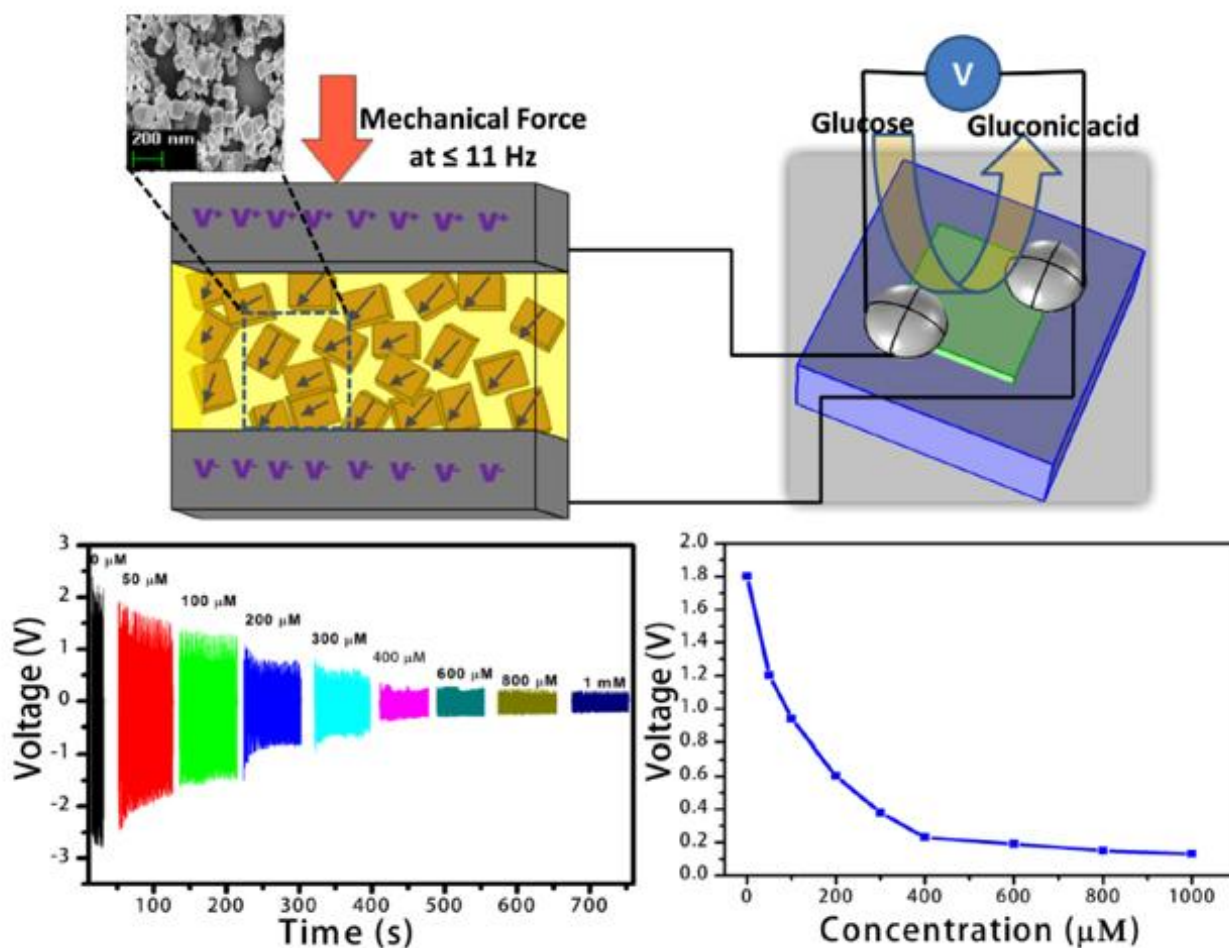
Figure 8. Self-powered glucose sensor. Reprinted from [199] with the permission from Elsevier.

Another glucose sensor was developed based on two composite films, a PVDF piezopolymer matrix loaded with BT nanocubes (≥100 nm, Figure S4f) that acted as a piezoelectric NG, and a PVA matrix containing BT NPs as the glucose-sensitive element (Figure 8) [199]. In the dynamic regime, at a cyclic frequency of 11 Hz, the NG device provided a peak to peak open circuit voltage of ~5 V under a mechanical force 11 N, which was sufficient to drive the PVA-based glucose sensing

element. The self-powered glucose sensor exhibited good selectivity towards glucose in the presence of interfering species such as galactose and uric acid, a reasonable sensitivity of 23.79 $\mu A/mM\ cm^2$, a low detection limit of 7.94 μM, and a detectable response in the concentration range of 0.1 μM to 1 mM; this, it could be useful for enzyme-free clinical applications.

3. Hybrid piezocomposites for biomedical applications

3.1. *In vivo* energy harvesters and tissue engineering materials

It is challenging to develop electroactive materials that can simultaneously trigger the regeneration of multiple tissues, such as bone and blood vessels. To overcome this challenge, scaffolds made of individual or hybrid piezoelectric polymers should be developed and implanted into the defects in these tissues to examine their capability to induce or promote multi-tissue regeneration *in vivo* in response to single or multiple stimuli. In-vivo experiments with large animal models are necessary for the further development and improvement of piezoelectric scaffolds that mimic living tissue [198]. To the best of our knowledge, implantable energy harvesters for energy collection from *in vivo* movements have been developed based only on non-biodegradable piezopolymers and without the use of nanofiller additives to improve their piezoelectric characteristics. In the first example [119], PVDF-TrFE electrospun fibres for an implanted energy harvester were demonstrated in Sprague Dawley rats for cell proliferation and cell alignment growth applications. The fibre morphology was optimised by varying the solution concentration and collection distance during the electrospinning process, and the highest piezoelectric coefficient d_{31} was found to be 15.73 pC/N for the poled PVDF-TrFE NF scaffolds with an area of $2\times2\ cm^2$. Piezoelectric performance testing revealed that the peak-to-peak output voltage reached more than 1.5 V, while the peak-to-peak output current was approximately 52.5 nA. Polarised PVDF-TrFE NF scaffolds implanted under the skin of rat legs generated a peak output voltage and output current of ~6 mV and ~6 nA when the legs were pulled upward by a linear motor via a wire to mimic the daily activity of a rat (Figure 9a). The PVDF-TrFE NF scaffolds fabricated under the optimised process conditions were also

demonstrated to have excellent cytocompatibility, and a 1.6-fold increase in the proliferation rate of fibroblast cells was measured, indicating that the polarised PVDF-TrFE NF scaffolds show great promise for tissue engineering and wound healing.

In the second study [210], a PDMS/Parylene-C packaged PVDF NG was implanted in a female mouse for six months. In order to prepare the piezopolymer-based energy harvester, a 15-20 μm Parylene-C thin film was deposited on both sides of a PDMS-encapsulated commercial PVDF film (thickness: ~50 μm, area: 5×5 mm^2). In response to *in vitro* bending at a frequency of 2 Hz, the NG provided a consistent peak-to-peak current of ~45 nA and a voltage of ~0.3 V. When implanted *in vivo* in the deep leg muscle at ~3 cm, the NG yielded a peak-to-peak voltage of ~0.05 V during stretching of the mouse leg muscle at a frequency of 1 Hz; the voltage increased to ~0.1 V at a stretching frequency of 2 Hz (Figure 9b). Note that the obtained *in vitro* piezoelectric output was higher due to the much more significant displacement. No signs of toxicity or incompatibility were observed in either the surrounding tissues or the whole organism during the 24 week implantation period, demonstrating the long-term biocompatibility and biosafety of the PVDF-based *in vivo* NG.
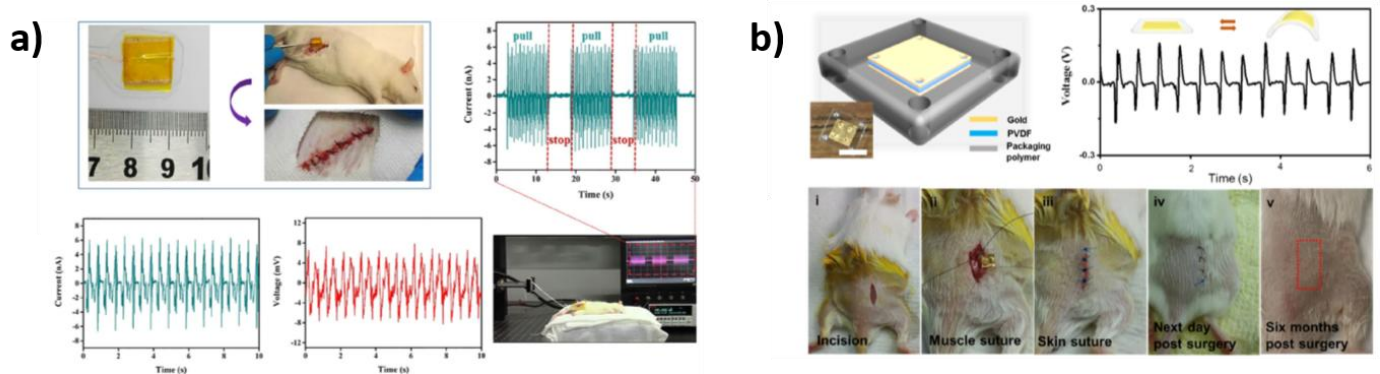
Figure 9. (a) In vivo NG made from an electrospun PVDF-TrFE NF scaffold [119] and (b) a PDMS/Parylene-C packaged PVDF film [210]. Reprinted with the permission from Elsevier.

Several non-biodegradable piezoelectric nanocomposites were recently created for use as tissue engineering scaffolds for blood vessel formation and bone regeneration. An electrospun

ZnO/PVDF-TrFE nanocomposite tissue engineering scaffold (2 wt% ZnO loading) demonstrated the ability to promote angiogenesis and enhanced the integration of the scaffold into the surrounding tissue [211]. The electrospun composite fibres with an average diameter of ~1.2 μm were found to be mainly in the piezoelectric β-phase. *In vitro* studies using human mesenchymal stem cells and human umbilical endothelial cells confirmed that the scaffolds, which had a highly porous morphology and randomly oriented fibres, were compatible with cells and promoted cell adhesion. *In vivo* studies in rats demonstrated the absence of visual inflammation or severe immunological responses at the scaffold implantation sites, as well as the ability of the scaffolds to facilitate angiogenesis. The best angiogenic response, which involved the formation of a highly branched vascular network over the whole scaffold, was observed for scaffolds pre-seeded with human mesenchymal stem cells.

BT/PVDF-TrFE membranes of were tested for *in vivo* support of bone repair. In an earlier study [78], a significant enhancement in bone response was observed in the presence of BT NPs (size: 500-620 nm) in piezoelectric membranes with a thickness of 90±10 μm cut into discs 6 mm in diameter. Six bone morphometric parameters (bone volume, bone surface, specific bone surface, trabecular number, trabecular thickness, and trabecular separation) were evaluated during the *in vivo* study, and four of these parameters were revealed to be similar for the BT/PVDF-TrFE and neat PVDF-TrFE membranes implanted in rat calvarial bone defects. However, a larger bone surface and lower trabecular separation were found at 4 and 8 weeks when a BT/PVDF-TrFE membrane was implanted, indicating that the BT loaded in the PVDF-TrFE matrix promoted bone formation.

In a later study [212], the same scientific group conducted a comparative test of the lab-made BT/PVDF-TrFE membrane and commercial PTFE membrane. Both membranes had a thickness of 0.25 mm and a surface roughness from 0.15 to 0.20, and were cut into 5 mm diameter discs. The results showed that the *Wistar* rats that received the BT/PVDF-TrFE membrane as a filler for the

created bone defects presented morphometric parameters that were similar to or even better than the rats that received the PTFE membrane. The composite membrane promoted the growth of new bone trabeculae above and below its structure. No inflammatory response was observed, and the resulting bone tissue showed higher resistance. Higher expression of genes associated with bone resorption, such as MMP9 and CALCR, was also detected. The increased expression of the latter gene could contribute to the greater amount of bone tissue in rats that received the BT/PVDF-TrFE membrane. A polydopamine-coated BT (coating thickness: ∼5 nm) were suspended in PVDF-TrFE to mimic the endogenous electric potential for the highly efficient repair of bone defects [76]. Piezocomposite membranes were fabricated with a BT loading of 5 vol% and an average thickness of 50-60 μm. A surface potential of approximately −76.8 mV was measured, which is comparable to the endogenous potential range of −60 to −100 mV. Further, *in vitro* studies of the biological performance of polarised nanocomposite membranes revealed enhanced activity and osteogenic differentiation of bone marrow mesenchymal stem cells, while *in vivo* experiments with 8-week-old male Sprague Dawley rats demonstrated facilitated repair of critical-sized calvarial defects in mature rats due to the sustained maintenance of the electrical microenvironment *in vivo*.

3.2. *In vitro* growth and development of living cells

Recently, piezoelectric ZnO/PVDF scaffolds were manufactured as a new type of orthopaedic material with cytocompatible and antibacterial properties [213]. ZnO NPs (<50 nm) were loaded into PVDF, and piezoelectric NFs were obtained. The average diameter of the NFs decreased from 360 nm to 240 nm as the ZnO loading of the PVDF solution was increased from 0 to 2 mg/ml. The β-phase content was 10% higher for a ZnO content of 2 mg/ml than for 0 mg/ml of ZnO, which led to an enhanced elasticity modulus, elongation at break, and maximum load. *In vitro* osteoblast assays demonstrated that the piezo-excited scaffolds exhibited a 30% greater osteoblast density compared to their non-piezoelectric-excited counterparts after 3 days of culturing. In addition, a

remarkable decrease in the density of three common etiologic agents of infection after orthopaedic surgery infection, namely, *Escherichia coli*, *Staphylococcus aureus,* and Methicillin-resistant *Staphylococcus aureus*, was detected for the 1 mg/ml ZnO/PVDF scaffolds without piezo-excitation; the density decrease was even greater for the piezo-excited scaffolds.

In another study, MgO whiskers (rod-shaped, average diameter: ~2.5 μm, length: ~15 μm) were added to the PVDF matrix to prepare scaffolds with an interconnected porous architecture [214]. MgO is well-known to provide excellent antibacterial properties and good biocompatibility and bioactivity. Loading PVDF with MgO whiskers improved the polymer crystallinity to a maximum value of 52.34% at a MgO whisker content of 2 wt%. The scaffold morphology became rougher in the presence of MgO due to the filaments. The tensile strength and elastic modulus of the scaffold were measured to be 62.17 MPa and 6018.83 MPa, respectively; these values were approximately 1.5 times higher than those of the neat scaffolds. *In vitro* cell culture experiments revealed that the 2 wt% MgO/PVDF scaffolds stimulated cell attachment and proliferation much more effectively than neat ones.

Aligned ultrafine BT/PVDF fibre meshes were developed for the use in cochlear implants for sensorineural hearing loss [51]. Fabricated PVDF fibres loaded with BT NPs (average particle size of 100 nm) showed an average diameter of 400 nm. An enhancement in the piezoelectric β-phase content was obtained as a result of the electrospinning processing. The fibres exhibited a direct piezoelectric coefficient g_{31} of 1.0 mV/N at a 20% BT loading, while the piezoelectric constant d_{31} was estimated to be 130 ± 30 pm/V. *In vitro* tests using inner-ear epithelial cells and neural-like cells showed very good biocompatibility and confirmed that the nanofibrous material possessed enhanced viability under simulated physiological conditions. An electrospun poly(3-hydroxybutyrate-co-4-hydroxybutyrate)/GO nanofibrous scaffold was fabricated. GO reduced the fibre diameter and enhanced the porosity, hydrophilicity, mechanical properties, cellular performance, and osteogenic differentiation of the scaffolds [215].

In an earlier approach, BT/PVDF-TrFE nanocomposite films were obtained and tested as substrates for the stimulation of neuronal model cells [79]. A 60 wt% loading of BT NPs (tetragonal, ~300 nm) was dispersed into a PVDF-TrFE matrix, which was used to prepare planar composite films that exhibited a surface roughness of ~212 nm; this value was three times greater than that of the neat polymer samples. The high BT loading increased the β-phase content to ~50 wt% and the Young's modulus to 784 ± 103 MPa. The films were cut into strips of $50 \times 5 \times 0.08$ mm^3 for piezoelectric performance measurements. A converse piezoelectric coefficient d_{31} of 53.5 pm/V and a direct piezoelectric coefficient g_{31} of 0.24 mV/N were determined for the improved piezocomposite material, which represented 4.5-fold and 2.2-fold increases over the d_{31} and g_{31} values of the neat PVDF-TrFE film. Both films demonstrated good viability and differentiation of SH-SY5Y neuroblastoma cells; however, the amplitude of Ca^{2+} transients under ultrasound stimulation, which serves as evidence of neuronal stimulation, was significantly higher for the composite film. Importantly, the neurite length was found to be significantly improved for the BT/PVDF-TrFE films subjected to ultrasound stimulation.

Similarly to in ref. [79], a piezoelectric film consisting of BN nanotubes suspended in a PVDF-TrFE matrix was fabricated for bone tissue regeneration [77]. Doping of the PVDF-TrFE piezopolymer with 1 wt% of BN nanotubes in the form of bundles of multi-walled tubes with an average diameter of 10 nm and lengths on the micrometre scale provided improved piezoelectric properties. The converse and direct piezoelectric coefficients d_{31} and g_{31} were found to be 11 pm/V and 0.155 V·m/N, respectively, representing a 1.8-fold increase over the undoped PVDF-TrFE film, whereas the effective transverse piezoelectric coefficient e_{31} increased 3.9-fold to 7.59 mC/m^2. Improved differentiation of SaOS-2 osteoblast-like cells in terms of calcium deposition, collagen I secretion, and the transcriptional levels of several marker genes (*Alpl*, *Col1a1*, *Ibsp*, and *Sparc*), was found for composite piezoelectric films subjected to ultrasound stimulation, which provided an amplitude of pressure variation of 2-6 kPa at the film site and a corresponding voltage of 23-61 mV on the PVDF-TrFE films.

Another PVDF piezocomposite containing MWCNTs with an average diameter of 9.5 nm and an average length of 1.5 μm was developed to stimulate muscle cell growth *in vitro* [216]. A 2 wt% loading of MWCNTs in the composite material enhanced the β-phase content to 59%, while the direct current conductivity was increased to $5 \cdot 10^{-5}$ S/cm. The viability results for C2C12 mouse myoblast cells demonstrated the absence of any cytotoxic effects *in vitro* in the absence of external field stimulation, and the optimal electric field to enhance cell proliferation was found to be 1 V/cm for the 2% MWCNTs/PVDF nanocomposite.

3.3 Piezo-catalysis and the piezoelectric antibacterial effect

Despite the fact that the piezoelectric phenomenon was first observed more than 100 years ago, the piezoelectric effect of nano/micrometre materials has been investigated only recently [163]. The induction of a piezoelectric effect by piezoelectric polarization has been widely applied in NGs, piezoelectric field effect transistors, and flexible self-powered systems [163, 201, 217, 218]. More recently, K. S. Hong et al. found that micro-scale ZnO fibres could directly split water into hydrogen with an ultrahigh energy conversion efficiency of ∼18% by simple vibration [219], and could also degrade organic pollutants in water [220]. Thus, the piezoelectric potential can be directly converted into piezo-chemical potential *in-situ* in aqueous solution [221]. This phenomenon is called the piezocatalytic effect. Numerous piezocatalytic studies for the degradation of methyl orange [222, 223], Rhodamine B [224], or acid orange [225] have been reported.

Despite the above-mentioned studies, research into the piezocatalytic effect has mainly focused on dyes. In 2017, S. Lan reported the successful degradation of the toxic compound 4-chlorophenol using piezocatalysis, as well as its simultaneous effective dechlorination [226]. Jinxi Feng et al. were the first to report the disinfection of media containing *E. coli* through the piezo-activity of BT [221]. They revealed that the most significant inactivation effect was achieved through a

combination of sonication and piezocatalysis [221]. Thus, piezo-active materials can be used to effectively kill bacteria.

In order to investigate the piezo-catalytic effect, piezoelectric ceramics with a high piezoelectric coefficient are most often used; however, these can be destroyed by mechanical force or by floating in the organic solution, and thus cause secondary pollution. Therefore, it is important to develop a highly reusable material without destroying its catalytic activity. Masimukku et. al. fabricated a piezoelectric brick based on PDMS with a high concentration of single-layer tungsten disulphide (WS_2) nanoflowers and successfully demonstrated the degradation of an organic dye (Rhodamine B, RB) and *E. coli*-killing ability in a dark environment through the piezocatalytic effect with mechanical vibration [227]. Although the polymer PDMS is usually used as an isolator, the single- and few-layered WS_2 nanoflowers could be piezoelectrically polarised through the mechanical force, and therefore, the induced electrical charges accumulated on the surfaces of the PDMS film to perform the redox process with polar water molecules (Figure 10). The mechanism by which ROS species are created in water using the piezo-catalytic effect, e.g. when using a PDMS/WS_2 NFs brick under mechanical force, can be described as follows [227]:

$$H_2O + h^+ \leftrightarrow OH^{\cdot} + H^+ \tag{1}$$

$$O_2 + e^- \rightarrow O^{\cdot}_2 \tag{2}$$

$$\cdot O_2^- + 2H^+ \rightarrow H_2O_2 \tag{3}$$

$$H_2O_2 + H^+ + e^- \rightarrow OH^{\cdot} + H_2O \tag{4}$$
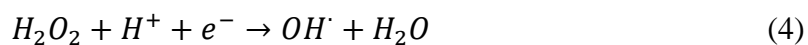
Figure 10 depicts the how the piezoelectric potential induces an internal electric field as a result of driving electrons (i.e. free carriers resulting from vacancies) to the left side to induce the positively charged surface. Meanwhile, the holes diffuse to the right side, inducing a negatively charged surface. Therefore, the negative side of the polar water molecule interacted with the positively charged surface (Figure 10A) and reacted to produce OH radicals and protons (see eq. 1). On the other side, the negatively charged surface further reacted with O_2 to produce $\cdot O_2^-$ free radicals (see eq. 2). While the created OH radicals interacted with the negatively charged surface and combined

with protons to reform molecules of water (Figure 10B, right side), hydrogen peroxide was produced via the reaction of the $\cdot O_2^-$ with protons (see eq. 3). Finally, Figure 10B (left side) shows that the hydrogen peroxide molecule regenerated a water molecule and an OH radical (see eq. 4) [227].
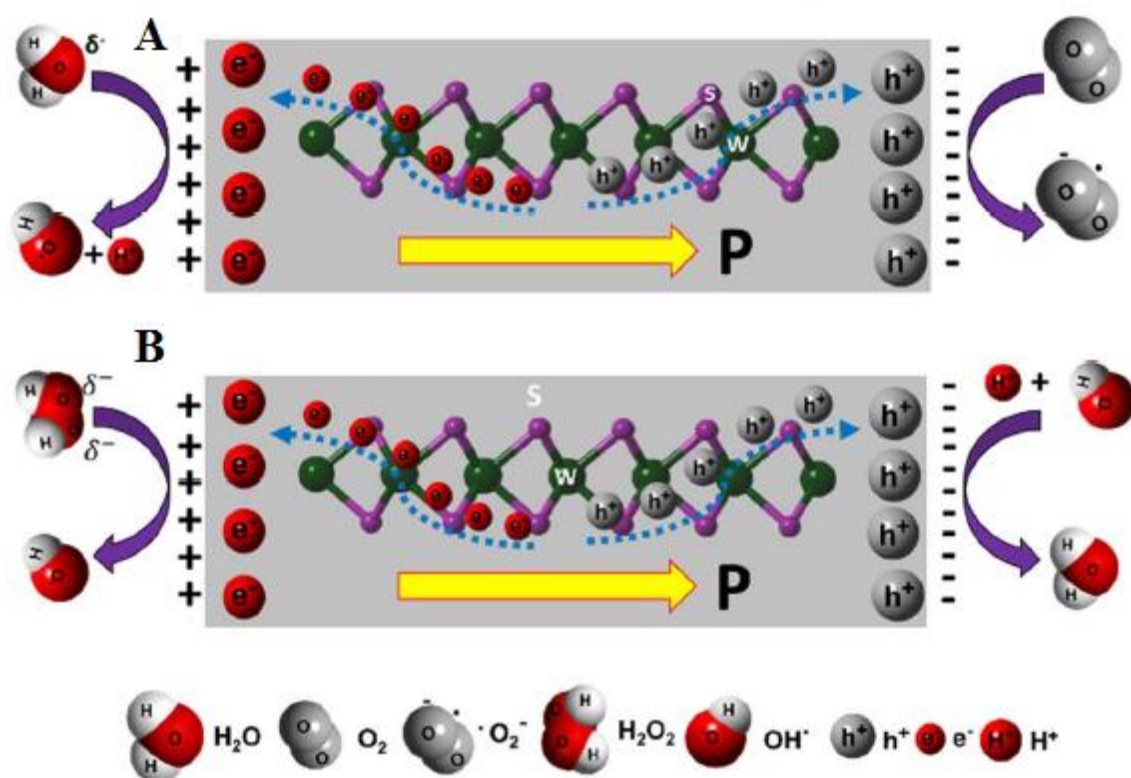
Figure 10. The working mechanism of creating the ROS species in water by the PDMS/WS$_2$ NFs brick under mechanical force. **A**. The induced positive charges were accumulated on the surface of the PDMS/WS$_2$ NFs brick to react with H$_2$O and form the OH with protons (H$^+$) radicals (left). Meanwhile, the induced negative charges reacted with O$_2$ and generated the $^\bullet$O$_2^-$ (right). **B**. The induced positive charges were accumulated on the surface of the PDMS/WS$_2$ NFs bricks, to react with H$_2$O$_2$ and form the OH (left). The induced negative charges reacted with the OH and protons (H$^+$) to re-generate the H$_2$O (right). Reprinted from [227] with the permission from Elsevier.

In spite of recent achievements, piezocatalysis has still scarcely been studied. Piezoelectric polymers such as PLLA, even those that do not contain piezoceramics with a strong piezoelectric performance, can also create ROS species that effectively kill bacteria, e.g. *staphylococcus aureus* [228]. Moreover, M. Ando et al. reported the strong electric field generated between PLLA yarns could inhibit bacteria via electroporation [228]. Also, the electrical current transported *via* humidity between yarns, fibres, or NPs of piezoceramics can affect the antibacterial activity, as bacterial damage due to electrical current has been reported [229]. Jiang Wu et al. demonstrated the presence of an electric current around BT NPs in water during ultrasonication [230]. Additionally, bacteria utilize an electron transport system to produce vital energy. Therefore, the operation of this system can be inhibited by an external electric field or current, killing or damaging the bacteria [228]. Thus, the antibacterial effect of piezoelectric synthetic materials and their hybrids can be attributed to a combination of the following three mechanisms: the generation of an electric field, electric current, and ROS species.

To conclude, compared with existing catalytic technologies such as photocatalysis and electrocatalysis, piezocatalysis is especially attractive because it predominantly uses mechanical vibration, which reduces dependence on other inputs such as light and electricity [230-234]. In addition, the antibacterial effect created by the strong electric field of the piezoelectric synthetic hybrid materials could be useful for clothing and sports goods, as well as for other biomedical applications.

Future outlook and challenges

As can be seen from the above literature data, hybrid piezocomposites can be efficiently utilized as mechano-, bio-, and gas sensors (Table S1), energy harvesters (Table S2), and tissue engineering materials (Table S3). However, their piezoelectric performance still requires further improvement for widespread use in biomedical devices and sensors. Doping with nanofillers of various shapes

and sizes, nanoinclusion patterning and alignment, and efficient sensor morphology play important roles in improving device performance. A piezopolymer loaded with microstructured ceramics provided an improved output voltage [204] and an increased current output [49] when a sample of the nanocomposite was bent by the fingers. In the presence of composite ceramic NPs, a simple planar piezopolymer film exhibited a remarkably high open circuit voltage of ~160 V under a small constant mechanical force [31]. rGO and Gr nanosheets seem to be promising nanofillers for obtaining strong sensing capabilities with low detection limits [31, 203, 206], especially in combination with specific film geometries and a multilayered sensor structure [203]. Good sensitivity was also obtained for microstructured piezopolymers loaded with metal oxides [200]. The first attempt to utilize the synergetic effect of Gr nanosheets and ceramic NPs yielded a high output voltage of ~112 V, but this value is still much lower than the ~200 V obtained using a PZT-based NG under bending deformation [7]. Structuring of the nanofiller particles, such as co-doping and coating, can also be useful for improving the performance of electroactive and bioactive materials [19, 45, 59, 76]. Importantly, only pristine piezopolymers have been tested *in vivo* as implanted NGs for energy harvesting from the daily activity of living organisms [119, 210].

Obviously, new developments towards high-efficient piezoelectric energy harvesters are associated with shaping and structuring of hybrid nanocomposites at the nano-, micro-, and macroscale. Loading nanofillers of various shapes and sizes (Figure S4), including complex doped [19, 31, 45, 55] and coated [59, 76, 208] fillers, into a piezopolymer matrix can efficiently increase its electroactive properties, while co-doping with several different types of nanofillers and optimising their content [27, 209] will provide further improvements in sensitivity. Furthermore, the much-less-explored and -exploited microscale patterning and the alignment of nanofiller particles inside the piezopolymer matrix are significant steps towards tuning and controlling the material properties (Figure S5). In addition to this, imparting a specific geometry in the piezocomposite material will further increase its electrical responsiveness to various external stimuli (Figure S6). Additional

cytotoxicity and biocompatibility tests will reveal the optimal piezocomposite materials for *in vivo* biomedical applications.

Thus, despite the progress that has been made in this rapidly advancing field, developing a fundamental understanding and common standard for consistently quantifying and evaluating the performance of various types of piezoelectric NGs is still a challenging task [235]. More in-depth work should be carried out to develop a comprehensive and sophisticated framework for evaluating NG materials and their structure and performance, which will result in the successful application of PENGs and self-powered systems. For example, the intrinsic material properties of piezoelectric materials, such as the internal carrier concentration, defect distribution, and internal strain, should be considered and included in the figures of merit (FOM). The structural parameters of PENG devices, e.g. contact properties, should also be taken into account, since the electrode contacts significantly affect the overall energy harvesting efficiency by affecting the impedance match and other properties [235].

Conclusions

Piezoresponsive polymer-based nanocomposite materials offer the potential of developing a new generation of high-performance and flexible energy harvesters for biomedical applications. By developing new polymer-based nanocomposites for piezoelectric energy harvesting, materials scientists now possess a number of potential lead-free alternatives that can be used. Future challenges in the preparation of piezoelectric scaffolds for use in bone tissue regeneration, sensors for various stimuli, *in vivo* implantable devices, and e-skin are presented. Given the fact that the energy conversion efficiencies of pure polymer materials is rather low, which is inhibitory for their use as mechanical transducers, the incorporation of a piezoactive secondary phase to create organic-inorganic nanocomposites is promising strategy to design new piezoelectric materials. In this context, PVDF and its copolymers with high piezoelectric strain constants are suitable matrix

71

materials. This review provides a snapshot of the progress in the development of piezoelectric materials is shown to depend on a specific set of material properties, and to require the fabrication of new hybrid materials that contain components such as inorganic and metallic NPs, conductive rGO nanosheets, and the other filler components discussed in this review. These materials allow significant improvement in the content of the electroactive phase in the piezoelectric polymers and enhance their energy-harvesting capability for various biomedical applications, with the main aim being the avoidance of external power sources in implantable and wearable biomedical devices. Despite the promising potential of implantable energy harvesting devices, their *in vivo* applications are challenged by the limited insights into their cytotoxicity and long-term behavior in the host organisms, which points out the necessity of more coherent and synergistic efforts among material scientists and medical experts.

Acknowledgements

References

[1] A.C. Wang, C. Wu, D. Pisignano, Z.L. Wang, L. Persano, Polymer nanogenerators: opportunities and challenges for large-scale applications, J. Appl. Polym. Sci. 134 (2017) 45674. https://doi.org/10.1002/app.45674.

[2] H. Li, C. Tian, Z. Daniel Deng, Energy harvesting from low frequency applications using piezoelectric materials, Appl. Phys. Rev. 1 (2014) 041301. https://doi.org/10.1063/1.4900845.

[3] H. Wu, Y.A. Huang, F. Xu, Y. Duan, Z. Yin, Energy Harvesters for Wearable and Stretchable Electronics: From Flexibility to Stretchability, Adv. Mater. 28 (2016) 9881-9919. https://doi.org/10.1002/adma.201602251.

[4] P.K. Panda, B. Sahoo, PZT to Lead Free Piezo Ceramics: A Review, Ferroelectrics 474 (2015) 128-143. https://doi.org/10.1080/00150193.2015.997146.

[5] R. Seveno, J. Carbajo, T. Dufay, B. Guiffard, J.C. Thomas, Flexible PET/Al/PZT/Al/PET multi-layered composite for low frequency energy harvesting, J. Phys. D: Appl. Phys. 50 (2017) 165502. https://doi.org/10.1088/1361-6463/aa6373.

[6] W. Jin, Z. Wang, H. Huang, X. Hu, Y. He, Meng Li, L. Li, Y. Gao, Y. Hu, H. Gu, High-performance piezoelectric energy harvesting of vertically aligned $Pb(Zr,Ti)O_3$ nanorod arrays, RSC Adv. 8 (2018) 7422-7427. https://doi.org/10.1039/C7RA13506H.

[7] K.-I. Park, J. H. Son, G.-T. Hwang, C.K. Jeong, J. Ryu, M. Koo, I. Choi, S. H. Lee, M. Byun, Z.L. Wang, K. J. Lee, Highly-Efficient, Flexible Piezoelectric PZT Thin Film Nanogenerator on Plastic Substrates, Adv. Mater. 26 (2014) 2514-2520. https://doi.org/10.1002/adma.201305659.

[8] S. Das, A. Kumar Biswal, K. Parida, R.N.P. Choudhary, A. Roy, Electrical and mechanical behavior of PMN-PT/CNT based polymer composite film for energy harvesting, Appl. Surf. Sci. 428 (2018) 356-363. https://doi.org/10.1016/j.apsusc.2017.09.077.

[9] X. Lu, H. Qu, M. Skorobogatiy, Piezoelectric Micro-and Nanostructured Fibers Fabricated from Thermoplastic Nanocomposites Using a Fiber Drawing Technique: Comparative Study and Potential Applications, ACS Nano 11 (2017) 2103-2114. https://doi.org/10.1021/acsnano.6b08290.

[10] X. Lu, H. Qu, M. Skorobogatiy, Piezoelectric microstructured fibers via drawing of multimaterial preforms, Sci. Rep. 7 (2017) 2907. https://doi.org/10.1038/s41598-017-01738-9.

[11] P. Panda, Review: environmental friendly lead-free piezoelectric materials, J. Mater. Sci. 44 (2009) 5049-5062. https://doi.org/10.1007/s10853-009-3643-0.

[12] H.B. Kang, C.S. Han, J.C. Pyun, W.H. Ryu, C.-Y.Kang, Y.S. Cho, $(Na,K)NbO_3$ nanoparticle-embedded piezoelectric nanofiber composites for flexible nanogenerators, Compos. Sci. Technol. 111 (2015) 1-8. https://doi.org/10.1016/j.compscitech.2015.02.015.

[13] R.V. Chernozem, M.A. Surmeneva, R.A. Surmenev, Hybrid biodegradable scaffolds of piezoelectric polyhydroxybutyrate and conductive polyaniline: Piezocharge constants and electric potential study, Mater. Lett. 220 (2018) 257-260. https://doi.org/10.1016/j.matlet.2018.03.022.

[14] X. Chen, H. Tian, X. Li, J. Shao, Y. Ding, N. An, Y. Zhoua, A high performance P(VDF-TrFE) nanogenerator with self-connected and vertically integrated fibers by patterned EHD pulling, Nanoscale 7 (2015) 11536-11544. https://doi.org/10.1039/C5NR01746G.

[15] J. Shi, S. Yong, S. Beeby, An easy to assemble ferroelectret for human body energy harvesting, Smart Mater. Struct. 27 (2018) 084005. https://doi.org/10.1088/1361-665X/aabdbc.

[16] F. Narita, M. Fox, A Review on Piezoelectric, Magnetostrictive, and Magnetoelectric Materials and Device Technologies for Energy Harvesting Applications, Adv. Eng. Mater. 2018, 20 (2018) 1700743. https://doi.org/110.1002/adem.201700743.

[17] P. Martins, A. Lopes, S. Lanceros-Mendez, Electroactive phases of poly (vinylidene fluoride): determination, processing and applications, Prog. Polym. Sci. 39 (2014) 683-706. https://doi.org/10.1016/j.progpolymsci.2013.07.006.

[18] N. Weber, Y.S. Lee, S. Shanmugasundaram, M. Jaffe, T.L. Arinzeh, Characterization and in vitro cytocompatibility of piezoelectric electrospun scaffolds, Acta Biomater 6 (2010) 3550-3556. https://doi.org/10.1016/j.actbio.2010.03.035.

[19] H. Parangusan, D. Ponnamma, M.A.A. Al-Maadeed, Stretchable electrospun PVDF-HFP/Co-ZnO nanofibers as piezoelectric nanogenerators, Sci. Rep. 8 (2018) 754. https://doi.org/10.1038/s41598-017-19082-3.

[20] J. Zhu, L. Jia, R. Huang, Electrospinning poly(l-lactic acid) piezoelectric ordered porous nanofibers for strain sensing and energy harvesting, J Mater Sci: Mater Electron 28 (2017) 12080-12085. https://doi.org/10.1007/s10854-017-7020-5.

[21] S.J. Lee, A. Anand Prabu, K.J. Kim, Piezoelectric properties of electrospun poly(L-lactic acid) nanofiber web, Mater. Lett. 148 (2015) 58-62. https://doi.org/10.1016/j.matlet.2015.02.038.

[22] Y.W. Kim, H. Bit Lee, S. Mo Yeon, J. Park, H. J. Lee, J. Yoon, S. H. Park, Enhanced Piezoelectricity in a Robust and Harmonious Multilayer Assembly of Electrospun Nanofiber Mats and Microbead-Based Electrodes, ACS Appl. Mater. Interfaces 10 (2018) 5723−5730. https://doi.org/10.1021/acsami.7b18259.

[23] B.-S. Lee, B. Park, H.-S. Yang, J. W. Han, C. Choong, J. Bae, K. Lee, W.-R. Yu, U. Jeong, U-I. Chung, J.-J. Park, O. Kim, Effects of Substrate on Piezoelectricity of Electrospun Poly(vinylidene fluoride)-Nanofiber-Based Energy Generators, ACS Appl. Mater. Interfaces 6 (2014) 3520−3527. https://doi.org/10.1021/am405684m.

[24] H. Shao, J. Fang, H. Wang, C. Lang, T. Lin, Robust Mechanical-to-Electrical Energy Conversion from Short-Distance Electrospun Poly(vinylidene fluoride) Fiber Webs, ACS Appl. Mater. Interfaces 7 (2015) 22551−22557. https://doi.org/10.1021/acsami.5b06863.

[25] D.-N. Nguyen, S. M. Yu, W. Moon, Electrospinning of poly(c-benzyl–a,L-glutamate) microfibers for piezoelectric polymer applications, J. Appl. Polym. Sci. 135 (2018) 46440. https://doi.org/10.1002/app.46440.

[26] M. Sajad Sorayani Bafqi, R. Bagherzadeh, M. Latifi, Fabrication of composite PVDF-ZnO nanofiber mats by electrospinning for energy scavenging application with enhanced efficiency, J. Polym. Res. 22 (2015) 130. https://doi.org/10.1007/s10965-015-0765-8.

[27] K. Shi, B. Sun, X. Huang, P. Jiang, Synergistic effect of graphene nanosheet and BaTiO$_3$ nanoparticles on performance enhancement of electrospun PVDF nanofiber mat for flexible piezoelectric nanogenerators, Nano Energy 52 (2018) 153-162. https://doi.org/10.1016/j.nanoen.2018.07.053.

[28] D. Dhakras, S. Ogale, High-Performance Organic–Inorganic Hybrid Piezo-Nanogenerator via Interface Enhanced Polarization Effects for Self-Powered Electronic Systems, Adv. Mater. Interfaces 3 (2016) 1600492. https://doi.org/10.1002/admi.201600492.

[29] S. Siddiqui, D.-I. Kima, E. Roh, L. Thai Duy, T. Quang Trung, M. Triet Nguyen, N.-E. Lee, A durable and stable piezoelectric nanogenerator with nanocomposite nanofibers embedded in an elastomer under high loading for a self-powered sensor system, Nano Energy 30 (2016) 434-442. https://doi.org/10.1016/j.nanoen.2016.10.034.

[30] A. Teka, S. Bairagi, M. Shahadat, M. Joshi, S. Ziauddin Ahammad, S. Wazed Ali, Poly (vinylidene fluoride)(PVDF)/potassium sodium niobate (KNN)–based nanofibrous web: A unique nanogenerator for renewable energy harvesting and investigating the role of KNN nanostructures, Polym. Adv. Technol. 29 (2018) 2537-2544. https://doi.org/10.1002/pat.4365.

[31] V. Vivekananthan, N. Rao Alluri, Y. Purusothaman, A. Chandrasekhar, S.-J. Kim, A flexible, planar energy harvesting device for scavenging road side waste mechanical energy via the synergistic piezoelectric response of $K_{0.5}Na_{0.5}NbO_3$-BaTiO$_3$/PVDF composite films, Nanoscale 9 (2017) 15122-15130. https://doi.org/10.1039/C7NR04115B.

[32] H. Paik, Y.-Y. Choi, S. Hong, K. No, Effect of Ag nanoparticle concentration on the electrical and ferroelectric properties of Ag/P(VDF-TrFE) composite films, Sci. Rep. 5 (2015) 13209. https://doi.org/10.1038/srep13209.

[33] U. Yaqoob, G.-S. Chung, Effect of reduced graphene oxide on the energy harvesting performance of P(VDF-TrFE)-BaTiO$_3$ nanocomposite devices, Smart Mater. Struct. 26 (2017) 095060. https://doi.org/10.1088/1361-665X/aa81a0.

[34] Y.-K. Fuh, J.-C. Ye, P.-C. Chen, H.-C. Ho, Z.-M. Huang, Hybrid Energy Harvester Consisting of Piezoelectric Fibers with Largely Enhanced 20 V for Wearable and Muscle-Driven Applications, ACS Appl. Mater. Interfaces 7 (2015) 16923−16931. https://doi.org/10.1021/acsami.5b03955.

[35] A. Talbourdet, F. Rault, G. Lemort, C. Cochrane, E. Devaux, C. Campagne, 3D interlock design 100% PVDF piezoelectric to improve energy harvesting, Smart Mater. Struct. 27 (2018) 075010. 10.1088/1361-665X/aab865.

[36] M. Boudriaux, F. Rault, C. Cochrane, G. Lemort, C. Campagne, E. Devaux, C. Courtois, Crystalline forms of PVDF fiber filled with clay components along processing steps, J. Appl. Polym. Sci. 133 (2016) 43244. https://doi.org/10.1002/app.43244.

[37] D. Ding, Z. Pan, D. Cuiuri, H. Li, Wire-feed additive manufacturing of metal components: technologies, developments and future interests, Int. J. Adv. Manuf. Technol. 81 (2015) 465-481. https://doi.org/10.1007/s00170-015-7077-3.

[38] Y. Cho, J.B. Park, B.-S. Kim, J. Lee, W.-K. Hong, I.-K. Park, J.E. Jang, J.I. Sohn, S.N. Cha, J. Min Kim, Enhanced energy harvesting based on surface morphology engineering of P(VDF-TrFE) film, Nano Energy 16 (2015) 524-532. https://doi.org/10.1016/j.nanoen.2015.07.006.

[39] M. Benz, W.B. Euler, O.J. Gregory, The role of solution phase wateron the deposition of thin films of poly(vinylidene fluoride), Macromolecules 35 (2002) 2682-2688. https://doi.org/10.1021/ma011744f.

[40] C.B. Lee, J.A Tarbutton, Electric Poling-Assisted Additive Manufacturing Process for Lead-Free Piezoelectric Device Fabrication, Procedia Manuf. 1 (2015) 320-326. https://doi.org/10.1016/j.promfg.2015.09.035.

[41] C. Lee, J.A. Tarbutton, Electric poling-assisted additive manufacturing process for PVDF polymer-based piezoelectric device applications, Smart Mater. Struct. 23 (2014) 095044. https://doi:10.1088/0964-1726/23/9/095044.

[42] J.H. Vinson, B.J. Jungnickel, Structure and stress dependence of pyroelectricity in poly(vinylidene fluoride), Ferroelectrics 216 (1998) 63−81. https://doi.org/10.1080/00150199808018228.

[43] J. Zhao, Z. You, A Shoe-Embedded Piezoelectric Energy Harvester for Wearable Sensors, Sensors 14 (2014) 12497-12510. https://doi.org/10.3390/s140712497.

[44] H.S. Nalwa, Ferroelectric polymers: chemistry: physics, and applications, CRC Press, 1995.

[45] S.K. Karan, D. Mandal, and B.B. Khatua, Self-powered flexible Fe-doped RGO/PVDF nanocomposite: an excellent material for a piezoelectric energy harvester, Nanoscale 7 (2015) 10655-10666. https://doi.org/10.1039/C5NR02067K.

[46] B. Ponraj, R. Bhimireddi, K. Varma, Effect of nano-and micron-sized $K_{0.5}Na_{0.5}NbO_3$ fillers on the dielectric and piezoelectric properties of PVDF composites, J. Adv. Ceram. 5 (2016) 308-320. https://doi.org/10.1007/s40145-016-0204-2.

[47] C. Wan, C.R. Bowen, Multiscale-structuring of polyvinylidene fluoride for energy harvesting: the impact of molecular-, micro-and macro-structure, J. Mater. Chem. A 5 (2017) 3091-3128. https://doi.org/10.1039/C6TA09590A.

[48] S. Bodkhe, G. Turcot, F.P. Gosselin, D. Therriault, One-step solvent evaporation-assisted 3D printing of piezoelectric PVDF nanocomposite structures, ACS Appl. Mater. Interfaces 9 (2017) 20833-20842. https://doi.org/10.1021/acsami.7b04095.

[49] C.K. Jeong, C. Baek, A.I. Kingon, K.-I. Park, S.-H. Kim, Lead-Free Perovskite Nanowire-Employed Piezopolymer for Highly Efficient Flexible Nanocomposite Energy Harvester, Small 14 (2018) 1704022. https://doi.org/10.1002/smll.201704022.

[50] A. Mandal, A.K. Nandi, Ionic liquid integrated multiwalled carbon nanotube in a poly (vinylidene fluoride) matrix: formation of a piezoelectric β-polymorph with significant reinforcement and conductivity improvement, ACS Appl. Mater. Interfaces 5 (2013) 747-760. https://doi.org/10.1021/am302275b.

[51] C. Mota, M. Labardi, L. Trombi, L. Astolfi, M. D'Acunto, D. Puppi, G. Gallone, F. Chiellini, S. Berrettini, L. Bruschini, and S. Danti, Design, fabrication and characterization of composite piezoelectric ultrafine fibers for cochlear stimulation, Mater. Design 122 (2017) 206-219. https://doi.org/10.1016/j.matdes.2017.03.013.

[52] T.G. Mofokeng, A.S. Luyt, V.P. Pavlović, V.B. Pavlović, D. Dudić, B. Vlahović, V. Djoković, Ferroelectric nanocomposites of polyvinylidene fluoride/polymethyl methacrylate blend and BaTiO$_3$ particles: Fabrication of β-crystal polymorph rich matrix through mechanical activation of the filler, J. Appl. Phys.115 (2014) 084109. https://doi.org/10.1063/1.4866694.

[53] B. Dutta, E. Kar, N. Bose, S. Mukherjee, Significant enhancement of the electroactive β-phase of PVDF by incorporating hydrothermally synthesized copper oxide nanoparticles, RSC Adv. 5 (2015) 105422-105434. https://doi.org/10.1039/C5RA21903E.

[54] C. Zhang, Y. Fan, H. Li, Y. Li, L. Zhang, S. Cao, S. Kuang, Y. Zhao, A. Chen, G. Zhu, Fully Rollable Lead-Free Poly (vinylidene fluoride)-Niobate-Based Nanogenerator with Ultra-Flexible Nano-Network Electrodes, ACS Nano 12 (2018) 4803-4811. https://doi.org/10.1021/acsnano.8b01534.

[55] N.R. Alluri, B. Saravanakumar, S.-J. Kim, Flexible, Hybrid Piezoelectric Film (BaTi$_{(1-x)}$Zr$_x$O$_3$)/PVDF Nanogenerator as a Self-Powered Fluid Velocity Sensor, ACS Appl. Mater. Interfaces 7 (2015) 9831-9840. https://doi.org/10.1021/acsami.5b01760.

[56] D. Rouxel, B. Vincent, L. Badie, F.D. Dos Santos, E. Lamouroux, Y. Fort, Influence of cluster size and surface functionalization of ZnO nanoparticles on the morphology, thermomechanical and piezoelectric properties of P (VDF-TrFE) nanocomposite films, Appl. Surf. Sci. 279 (2013) 204-211. https://doi.org/10.1016/j.apsusc.2013.04.070.

[57] M. Choi, G. Murillo, S. Hwang, J.W. Kim, J.H. Jung, C.-Y. Chen, M. Lee, Mechanical and electrical characterization of PVDF-ZnO hybrid structure for application to nanogenerator, Nano Energy 33 (2017) 462-468. https://doi.org/10.1016/j.nanoen.2017.01.062.

[58] D. Singh, A. Choudhary, A. Garg, Flexible and robust piezoelectric polymer nanocomposites based energy harvesters, ACS Appl. Mater. Interfaces 10 (2018) 2793-2800. https://doi.org/10.1021/acsami.7b16973.

[59] B. Dutta, E. Kar, N. Bose, S. Mukherjee, NiO@SiO$_2$/PVDF: A Flexible Polymer Nanocomposite for a High Performance Human Body Motion-Based Energy Harvester and Tactile e-Skin Mechanosensor, ACS Sustain. Chem. Eng. 6 (2018) 10505-10516. https://doi.org/10.1021/acssuschemeng.8b01851.

[60] N.R. Alluri, A. Chandrasekhar, J.H. Jeong, S.-J. Kim, Enhanced electroactive β-phase of the sonication-process-derived PVDF-activated carbon composite film for efficient energy conversion and a battery-free acceleration sensor, J. Mater. Chem. C 5 (2017) 4833-4844. https://doi.org/10.1039/C7TC00568G.

[61] S. Begum, A. Kausar, H. Ullah, M. Siddiq, Exploitation of carbon nanotubes in high performance polyvinylidene fluoride matrix composite: A review, Polymer-Plastics Technol. Eng. 55 (2016) 199-222. https://doi.org/10.1080/03602559.2015.1055505.

[62] G.G. Genchi, A. Marino, A. Rocca, V. Mattoli, G. Ciofani, Barium titanate nanoparticles: promising multitasking vectors in nanomedicine, Nanotechnology 27 (2016) 232001. https://doi.org/10.1088/0957-4484/27/23/232001.

[63] E. Kabir, M. Khatun, L. Nasrin, M.J. Raihan, M. Rahman, Pure β-phase formation in polyvinylidene fluoride (PVDF)-carbon nanotube composites, J. Phys. D: Appl. Phys. 50 (2017) 163002. https://doi.org/10.1088/1361-6463/aa5f85.

[64] J.K.Y. Lee, N. Chen, S. Peng, L. Li, L. Tian, N. Thakor, S. Ramakrishna, Polymer-based composites by electrospinning: Preparation & functionalization with nanocarbons, Prog. Polym. Sci. (2018) 40-84. https://doi.org/10.1016/j.progpolymsci.2018.07.002.

[65] C.M. Wu, M.H. Chou, Polymorphism, piezoelectricity and sound absorption of electrospun PVDF membranes with and without carbon nanotubes, Compos. Sci. Technol. 127 (2016) 127-133. https://doi.org/10.1016/j.compscitech.2016.03.001.

[66] M. Abbasipour, R. Khajavi, A. Akbar Yousefi, M. Esmail Yazdanshenas, F. Razaghian, The piezoelectric response of electrospun PVDF nanofibers with graphene oxide, graphene, and halloysite nanofillers: a comparative study, J. Mater. Sci: Mater. Electron. 28 (2017) 15942-15952. https://doi.org/ 10.1007/s10854-017-7491-4.

[67] D. Bitounis, H. Ali-Boucetta, B. Hee Hong , D.-H. Min, K. Kostarelos, Prospects and Challenges of Graphene in Biomedical Applications, Adv. Mater. 25 (2013) 2258-2268. https://doi.org/10.1002/adma.201203700.

[68] N.A. Hoque, P. Thakur, S. Roy, A. Kool, B. Bagchi, P. Biswas, M.M. Saikh, F. Khatun, S. Das, P.P. Ray, Er^{3+}/Fe^{3+} Stimulated Electroactive, Visible Light Emitting, and High Dielectric Flexible PVDF Film Based Piezoelectric Nanogenerators: A Simple and Superior Self-Powered Energy Harvester with Remarkable Power Density, ACS Appl. Mater. Interfaces 9 (2017) 23048-23059. https://doi.org/10.1021/acsami.7b08008.

[69] Y. Xin, X. Qi, H. Tian, C. Guo, X. Li, J. Lin, C. Wang, Full-fiber piezoelectric sensor by straight PVDF/nanoclay nanofibers, Mater. Lett. 164 (2016) 136-139. https://doi.org/10.1016/j.matlet.2015.09.117.

[70] P. Thakur, A. Kool, B. Bagchi, S. Das, P. Nandy, Enhancement of β phase crystallization and dielectric behavior of kaolinite/halloysite modified poly (vinylidene fluoride) thin films, Appl. Clay Sci. 99 (2014) 149-159. https://doi.org/10.1016/j.clay.2014.06.025.

[71] S.K. Ghosh, T.K. Sinha, B. Mahanty, D. Mandal, Self-poled Efficient Flexible "Ferroelectretic" Nanogenerator: A New Class of Piezoelectric Energy Harvester, Energy Technol. 3 (2015) 1190-1197. https://doi.org/10.1002/ente.201500167.

[72] C.H. Liow, X. Lu, C.F. Tan, K.H. Chan, K. Zeng, S. Li, G.W. Ho, Spatially Probed Plasmonic Photothermic Nanoheater Enhanced Hybrid Polymeric–Metallic PVDF-Ag Nanogenerator, Small 14 (2018) 1702268. https://doi.org/10.1002/smll.201702268.

[73] S. Siddiqui, D.-I. Kim, L.T. Duy, M.T. Nguyen, S. Muhammad, W.-S. Yoon, N.-E. Lee, High-performance flexible lead-free nanocomposite piezoelectric nanogenerator for biomechanical

energy harvesting and storage, Nano Energy 15 (2015) 177-185. https://doi.org/10.1016/j.nanoen.2015.04.030.

[74] S.-H. Shin, Y.-H. Kim, M.H. Lee, J.-Y. Jung, J. Nah, Hemispherically aggregated $BaTiO_3$ nanoparticle composite thin film for high-performance flexible piezoelectric nanogenerator, ACS Nano 8 (2014) 2766-2773. https://doi.org/10.1021/nn406481k.

[75] S. Cho, J.S. Lee, J. Jang, Enhanced Crystallinity, Dielectric, and Energy Harvesting Performances of Surface-Treated Barium Titanate Hollow Nanospheres/PVDF Nanocomposites, Adv. Mater. Interfaces 2 (2015) 1500098. https://doi.org/10.1002/admi.201500098.

[76] X. Zhang, C. Zhang, Y. Lin, P. Hu, Y. Shen, K. Wang, S. Meng, Y. Chai, X. Dai, X. Liu, Y. Liu, X. Mo, C. Cao, S. Li, X. Deng, L. Chen, Nanocomposite membranes enhance bone regeneration through restoring physiological electric microenvironment, ACS Nano 10 (2016) 7279-7286. https://doi.org/10.1021/acsnano.6b02247.

[77] G.G. Genchi, E. Sinibaldi, L. Ceseracciu, M. Labardi, A. Marino, S. Marras, G. de Simoni, V. Mattoli, G. Ciofani, Ultrasound-activated piezoelectric P(VDF-TrFE)/boron nitride nanotube composite films promote differentiation of human SaOS-2 osteoblast-like cells, Nanomedicine: NBM 14 (2017) 2421-2432. https://doi.org/10.1016/j.nano.2017.05.006.

[78] H.B. Lopes, T.de S. Santos, F.S. de Oliveira, G.P. Freitas, A.L.G. de Almeida, R. Gimenes, A.L. Rosa, and M.M. Beloti, Poly (vinylidene-trifluoroethylene)/barium titanate composite for in vivo support of bone formation, J. Biomat. Appl. 29 (2014) 104-112. https://doi.org/10.1177/0885328213515735.

[79] G.G. Genchi, L. Ceseracciu, A. Marino, M. Labardi, S. Marras, F. Pignatelli, L. Bruschini, V. Mattoli, G. Ciofani, P(VDF-TrFE)/$BaTiO_3$ Nanoparticle Composite Films Mediate Piezoelectric Stimulation and Promote Differentiation of SH-SY5Y Neuroblastoma Cells, Adv. Healthcare Mater. 5 (2016) 1808-1820. https://doi.org/10.1002/adhm.201600245.

[80] J. Nunes-Pereira, V. Sencadas, V. Correia, V.F. Cardoso, W. Han, J.G. Rocha, S. Lanceros-Méndez, Energy harvesting performance of $BaTiO_3$/poly (vinylidene fluoride–trifluoroethylene)

spin coated nanocomposites, Compos. Part B: Eng. 72 (2015) 130-136. https://doi.org/10.1016/j.compositesb.2014.12.001.

[81] J. Nunes-Pereira, V. Sencadas, V. Correia, J.G. Rocha, S. Lanceros-Méndez, Energy harvesting performance of piezoelectric electrospun polymer fibers and polymer/ceramic composites, Sens. Actuators A: Phys. 196 (2013) 55-62. https://doi.org/10.1016/j.sna.2013.03.023.

[82] Y. Feng, W. Li, Y. Hou, Y. Yu, W. Cao, T. Zhang, W. Fei, Enhanced dielectric properties of PVDF-HFP/BaTiO 3-nanowire composites induced by interfacial polarization and wire-shape, J. Mater. Chem. C 3 (2015) 1250-1260. https://doi.org/10.1039/C4TC02183E.

[83] D. Guo, K. Cai, Y. Wang, A distinct mutual phase transition in a new PVDF based lead-free composite film with enhanced dielectric and energy storage performance and low loss, J. Mater. Chem. C 5 (2017) 2531-2541. https://doi.org/10.1039/C6TC04648G.

[84] J. Fu, Y. Hou, M. Zheng, M. Zhu, Comparative study of dielectric properties of the PVDF composites filled with spherical and rod-like $BaTiO_3$ derived by molten salt synthesis method, J. Mater. Sci. 53 (2018) 7233-7248. https://doi.org/10.1007/s10853-018-2114-x.

[85] C. Li, L. Wang, W. Chen, L. Lu, H. Nan, D. Wang, Y. Zhang, Y. Yang, C.L. Jia, A Novel Multiple Interface Structure with the Segregation of Dopants in Lead-Free Ferroelectric $(K_{0.5}Na_{0.5})$ NbO_3 Thin Films, Adv. Mater. Interfaces 5 (2018) 1700972. https://doi.org/10.1002/admi.201700972.

[86] X. Vendrell, J. García, X. Bril, D. Ochoa, L. Mestres, G. Dezanneau, Improving the functional properties of $(K_{0.5}Na_{0.5})NbO_3$ piezoceramics by acceptor doping, J. Eur. Ceram. Soc. 35 (2015) 125-130. https://doi.org/10.1016/j.jeurceramsoc.2014.08.033.

[87] Y. Lu, N.W. Emanetoglu, Y. Chen, ZnO piezoelectric devices, in: C. Jagadish, S.J. Pearton (Eds.), Zinc Oxide Bulk, Thin Films and Nanostructures, Elsevier, 2006, pp. 443-489.

[88] L. Le Brizoual, J. Krüger, O. Elmazria, B. Vincent, L. Bouvot, M. Kolle, D. Rouxel, P. Alnot, Mapping of microwave-induced phonons by μ-Brillouin spectroscopy: hypersons in ZnO on silicon, J. Phys. D: Appl. Phys. 41 (2008) 105502. https://doi.org/10.1088/0022-3727/41/10/105502.

[89] S. Xu, Y. Wei, M. Kirkham, J. Liu, W. Mai, D. Davidovic, R.L. Snyder, Z.L. Wang, Patterned growth of vertically aligned ZnO nanowire arrays on inorganic substrates at low temperature without catalyst, J. Am. Chem. Soc. 130 (2008) 14958-14959. https://doi.org/10.1021/ja806952j.

[90] P. Thakur, A. Kool, N.A. Hoque, B. Bagchi, F. Khatun, P. Biswas, D. Brahma, S. Roy, S. Banerjee, S. Das, Superior performances of in situ synthesized ZnO/PVDF thin film based self-poled piezoelectric nanogenerator and self-charged photo-power bank with high durability, Nano Energy 44 (2018) 456-467. https://doi.org/10.1016/j.nanoen.2017.11.065.

[91] M.M. Alam, A. Sultana, D. Mandal, Biomechanical and Acoustic Energy Harvesting from TiO_2 Nanoparticle Modulated PVDF Nanofiber Made High Performance Nanogenerator, ACS Appl. Energy Mater. 1 (2018) 3103-3112. https://doi.org/10.1021/acsaem.8b00216.

[92] Y. Zhou, J. He, J. Hu, B. Dang, Surface-modified MgO nanoparticle enhances the mechanical and direct-current electrical characteristics of polypropylene/polyolefin elastomer nanodielectrics, J. Appl. Polym. Sci. 132 (2016). 42863 https://doi.org/10.1002/app.42863.

[93] S. Peng, J. He, J. Hu, X. Huang, P. Jiang, Influence of functionalized MgO nanoparticles on electrical properties of polyethylene nanocomposites, IEEE Trans. Dielectr. Electr. Insul. 22 (2015) 1512-1519. https://doi.org/10.1109/TDEI.2015.7116346.

[94] A. Hassen, T. Hanafy, S. El-Sayed, A. Himanshu, Dielectric relaxation and alternating current conductivity of polyvinylidene fluoride doped with lanthanum chloride, J. Appl. Phys. 110 (2011) 114119. https://doi.org/10.1063/1.3669396.

[95] S. El-Sayed, T. Abdel-Baset, A. Hassen, Dielectric properties of PVDF thin films doped with 3 wt.% of RCl_3 (R= Gd or Er), AIP Adv. 4 (2014) 037114. https://doi.org/10.1063/1.4869093.

[96] P. Thakur, A. Kool, B. Bagchi, N.A. Hoque, S. Das, P. Nandy, The role of cerium (iii)/yttrium (iii) nitrate hexahydrate salts on electroactive β phase nucleation and dielectric properties of poly (vinylidene fluoride) thin films, RSC Adv. 5 (2015) 28487-28496. https://doi.org/10.1039/C5RA03524D.

[97] S. Garain, T.K. Sinha, P. Adhikary, K. Henkel, S. Sen, S. Ram, C. Sinha, D. Schmeißer, D. Mandal, Self-poled transparent and flexible UV light-emitting cerium complex–PVDF composite: a high-performance nanogenerator, ACS Appl. Mater. Interfaces 7 (2015) 1298-1307. https://doi.org/10.1021/am507522r.

[98] S.K. Ghosh, A. Biswas, S. Sen, C. Das, K. Henkel, D. Schmeisser, D. Mandal, Yb^{3+} assisted self-polarized pvdf based ferroelectretic nanogenerator: a facile strategy of highly efficient mechanical energy harvester fabrication, Nano Energy 30 (2016) 621-629. https://doi.org/10.1016/j.nanoen.2016.10.042.

[99] P. Adhikary, D. Mandal, Enhanced electro-active phase in a luminescent P (VDF–HFP)/Zn^{2+} flexible composite film for piezoelectric based energy harvesting applications and self-powered UV light detection, Phys. Chem. Chem. Phys.19 (2017) 17789-17798. https://doi.org/10.1039/C7CP01714F.

[100] P. Adhikary, S. Garain, D. Mandal, The co-operative performance of a hydrated salt assisted sponge like P (VDF-HFP) piezoelectric generator: an effective piezoelectric based energy harvester, Phys. Chem. Chem. Phys. 17 (2015) 7275-7281. https://doi.org/10.1039/C4CP05513F.

[101] P. Adhikary, S. Garain, S. Ram, D. Mandal, Flexible hybrid Eu^{3+} doped P(VDF-HFP) nanocomposite film possess hypersensitive electronic transitions and piezoelectric throughput, J. Polym. Sci. Part B: Polym. Phys.54 (2016) 2335-2345. https://doi.org/10.1002/polb.24144.

[102] Y.M. Yousry, K. Yao, S. Chen, W.H. Liew, S. Ramakrishna, Mechanisms for Enhancing Polarization Orientation and Piezoelectric Parameters of PVDF Nanofibers, Adv. Electron. Mater. 4 (2018) 1700562. https://doi.org/10.1002/aelm.201700562.

[103] A.A. Issa, M.A. Al-Maadeed, A.S. Luyt, D. Ponnamma, M.K. Hassan, Physico-mechanical, dielectric, and piezoelectric properties of PVDF electrospun mats containing silver nanoparticles, C 3 (2017) 30. https://doi.org/10.3390/c3040030.

[104] S. Barrau, A. Ferri, A. Da Costa, J. Defebvin, S. Leroy, R. Desfeux, J.-M. Lefebvre, Nanoscale Investigations of α-and γ-Crystal Phases in PVDF-Based Nanocomposites, ACS Appl. Mater. Interfaces 10 (2018) 13092-13099. https://doi.org/10.1021/acsami.8b02172.

[105] S. Lee, Y. Lim, Generating Power Enhancement of Flexible PVDF Generator by Incorporation of CNTs and Surface Treatment of PEDOT: PSS Electrodes, Macromolecular Mater. Eng. (2018) 1700588. https://doi.org/10.1002/mame.201700588.

[106] S. Huang, W.A. Yee, W.C. Tjiu, Y. Liu, M. Kotaki, Y.C.F. Boey, J. Ma, T. Liu, X. Lu, Electrospinning of polyvinylidene difluoride with carbon nanotubes: synergistic effects of extensional force and interfacial interaction on crystalline structures, Langmuir 24 (2008) 13621-13626. https://doi.org/10.1021/la8024183.

[107] H. Ye, H. Lam, N. Titchenal, Y. Gogotsi, F. Ko, Reinforcement and rupture behavior of carbon nanotubes–polymer nanofibers, Appl. Phys. Lett. 85 (2004) 1775-1777. https://doi.org/10.1063/1.1787892.

[108] P.-C. Ma, N.A. Siddiqui, G. Marom, J.-K. Kim, Dispersion and functionalization of carbon nanotubes for polymer-based nanocomposites: a review, Compos. Part A: Appl. Sci. Manuf. 41 (2010) 1345-1367. https://doi.org/10.1016/j.compositesa.2010.07.003.

[109] S. Manna, A.K. Nandi, Piezoelectric β polymorph in poly (vinylidene fluoride)-functionalized multiwalled carbon nanotube nanocomposite films, J. Phys. Chem. C 111 (2007) 14670-14680. https://doi.org/10.1021/jp073102l.

[110] G. O'Bryan, E. Yang, T. Zifer, K. Wally, J. Skinner, A. Vance, Nanotube surface functionalization effects in blended multiwalled carbon nanotube/PVDF composites, J. Appl. Polym. Sci. 120 (2011) 1379-1384. https://doi.org/10.1002/app.33264.

[111] Z.M. Dang, L. Wang, Y. Yin, Q. Zhang, Q.Q. Lei, Giant dielectric permittivities in functionalized carbon-nanotube/electroactive-polymer nanocomposites, Adv. Mater. 19 (2007) 852-857. https://doi.org/10.1002/adma.20060070.

[112] K. Ke, P. Pötschke, D. Jehnichen, D. Fischer, B. Voit, Achieving β-phase poly (vinylidene fluoride) from melt cooling: Effect of surface functionalized carbon nanotubes, Polymer 55 (2014) 611-619. https://doi.org/10.1016/j.polymer.2013.12.014.

[113] Y. Ahn, J.Y. Lim, S.M. Hong, J. Lee, J. Ha, H.J. Choi, Y. Seo, Enhanced piezoelectric properties of electrospun poly (vinylidene fluoride)/multiwalled carbon nanotube composites due to high β-phase formation in poly (vinylidene fluoride), J. Phys. Chem. C 117 (2013) 11791-11799. https://doi.org/10.1021/jp4011026.

[114] L. Yang, H. Ji, K. Zhu, J. Wang, J. Qiu, Dramatically improved piezoelectric properties of poly (vinylidene fluoride) composites by incorporating aligned TiO_2@MWCNTs, Composi. Sci. Technol. 123 (2016) 259-267. https://doi.org/10.1016/j.compscitech.2015.11.032.

[115] M. Wang, L. Li, S. Zhou, R. Tang, Z. Yang, X. Zhang, Influence of CNTs on crystalline microstructure and ferroelectric behavior of P (VDF-TrFE), Langmuir 34 (2018) 10702-10710. https://doi.org/10.1021/acs.langmuir.8b02392.

[116] F. Mokhtari, M. Shamshirsaz, M. Latifi, S. Asadi, Comparative evaluation of piezoelectric response of electrospun PVDF (polyvinilydine fluoride) nanofiber with various additives for energy scavenging application, J. Text. I. 108 (2017) 906-914. https://doi.org/10.1080/00405000.2016.1202091.

[117] A. Gaur, C. Kumar, S. Tiwari, P. Maiti, Efficient energy harvesting using processed poly (vinylidene fluoride) nanogenerator, ACS Appl. Energy Mater. 1 (2018) 3019-3024. https://doi.org/10.1021/acsaem.8b00483.

[118] V. Cauda, S. Stassi, K. Bejtka, G. Canavese, Nanoconfinement: an effective way to enhance PVDF piezoelectric properties, ACS Appl. Mater. Interfaces 5 (2013) 6430. https://doi.org/10.1021/am4016878.

[119] A. Wang, Z. Liu, M. Hu, C. Wang, X. Zhang, B. Shi, Y. Fan, Y. Cui, Z. Li, and K. Ren, Piezoelectric nanofibrous scaffolds as in vivo energy harvesters for modifying fibroblast alignment

and proliferation in wound healing, Nano Energy 43 (2018) 63-71. https://doi.org/10.1016/j.nanoen.2017.11.023.

[120] N. Soin, D. Boyer, K. Prashanthi, S. Sharma, A. A. Narasimulu, J. Luo, T. H. Shah, E. Siores, T. Thundat, Exclusive self-aligned b-phase PVDF films with abnormal piezoelectric coefficient prepared via phase inversion, Chem. Commun. 51 (2015) 8257-8260. https://doi.org/10.1039/C5CC01688F.

[121] X. Liu, J. Ma, X. Wu, L. Lin, X. Wang, Polymeric nanofibers with ultrahigh piezoelectricity via self-orientation of nanocrystals, ACS Nano 11 (2017) 1901-1910. https://doi.org/10.1021/acsnano.6b07961.

[122] M. Sharma, V. Srinivas, G. Madras, S. Bose, Outstanding dielectric constant and piezoelectric coefficient in electrospun nanofiber mats of PVDF containing silver decorated multiwall carbon nanotubes: assessing through piezoresponse force microscopy, RSC Adv. 6 (2016) 6251-6258. https://doi.org/10.1039/C5RA25671B.

[123] S. Bodkhe, P. Rajesh, F.P. Gosselin, D. Therriault, Simultaneous 3D Printing and Poling of PVDF and Its Nanocomposites, ACS Appl. Energy Mater. 1 (2018) 2474-2482. https://doi.org/10.1021/acsaem.7b00337.

[124] M. Mishra, A. Roy, S. Dash, S. Mukherjee, Flexible nano-GFO/PVDF piezoelectric-polymer nanocomposite films for mechanical energy harvesting, IOP Conf. Series: Mater. Sci. Eng. 338 (2018) 012026. https://doi.org/10.1088/1757-899X/338/1/012026.

[125] S. Siddiqui, H. B. Lee, D.-I. Kim, L. Thai Duy, A. Hanif, N.-E. Lee, An Omnidirectionally Stretchable Piezoelectric Nanogenerator Based on Hybrid Nanofibers and Carbon Electrodes for Multimodal Straining and Human Kinematics Energy Harvesting, Adv. Energy Mater. 8 (2018) 1701520. https://doi.org/10.1002/aenm.201701520.

[126] U. Yaqoob, A.S.M. Iftekhar Uddin, G.-S. Chung, A novel tri-layer flexible piezoelectric nanogenerator based on surface- modified graphene and PVDF-BaTiO$_3$ nanocomposites, Appl. Surf. Sci. 405 (2017) 420-426. https://doi.org/10.1016/j.apsusc.2017.01.314.

[127] S. Kumar Si, S. Kumar Karan, S. Paria, A. Maitra, A. K. Das, R. Bera, A. Bera, L. Halder, B. B. Khatua, A strategy to develop an efficient piezoelectric nanogenerator through ZTO assisted g-phase nucleation of PVDF in ZTO/PVDF nanocomposite for harvesting bio-mechanical energy and energy storage application, Mater. Chem. Phys. 213 (2018) 525-537. https://doi.org/10.1016/j.matchemphys.2018.04.013.

[128] Y. Yu, H. Sun, H. Orbay, F. Chen, C. G. England, W. Cai, X. Wang, Biocompatibility and in vivo operation of implantable mesoporous PVDF-based nanogenerators, Nano Energy 27 (2016) 275-281. https://doi.org/10.1016/j.nanoen.2016.07.015.

[129] E.J. Lee, T.Y. Kim, S.-W. Kim, S. Jeong, Y. Choi, S.Y. Lee, High-performance piezoelectric nanogenerators based on chemically-reinforced composites, Energy Environ. Sci. 11 (2018) 1425-1430. https://doi.org/10.1039/C8EE00014J.

[130] R. Md Habibur, U. Yaqoob, S. Muhammad, A.S.M.I. Uddin , H.C. Kim, The effect of RGO on dielectric and energy harvesting properties of P(VDF-TrFE) matrix by optimizing electroactive b phase without traditional polling process, Mater. Chem. Phys. 215 (2018) 46-55. https://doi.org/10.1016/j.matchemphys.2018.05.010.

[131] M. Mahdi Abolhasania, K. Shirvanimoghaddam, M. Naebe, PVDF/graphene composite nanofibers with enhanced piezoelectric performance for development of robust nanogenerators, Compos. Sci. Technol. 138 (2017) 49-56. https://doi.org/10.1016/j.compscitech.2016.11.017.

[132] T. Kumar Sinha, S. Kumar Ghosh, R. Maiti, S. Jana, B. Adhikari, D. Mandal, S. K. Ray, Graphene-Silver-Induced Self-Polarized PVDF-Based Flexible Plasmonic Nanogenerator Toward the Realization for New Class of Self Powered Optical Sensor, ACS Appl. Mater. Interfaces 8 (2016) 14986-14993. https://doi.org/10.1021/acsami.6b01547.

[133] M. Pusty, A. Sharma, L. Sinha, A. Chaudhary, P. Shirage, Comparative Study with a Unique Arrangement to Tap Piezoelectric Output to Realize a Self Poled PVDF Based Nanocomposite for Energy Harvesting Applications, ChemistrySelect 2 (2017) 2774-2782. https://doi.org/10.1002/slct.201602046.

[134] C. Kumar, A. Gaur, S. Kumar Rai, P. Maiti, Piezo devices using poly(vinylidene fluoride)/reduced graphene oxide hybrid for energy harvesting, Nano-Struct. Nano-Objects 12 (2017) 174-181. https://doi.org/10.1016/j.nanoso.2017.10.006.

[135] W. Tong, Y. Zhang, L. Yu, X. Luan, Q. An, Q. Zhang, F. Lv, P. K. Chu, B. Shen, Z. Zhang, Novel Method for the Fabrication of Flexible Film with Oriented Arrays of Graphene in Poly(vinylidene fluoride-cohexafluoropropylene) with Low Dielectric Loss, J. Phys. Chem. C 118 (2014) 10567−10573. https://doi.org/10.1021/jp411828e.

[136] S. Kumar Karan, R. Bera, S. Paria, A. Kumar Das, S. Maiti, A. Maitra, B. Bhusan Khatua, An Approach to Design Highly Durable Piezoelectric Nanogenerator Based on Self-Poled PVDF/AlO-rGO Flexible Nanocomposite with High Power Density and Energy Conversion Efficiency, Adv. Energy Mater. 6 (2016) 1601016. https://doi.org/10.1002/aenm.201601016.

[137] Y. Tajitsu, Piezoelectricity of chiral polymeric fiber and its application in biomedical engineering, IEEE Trans. Ultrason., Ferroelectr., Freq. Control 55 (2008) 1000-1008. https://doi.org/10.1109/TUFFC.2008.746.

[138] T. Kaura, R. Nath, M. Perlman, Simultaneous stretching and corona poling of PVDF films, J. Phys.D: Appl. Phys. 24 (1991) 1848. https://doi.org/10.1088/0022-3727/24/10/020.

[139] G.W. Day, C.A. Hamilton, R. Peterson, R. Phelan Jr, L. Mullen, Effects of poling conditions on responsivity and uniformity of polarization of PVF_2 pyroelectric detectors, Appl. Phys. Lett. 24 (1974) 456-458. https://doi.org/10.1063/1.1655010.

[140] V. Kochervinskii, D. Kiselev, M. Malinkovich, N. Shmakova, An effect of the film texture on high-voltage polarization and local piezoelectric properties of the ferroelectric copolymer of vinylidene fluoride, Colloid Polym. Sci. 296 (2018) 1057-1070. https://doi.org/10.1007/s00396-018-4317-8.

[141] J. Wu, D. Xiao, W. Wu, Q. Chen, J. Zhu, Z. Yang, J. Wang, Composition and poling condition-induced electrical behavior of $(Ba_{0.85}Ca_{0.15})(Ti_{1−x}Zr_x)O_3$ lead-free piezoelectric ceramics, J. Eur. Ceram.Soc. 32 (2012) 891-898. https://doi.org/10.1016/j.jeurceramsoc.2011.11.003.

[142] E.M. Fuentes-Fernandez, B.E. Gnade, M.A. Quevedo-Lopez, P. Shah, H.N. Alshareef, The effect of poling conditions on the performance of piezoelectric energy harvesters fabricated by wet chemistry, J. Mater. Chem. A 3 (2015) 9837-9842. https://doi.org/10.1039/C5TA00447K.

[143] M.H.M. Radzi, K.S. Leong, Investigation of the piezoelectric charge coefficient d_{33} of thick-film piezoelectric ceramics by varying poling and repoling conditions, AIP Conference Proceedings, AIP Publishing, 1660 (2015) 070083. https://doi.org/10.1063/1.4915801.

[144] E. Nilsson, A. Lund, C. Jonasson, C. Johansson, B. Hagström, Poling and characterization of piezoelectric polymer fibers for use in textile sensors, Sens. Actuators A: Phys. 201 (2013) 477-486. https://doi.org/10.1016/j.sna.2013.08.011.

[145] A. Kumar, M. Periman, Simultaneous stretching and corona poling of PVDF and P(VDF-TriFE) films. II, J.Phys. D: Appl. Phys. 26 (1993) 469. https://doi.org//10.1088/0022-3727/26/3/020.

[146] M. Wegener, R. Gerhard-Multhaupt, Electric poling and electromechanical characterization of 0.1-mm-thick sensor films and 0.2-mm-thick cable layers from poly (vinylidene fluoride-trifluroethylene), IEEE Trans. Ultrason., Ferroelectr., Freq. Control 50 (2003) 921-931. https://doi.org/10.1109/TUFFC.2003.1214511.

[147] Y.-S. Kim, Y. Xie, X. Wen, S. Wang, S.J. Kim, H.-K. Song, Z.L. Wang, Highly porous piezoelectric PVDF membrane as effective lithium ion transfer channels for enhanced self-charging powercell, Nano Energy 14 (2015) 77-86. https://doi.org/10.1016/j.nanoen.2015.01.006.

[148] N. Murayama, T. Oikawa, T. Katto, K. Nakamura, Persistent polarization in poly(vinylidene fluoride). II. Piezoelectricity of poly(vinylidene fluoride) thermoelectrets, J. Polym. Sci. Polym. Phys. Ed. 13 (1975) 1033. https://doi.org/10.1002/pol.1975.180130515.

[149] Y. Zhao, Q. Liao, G. Zhang, Z. Zhang, Q. Liang, X. Liao, Y. Zhang, High output piezoelectric nanocomposite generators composed of oriented $BaTiO_3$ NPs@PVDF, Nano Energy 11 (2015) 719-727. https://doi.org/10.1016/j.nanoen.2014.11.061.

[150] K. Arlt, M. Wegener, Piezoelectric PZT/PVDF-copolymer 0-3 composites: aspects on film preparation and electrical poling, IEEE Trans. Dielectr. Electr. Insul. 17 (2010) 1178-1184. https://doi.org/10.1109/TDEI.2010.5539688.

[151] J. Malmonge, L. Malmonge, G. Fuzari Jr, S. Malmonge, W. Sakamoto, Piezo and dielectric properties of PHB–PZT composite, Polym. Compos. 30 (2009) 1333-1337. https://doi.org/10.1002/pc.20719.

[152] J.-S. Chang, P.A. Lawless, T. Yamamoto, Corona discharge processes, IEEE Trans. Plasma Sci. 19 (1991) 1152-1166. https://doi.org/10.1109/27.125038.

[153] R. Gonçalves, V. F. Cardoso, Nelson Pereira, Juliana Oliveira, J.Nunes-Pereira, C.M. Costa, S. Lanceros-Méndez, Evaluation of the Physicochemical Properties and Active Response of Piezoelectric Poly(vinylidene fluoride-co-trifluoroethylene) as a Function of Its Microstructure, J. Phys. Chem. C 122 (2018) 11433−11441. https://doi.org/10.1021/acs.jpcc.8b02605.

[154] J. Pärssinen, H. Hammarén, R. Rahikainen, V. Sencadas, C. Ribeiro, S. Vanhatupa, S. Miettinen, S. Lanceros-Méndez, V.P. Hytönen, Enhancement of adhesion and promotion of osteogenic differentiation of human adipose stem cells by poled electroactive poly (vinylidene fluoride), J. Biomed. Mater. Res. Part A 103 (2015) 919-928. https://doi.org/10.1002/jbm.a.35234.

[155] H. Kim, F. Torres, Y. Wu, D. Villagran, Y. Lin, T.-L.B.J.S.M. Tseng, Integrated 3D printing and corona poling process of PVDF piezoelectric films for pressure sensor application, Smart Mater. Struct. 26 (2017) 085027. https://doi.org/10.1088/1361-665X/aa738.

[156] V. Sencadas, C. Ribeiro, A. Heredia, I. Bdikin, A.L. Kholkin, S. Lanceros-Méndez, Local piezoelectric activity of single poly (L-lactic acid)(PLLA) microfibers, Appl. Phys. A 109 (2012) 51-55. https://doi.org/10.1007/s00339-012-7095-z.

[157] Y. Tajitsu, Fundamental study on improvement of piezoelectricity of poly (ι-lactic acid) and its application to film actuators, IEEE Trans. Ultrason., Ferroelectr., Freq. Control 60 (2013) 1625-1629. https://doi.org/10.1109/TUFFC.2013.2744.

[158] M.C. Garcia-Gutierrez, A. Linares, J.J. Hernandez, D. R. Rueda, T.A. Ezquerra, P. Poza, R.J. Davies, Confinement-Induced One-Dimensional Ferroelectric Polymer Arrays, Nano Lett. 10 (2010) 1472. https://doi.org/10.1021/nl100429u.

[159] V. Cauda, B. Torre, A. Falqui, G. Canavese, S. Stassi, T. Bein, M. Pizzi, Confinement in Oriented Mesopores Induces Piezoelectric Behavior of Polymeric Nanowires, Chem. Mater. 24 (2012) 4215. https://doi.org/10.1021/cm302594s.

[160] A. Tamang, S. Kumar Ghosh, S. Garain, Md. Mehebub Alam, J. Haeberle, K. Henkel, D. Schmeisser, D. Mandal, DNA-Assisted β-phase Nucleation and Alignment of Molecular Dipoles in PVDF Film: A Realization of Self-Poled Bioinspired Flexible Polymer Nanogenerator for Portable Electronic Devices, ACS Appl. Mater. Interfaces 7 (2015) 16143−16147. https://doi.org/10.1021/acsami.5b04161.

[161] S.T. Chen, X. Li, K. Yao, F.H. Tay, A. Kumar, K. Zeng, Self-polarized ferroelectric PVDF homopolymer ultra-thin films derived from Langmuir–Blodgett deposition, Polymer 53 (2012) 1404. https://doi.org/10.1016/j.polymer.2012.01.058.

[162] B.J. Rodriguez, S. Jesse, S.V. Kalinin, J. Kim, S. Ducharme, V.M. Fridkin, Nanoscale polarization manipulation and imaging of ferroelectric Langmuir-Blodgett polymer films, Appl. Phys. Lett. 90 (2007) 122904. https://doi.org/10.1063/1.2715102.

[163] Z.L. Wang, J. Song, Piezoelectric nanogenerators based on zinc oxide nanowire arrays, Science 312 (2006) 242-246. https://doi.org/10.1126/science.1124005.

[164] S. Cha, S.M. Kim, H. Kim, J. Ku, J.I. Sohn, Y.J. Park, B.G. Song, M.H. Jung, E.K. Lee, B.L. Choi, Porous PVDF as effective sonic wave driven nanogenerators, Nano letters 11 (2011) 5142-5147. https://doi.org/10.1021/nl202208n.

[165] D. Chen, T. Sharma, J.X. Zhang, Mesoporous surface control of PVDF thin films for enhanced piezoelectric energy generation, Sens. Actuators A: Phys. 216 (2014) 196-201. https://doi.org/10.1016/j.sna.2014.05.027.

[166] Y. Duan, Y. Huang, Z. Yin, N. Bu, W. Dong, Non-wrinkled, highly stretchable piezoelectric devices by electrohydrodynamic direct-writing, Nanoscale 6 (2014) 3289-3295. https://doi.org/10.1039/C3NR06007A.

[167] J. Fang, H. Niu, H. Wang, X. Wang, T. Lin, Enhanced mechanical energy harvesting using needleless electrospun poly (vinylidene fluoride) nanofibre webs, Energ Environ. Sci. 6 (2013) 2196-2202. https://doi.org/10.1039/C3EE24230G.

[168] J.H. Lee, H.J. Yoon, T.Y. Kim, M.K. Gupta, J.H. Lee, W. Seung, H. Ryu, S.W. Kim, Micropatterned P (VDF-TrFE) Film-Based Piezoelectric Nanogenerators for Highly Sensitive Self-Powered Pressure Sensors, Adv. Funct. Mater. 25 (2015) 3203-3209. https://doi.org/10.1002/adfm.201500856.

[169] R.A. Whiter, V. Narayan, S. Kar-Narayan, A scalable nanogenerator based on self-poled piezoelectric polymer nanowires with high energy conversion efficiency, Adv. Energy Mater. 4 (2014) 1400519. https://doi.org/10.1002/aenm.201400519.

[170] W.H. Liew, M.S. Mirshekarloo, S. Chen, K. Yao, F.E.H. Tay, Nanoconfinement induced crystal orientation and large piezoelectric coefficient in vertically aligned P (VDF-TrFE) nanotube array, Sci. Rep. 5 (2015) 09790. https://doi.org/doi.org/10.1038/srep09790.

[171] Y.-Y. Choi, T.G. Yun, N. Qaiser, H. Paik, H.S. Roh, J. Hong, S. Hong, S.M. Han, K. No, Vertically aligned P (VDF-TrFE) core-shell structures on flexible pillar arrays, Sci. Rep. 5 (2015) 10728. https://doi.org/doi.org/10.1038/srep10728.

[172] V. Bhavanasi, D.Y. Kusuma, P.S. Lee, Polarization Orientation, Piezoelectricity, and Energy Harvesting Performance of Ferroelectric PVDF-TrFE Nanotubes Synthesized by Nanoconfinement, Adv. Energy Mater. 4 (2014) 1400723. https://doi.org/doi.org/10.1002/aenm.201400723.

[173] B.-S. Lee, B. Park, H.-S. Yang, J.W. Han, C. Choong, J. Bae, K. Lee, W.-R. Yu, U. Jeong, U.-I. Chung, Effects of substrate on piezoelectricity of electrospun poly (vinylidene fluoride)-nanofiber-based energy generators, ACS Appl. Mater. Interfaces 6 (2014) 3520-3527. https://doi.org/doi.org/10.1021/am405684m.

[174] J. Ma, Q. Zhang, K. Lin, L. Zhou, Z. Ni, Piezoelectric and optoelectronic properties of electrospinning hybrid PVDF and ZnO nanofibers, Mater. Res. Express 5 (2018) 035057. https://doi.org/doi.org/10.1088/2053-1591/aab747.

[175] C.-C. Hong, S.-Y. Huang, J. Shieh, S.-H. Chen, Enhanced piezoelectricity of nanoimprinted sub-20 nm poly (vinylidene fluoride–trifluoroethylene) copolymer nanograss, Macromolecules 45 (2012) 1580-1586. https://doi.org/doi.org/10.1021/ma202481t.

[176] E. Fukada, Recent developments of polar piezoelectric polymers, IEEE Trans. Dielectr. Electr. Insul.13 (2006) 1110-1119. https://doi.org/doi.org/10.1109/TDEI.2006.247839.

[177] R. Fu, S. Chen, Y. Lin, S. Zhang, J. Jiang, Q. Li, Y. Gu, Improved piezoelectric properties of electrospun poly (vinylidene fluoride) fibers blended with cellulose nanocrystals, Mater. Lett. 187 (2017) 86-88. https://doi.org/doi.org/10.1016/j.matlet.2016.10.068.

[178] Q. Zheng, B. Shi, Z. Li, Z.L. Wang, Recent progress on piezoelectric and triboelectric energy harvesters in biomedical systems, Adv. Sci. 4 (2017) 1700029. https://doi.org/10.1002/advs.201700029.

[179] M. Salim, D. Salim, D. Chandran, H.S. Aljibori, A. Sh. Kherbeet, Review of nano piezoelectric devices in biomedicine applications, J. Intell. Material Syst. Struct. 29 (2018) 2105-2121. https://doi.org/10.1177/1045389X17754272.

[180] G.-T. Hwang, M. Byun, C.K. Jeong, K.J. Lee, Flexible piezoelectric thin-film energy harvesters and nanosensors for biomedical applications, Adv. Healthcare Mater. 4 (2015) 646-658. https://doi.org/10.1002/adhm.201400642.

[181] C. Dagdeviren, P. Joe, O.L. Tuzman, K.-I. Park, K.J. Lee, Y. Shi, Y. Huang, and J.A. Rogers, Recent progress in flexible and stretchable piezoelectric devices for mechanical energy harvesting, sensing and actuation, Extreme Mech. Lett. 9 (2016) 269-281. https://doi.org/10.1016/j.eml.2016.05.015.

[182] F.R. Fan, W. Tang, Z.L. Wang, Flexible nanogenerators for energy harvesting and self-powered electronics, Adv. Mater. 28 (2016) 4283-4305. https://doi.org/10.1002/adma.201504299.

[183] T.Q. Trung, N.-E. Lee, Flexible and stretchable physical sensor integrated platforms for wearable human-activity monitoring and personal healthcare, Adv. Mater. 28 (2016) 4338-4372. https://doi.org/10.1002/adma.201504244.

[184] C.Y.S. Dagdeviren, P. Joe, R. Yona, Y. Liu, Y. Kim, Y Huang, A.R. Damadoran, J. Xia, L.W. Martin, Y. Huang, J.A. Rogers, Conformable amplified lead zirconate titanate sensors with enhanced piezoelectric response for cutaneous pressure monitoring, Nat. Commun. 5 (2014) 4496. https://doi.org/10.1038/ncomms5496.

[185] T.D. Nguyen, N. Deshmukh, J.M. Nagarah, T. Kramer, P.K. Purohit, M.J. Berry, M.C. McAlpine, Piezoelectric nanoribbons for monitoring cellular deformations, Nat. Nanotechnol. 7 (2012) 587-593. https://doi.org/10.1038/nnano.2012.112.

[186] G.-T. Hwang, H. Park, J.-H. Lee, S. Oh, K.-I. Park, M. Byun, H. Park, G. Ahn, C.K. Jeong, K. No, H. Kwon, S.-G. Lee, B. Joung, K.J. Lee, Self-powered cardiac pacemaker enabled by flexible single crystalline PMNPT piezoelectric energy harvester, Adv. Mater. 26 (2014) 4880-4887. https://doi.org/10.1002/adma.201400562.

[187] A. Marino, G.G. Genchi, E. Sinibaldi, G. Ciofani, Piezoelectric effects of materials on biointerfaces, ACS Appl. Mater. Interfaces 9 (2017) 17663-17680. https://doi.org/10.1021/acsami.7b04323.

[188] B. Tandon, J.J. Blaker, S.H. Cartmell, Piezoelectric materials as stimulatory biomedical materials and scaffolds for bone repair, Acta Biomater. 73 (2018) 1-20. https://doi.org/10.1016/j.actbio.2018.04.026.

[189] L. Ruan, X. Yao, Y. Chang, L. Zhou, G. Qin, X. Zhang, Properties and applications of the β phase poly(vinylidene fluoride), Polymers 10 (2018) 228. https://doi.org/10.3390/polym10030228.

[190] K.-I. Park, C.K. Jeong, N.K. Kim, K.J. Lee, Stretchable piezoelectric nanocomposite generator, Nano Convergence 3 (2016) 12. https://doi.org/10.1186/s40580-016-0072-z.

[191] J. Li, R. Bao, J. Tao, Y. Peng, C. Pan, Recent progress in flexible pressure sensor arrays: from design to applications, J. Mater. Chem. C (2018). https://doi.org/10.1039/C8TC02946F.

[192] Q. Jing, S. Kar-Narayan, Nanostructured polymer-based piezoelectric and triboelectric materials and devices for energy harvesting applications, J. Phys. D: Appl. Phys. 51 (2018) 303001. https://doi.org/10.1088/1361-6463/aac827.

[193] Y. Hu, Z.L. Wang, Recent progress in piezoelectric nanogenerators as a sustainable power source in self-powered systems and active sensors, Nano Energy 14 (2015) 3-14. https://doi.org/10.1016/j.nanoen.2014.11.038.

[194] W.-S. Jung, M.-J. Lee, M.-G. Kang, H.G. Moon, S.-J. Yoon, S.-H. Baek, C.-Y. Kang, Powerful curved piezoelectric generator for wearable applications, Nano Energy 13 (2015) 174-181. https://doi.org/10.1016/j.nanoen.2015.01.051.

[195] S.-H. Shin, S.-Y. Choi, M.H. Lee, J. Nah, High-performance piezoelectric nanogenerators via imprinted sol−gel $BaTiO_3$ nanopillar array, ACS Appl. Mater. Interfaces 9 (2017) 41099-41103. https://doi.org/10.1021/acsami.7b11773.

[196] S. Shin, D. Park, J.-Y. Jung, M.H. Lee, J. Nah, Ferroelectric zinc oxide nanowire embedded flexible sensor for motion and temperature sensing, ACS Appl. Mater. Interfaces 9 (2017) 9233-9238. https://doi.org/10.1021/acsami.7b00380.

[197] C. Ribeiro, V. Sencadas, D.M. Correia, S. Lanceros-Méndez, Piezoelectric polymers as biomaterials for tissue engineering applications, Colloids Surf. B: Biointerfaces 136 (2015) 46-55. https://doi.org/10.1016/j.colsurfb.2015.08.043.

[198] C. Ning, Z. Zhoua, G. Tan, Ye Zhu, C. Mao, Electroactive polymers for tissue regeneration: Developments and perspectives, Prog. Polym. Sci. 81 (2018) 144-162. https://doi.org/10.1016/j.progpolymsci.2018.01.001.

[199] S. Selvarajan, N.R. Alluri, A. Chandrasekhar, S.-J. Kim, $BaTiO_3$ nanoparticles as biomaterial film for self-powered glucosesensor application, Sens. Actuators B Chem. 234 (2016) 395-403. https://doi.org/10.1016/j.snb.2016.05.004.

[200] J.S. Lee, K.-Y. Shin, O.J. Cheong, J.H. Kim, J. Jang, Highly sensitive and multifunctional tactile sensor using free-standing ZnO/PVDF thin film with graphene electrodes for pressure and temperature monitoring, Sci. Rep. 5 (2015) 7887. https://doi.org/10.1038/srep07887.

[201] H H. He, Y. Fu, W. Zang, Q. Wang, L. Xing, Y. Zhang, X. Xue, A flexible self-powered T-ZnO/PVDF/fabric electronic-skin with multifunctions of tactile-perception, atmosphere-detection and self-clean, Nano Energy 31 (2017) 37-48. https://doi.org/10.1016/j.nanoen.2016.11.020.

[202] T. Huang, S. Yang, P. He, J. Sun, S. Zhang, D. Li, Y. Meng, J. Zhou, H. Tang, J. Liang, G. Ding, X. Xie, Phase separation induced PVDF/Graphene coating on fabrics towards flexible piezoelectric sensors, ACS Appl. Mater. Interfaces 10 (2018) 30732-30740. https://doi.org/10.1021/acsami.8b10552.

[203] Y. Lee, J. Park, S. Cho, Y.-E. Shin, H. Lee, J. Kim, J. Myoung, S. Cho, S. Kang, C. Baig, H. Ko, Flexible ferroelectric sensors with ultrahigh pressure sensitivity and linear response over exceptionally broad pressure range, ACS Nano 12 (2018) 4045-4054. https://doi.org/10.1021/acsnano.8b01805.

[204] X. Chen, X. Li, Jinyou Shao, N. An, H. Tian, C. Wang, T. Han, L. Wang, B. Lu, High-Performance Piezoelectric Nanogenerators with Imprinted P(VDF-TrFE)/BaTiO$_3$ Nanocomposite Micropillars for Self-Powered Flexible Sensors, Small 13 (2017) 1604245. https://doi.org/10.1002/smll.201604245.

[205] Z. Lou, S. Chen, L. Wang, K. Jiang, G. Shen, An ultra-sensitive and rapid response speed graphene pressure sensors for electronic skin and health monitoring, Nano Energy 23 (2016) 7-14. https://doi.org/10.1016/j.nanoen.2016.02.053.

[206] J. Park, M. Kim, Y. Lee, H.S. Lee, H. Ko, Fingertip skin-inspired microstructured ferroelectric skins discriminate static/dynamic pressure and temperature stimuli, Sci. Adv. 1 (2015) e1500661. https://doi.org/10.1126/sciadv.1500661.

[207] W. Zeng, X.-M. Tao, S. Chen, S. Shang, H.L.W. Chan, S.H. Choy, Highly durable all-fiber nanogenerator for mechanical energy harvesting, Energy Environ. Sci. 6 (2013) 2631-2638. https://doi.org/10.1039/C3EE41063C.

[208] W. Tong, Y. Zhang, Q. Zhang, X. Luan, F. Lv, L. Liu, Q. An, An all-solid-state flexible piezoelectric high-k film functioning as both a generator and in situ storage unit, Adv. Funct. Mater. 25 (2015) 7029-7037. https://doi.org/10.1002/adfm.201503514.

[209] P. Zhang, X. Zhao, X Zhang, Y. Lai, X. Wang, J. Li, G. Wei, Z. Su, Electrospun doping of carbon nanotubes and platinum nanoparticles into the β-phase polyvinylidene difluoride nanofibrous membrane for biosensor and catalysis applications, ACS Appl. Mater. Interfaces 6 (2014) 7563-7571. https://doi.org/10.1021/am500908v.

[210] J. Li, L. Kang, Y. Yu, Y. Long, J.J. Jeffery, W. Cai, X. Wang, Study of long-term biocompatibility and bio-safety of implantable nanogenerators, Nano Energy 51 (2018) 728-735. https://doi.org/10.1016/j.nanoen.2018.07.008.

[211] R. Augustine, P. Dan, A. Sosnik, N. Kalarikkal, N. Tran, B. Vincent, S. Thomas, P. Menu, D. Rouxel, Electrospun poly(vinylidene fluoride-trifluoroethylene)/zinc oxide nanocomposite tissue engineering scaffolds with enhanced cell adhesion and blood vessel formation, Nano Research 10 (2017) 3358-3376. https://doi.org/10.1007/s12274-017-1549-8.

[212] P.H. Scalize, K.F. Bombonato-Prado, L.G. de Sousa, A.L. Rosa, M.M. Beloti, M. Semprini, R Gimenes, A.L.G. de Almeida, F.S. de Oliveira, S.C.H. Regalo, S. Siessere, Poly(Vinylidene Fluoride-Trifluorethylene)/barium titanate membrane promotes de novo bone formation and may modulate gene expression in osteoporotic rat model, J. Mater. Sci.: Mater. Med. (2016) 27180. https://doi.org/10.1007/s10856-016-5799-x.

[213] Y. Li, L. Sun, T.J. Webster, The investigation of ZnO/Poly(vinylidene fluoride) nanocomposites with improved mechanical, piezoelectric, and antimicrobial properties for orthopedic applications, J. Biomed. Nanotechnol. 14 (2018) 536-545. https://doi.org/10.1166/jbn.2018.2519.

[214] W. Huang, P. Wu, P. Feng, Y. Yang, W. Guo, D. Lai, Z. Zhou, X. Liu, C. Shuai, MgO whiskers reinforced poly(vinylidene fluoride) scaffolds, RSC Adv. 6 (2016) 108196-108202. https://doi.org/10.1039/C6RA22386A.

[215] T. Zhou, G. Li, S. Lin, T. Tian, Q. Ma, Q. Zhang, S. Shi, C. Xue, W. Ma, X. Cai, Y. Lin, Electrospun Poly(3-hydroxybutyrate-co-4-hydroxybutyrate)/Graphene Oxide Scaffold: Enhanced Properties and Promoted in Vivo Bone Repair in Rats, ACS Appl. Mater. Interfaces 9 (2017) 42589-42600. https://doi.org/10.1021/acsami.7b14267.

[216] K. Ravikumar, G.P. Kar, S. Bose, B. Basu, Synergistic effect of polymorphism, substrate conductivity and electric field stimulation towards enhancing muscle cell growth in vitro, RSC Adv. 6 (2016) 10837-10845. https://doi.org/10.1039/C5RA26104J.

[217] Y. Hu, Y. Chang, P. Fei, R.L. Snyder, Z.L. Wang, Designing the electric transport characteristics of ZnO micro/nanowire devices by coupling piezoelectric and photoexcitation effects, ACS Nano 4 (2010) 1234-1240. https://doi.org/10.1021/nn901805g.

[218] Y. Feng, L. Ling, Y. Wang, Z. Xu, F. Cao, H. Li, Z. Bian, Engineering spherical lead zirconate titanate to explore the essence of piezo-catalysis, Nano Energy 40 (2017) 481-486. https://doi.org/10.1016/j.nanoen.2017.08.058.

[219] K.-S. Hong, H. Xu, H. Konishi, X. Li, Direct water splitting through vibrating piezoelectric microfibers in water, J. Phys. Chem. Lett. 1 (2010) 997-1002. https://doi.org/10.1021/jz100027t.

[220] K.-S. Hong, H. Xu, H. Konishi, X. Li, Piezoelectrochemical effect: a new mechanism for azo dye decolorization in aqueous solution through vibrating piezoelectric microfibers, J. Phys. Chem. C 116 (2012) 13045-13051. https://doi.org/10.1021/jp211455z.

[221] J. Feng, Y. Fu, X. Liu, S. Tian, S. Lan, Y. Xiong, Significant Improvement and Mechanism of Ultrasonic Inactivation to Escherichia coli with Piezoelectric Effect of Hydrothermally Synthesized t-BaTiO$_3$, ACS Sustain. Chem. Eng. 6 (2018) 6032-6041. https://doi.org/10.1021/acssuschemeng.7b04666.

[222] Y. Yang, H. Zang, S. Lee, D. Kim, W. Hwang, Z. L Wang, Hybrid energy cell for degradation of methyl orange by self-powered electrocatalytic oxidation, Nano Lett. 13 (2013) 803-818. https://doi.org/10.1021/nl3046188.

[223] C.F. Tan, W.L. Ong, G.W. Ho, Self-biased hybrid piezoelectric-photoelectrochemical cell with photocatalytic functionalities, ACS Nano 9 (2015) 7661-7670. https://doi.org/10.1021/acsnano.5b03075.

[224] J.M. Wu, W.E. Chang, Y.T. Chang, C.K. Chang, Piezo-Catalytic Effect on the Enhancement of the Ultra-High Degradation Activity in the Dark by Single-and Few-Layers MoS_2 Nanoflowers, Advanced Materials 28 (2016) 3718-3725. https://doi.org/10.1002/adma.201505785.

[225] H. Lin, Z. Wu, Y. Jia, W. Li, R.-K. Zheng, H. Luo, Piezoelectrically induced mechano-catalytic effect for degradation of dye wastewater through vibrating Pb $(Zr_{0.52}Ti_{0.48})O_3$ fibers, Appl. Phys. Lett. 104 (2014) 162907. https://doi.org/10.1063/1.4873522.

[226] S. Lan, J. Feng, Y. Xiong, S. Tian, S. Liu, L. Kong, Performance and Mechanism of Piezo-Catalytic Degradation of 4-Chlorophenol: Finding of Effective Piezo-Dechlorination, Environ. Sci. Technol. 51 (2017) 6560-6569. https://doi.org/10.1021/acs.est.6b06426.

[227] S. Masimukku, Y.-C. Hu, Z.-H. Lin, S.-W. Chan, T.-M. Chou, J.M. Wu, High efficient degradation of dye molecules by PDMS embedded abundant single-layer tungsten disulfide and their antibacterial performance, Nano energy 46 (2018) 338-346. https://doi.org/10.1016/j.nanoen.2018.02.008.

[228] M. Ando, S. Takeshima, Y. Ishiura, K. Ando, O. Onishi, Piezoelectric antibacterial fabric comprised of poly (l-lactic acid) yarn, Jap. J. Appl. Phys. 56 (2017) 10PG01. https://doi.org/10.7567/JJAP.56.10PG01.

[229] J.L. Del Pozo, M.S. Rouse, J.N. Mandrekar, J.M. Steckelberg, R. Patel, The electricidal effect: reduction of Staphylococcus and Pseudomonas biofilms by prolonged exposure to low-intensity electrical current, Antimicrob. Agents Chemother. 53 (2009) 41-45. https://doi.org/10.1128/AAC.00680-08.

[230] J. Wu, Q. Xu, E. Lin, B. Yuan, N. Qin, S.K. Thatikonda, D. Bao, Insights into the Role of Ferroelectric Polarization in Piezocatalysis of Nanocrystalline $BaTiO_3$, ACS Appl. Mater. Interfaces 10 (2018) 17842-17849. https://doi.org/10.1021/acsami.8b01991.

[231] W. Zhao, C. Liang, B. Wang, S. Xing, Enhanced Photocatalytic and Fenton-like Performance of CuO_x-Decorated $ZnFe_2O_4$, ACS Appl. Mater. Interfaces 9 (2017) 41927-41936. https://doi.org/10.1021/acsami.7b14799.

[232] Q. Mo, N. Chen, M. Deng, L. Yang, Q. Gao, Metallic Cobalt@Nitrogen-Doped Carbon Nanocomposites: Carbon-Shell Regulation toward Efficient Bi-Functional Electrocatalysis, ACS Appl. Mater. Interfaces 9 (2017) 37721-37730. https://doi.org/10.1021/acsami.7b10853.

[233] X. Xiong, T. Zhou, X. Liu, S. Ding, J. Hu, Surfactant-mediated synthesis of single-crystalline Bi_3O_4Br nanorings with enhanced photocatalytic activity, J. Mater. Chem. A 5 (2017) 15706-15713. https://doi.org/10.1039/C7TA04507G.

[234] M.A. Sayeed, A.P. O'Mullane, A multifunctional gold doped Co $(OH)_2$ electrocatalyst tailored for water oxidation, oxygen reduction, hydrogen evolution and glucose detection, J. Mater. Chem. A 5 (2017) 23776-23784. https://doi.org/10.1039/C7TA08928G.

[235] W. Wu, High-performance piezoelectric nanogenerators for self-powered nanosystems: quantitative standards and figures of merit, Nanotechnology 27 (2016) 112503. https://doi.org/10.1088/0957-4484/27/11/112503.

Supporting Information

Click here to download Supporting Information: Plan of the article2_Supporting info final.docx

Supporting Information

Click here to download Supporting Information: Permissions.rar

Supporting Information

Click here to download Supporting Information: Certificate_Surmenev Roman.pdf

*Graphical Abstract